NUCLEON - NUCLEON TWO - PION - EXCHANGE

Dissertation for the Degree of Ph. D.
MICHIGAN STATE UNIVERSITY
GEORGE EDMOND BOHANNON
1974

THESIS

LIBRARY
Michigan State
University

This is to certify that the

thesis entitled

NUCLEON-NUCLEON
TWO-PION-EXCHANGE

presented by

George Edmond Bohannon

has been accepted towards fulfillment
of the requirements for

Ph.D. degree in Physics

Peter Signell
Major professor

Date April 30, 1974

O-7639

BINDING BY
HOAG & SONS'
BOOK BINDERY INC.
LIBRARY BINDERS
SPRINGPORT, MICHIGAN

RARY
g. n State
iversity

BINDING BY
HOAG & SONS'
BOOK BINDERY INC.
LIBRARY BINDERS
SPRINGPORT, MICHIGAN

NU

The J=0

pseudophysical

nucleon-nucleon

which entered t

$N\bar{N}\to\pi\pi$ amplitude

given for sever

δ_0^0.

The πN

$\frac{\partial}{\partial t} A^{(+)}(s=u,t)$

relations to b

tively. These

a fixed $\nu=(s-u$

shift δ_0^0 as in

for $A^{(+)}(t=4\mu^2$

used; values o

The va

mination of th

and Watanabe[1]

ABSTRACT

NUCLEON-NUCLEON TWO-PION-EXCHANGE

By

George Edmond Bohannon

The $J=0,1,2$ $N\bar{N}\to\pi\pi$ amplitudes were evaluated in the pseudophysical region $t\geq 4\mu^2$ and used in a calculation of nucleon-nucleon two-pion-exchange. The $\pi\pi$ phase shifts, which entered the calculation as the phases of the $t\geq 4\mu^2$ $N\bar{N}\to\pi\pi$ amplitudes, are discussed in detail. Results are given for several forms of the inputed $I=J=0$ $\pi\pi$ phase shift δ_0^0.

The πN amplitudes $A^{(+)}(s=u,t=0)$ and $\frac{\partial}{\partial t}A^{(+)}(s=u,t)\big|_{t=0}$ were determined from fixed-t dispersion relations to be $25.9 \pm .5\ \mu^{-1}$ and $1.16 \pm .05\ \mu^{-3}$ respectively. These values were used as subtraction constants in a fixed $\nu=(s-u)/(4m)=0$ dispersion relation with the phase shift δ_0^0 as input to continue to positive t. The results for $A^{(+)}(t=4\mu^2)$ were somewhat dependent upon the form of δ_0^0 used; values obtained were between $32\ \mu^{-1}$ and $34\ \mu^{-1}$.

The values of $A^{(+)}(t=0)$, $A^{(+)}(t=4\mu^2)$ and a determination of the $J=0$ $N\bar{N}\to\pi\pi$ amplitude $f_+^0(t=0)$ by Furuichi and Watanabe[1] were used for subtraction constants along

with the phase

to determine |f

enhancement in

Saclay K_{e4} expe

For the

partial wave d

Nielsen's fixe

requiring that

nucleon form f

with a total o

form factors G

with experimen

required in th

dominance of t

with experimen

imaginary part

with resonance

constants as d

found are $g^2_{\rho NN}$

The J=

partial wave

where the subt

work.[3]

The J=

subtracted pa

shown with an

C 12139

with the phase shift δ_o^o in partial wave dispersion relations to determine $|f_+^o(t)|$. It was found that introducing an enhancement in the low energy δ_o^o, as seen in the Geneva-Saclay K_{e4} experiment,[2] resulted in a smaller $|f_+^o(t\gtrsim 6\mu^2)|$.

For the J=1 case the subtraction constants in a partial wave dispersion relation were determined from Nielsen's fixed-t dispersion relation results[3] and by requiring that the two pion intermediate state dominate the nucleon form factors. The resulting J=1 $N\bar{N}\to\pi\pi$ amplitudes with a total of two adjusted subtraction constants produced form factors G_E^V and G_M^V which are in excellent agreement with experimental results. The pion form factor, which was required in the calculation, was evaluated assuming dominance of the two pion intermediate state and compared with experimental results in the timelike region. The imaginary parts of the J=1 $N\bar{N}\to\pi\pi$ amplitudes were fitted with resonance expressions to determine the ρNN coupling constants as defined at the rho meson pole. The values found are $g^2_{\rho NN}/4\pi = 0.44\pm0.05$ and $f_{\rho NN}/g_{\rho NN} = 5.8\pm0.2$.

The J=0,1 $N\bar{N}\to\pi\pi$ amplitudes were also evaluated via partial wave dispersion relations subtracted twice at t=0, where the subtraction constants were taken from Nielsen's work.[3]

The J=2 $N\bar{N}\to\pi\pi$ amplitudes were evaluated with once subtracted partial wave dispersion relations. Results are shown with and without the right-hand ($\pi\pi$) cut.

The fi

exchange, one-

tudes. The NN

MAW-X phase sh

exchange fits[5]

amplitude. It

enhancement in

ment of most L

The NN

with the Hamad

Variou

coupling const

meson-dominanc

[1]S. Fu

37, 465 (1967)

[2]A. Zy

(1971).

[3]H. N

[4]M. H

Phys. Rev. 18

[5]R. A

(1972).

[6]T. H

(1962).

The final NN amplitude was the sum of the one-pion-exchange, one-omega-exchange and two-pion-exchange amplitudes. The NN phase shifts were compared with those of the MAW-X phase shift analyses,[4] the Bryan-Gersten one-boson exchange fits[5] and the pseudoscalar coupling nucleon box amplitude. It was found that introducing a low energy enhancement into the $\pi\pi$ phase shift δ_0^0 improved the agreement of most $L \geq 2$ phase shifts with the phase shift analyses.

The NN potential was calculated and shown along with the Hamada-Johnston[6] and nucleon box potentials.

Various methods are discussed for finding the ωNN coupling constants based on the quark model and vector-meson-dominance.

[1]S. Furuichi and K. Watanabe, Prog. Theoret. Phys. 37, 465 (1967).

[2]A. Zylbersztejn et al., Phys. Letters 38B, 457 (1971).

[3]H. Nielsen, Nucl. Phys. B33, 152 (1971).

[4]M. H. MacGregor, R. A. Arndt and R. M. Wright, Phys. Rev. 182, 1714 (1969).

[5]R. A. Bryan and A. Gersten, Phys. Rev. D6, 341 (1972).

[6]T. Hamada and I. D. Johnston, Nucl. Phys. 34, 382 (1962).

NU

in pa

NUCLEON-NUCLEON TWO-PION-EXCHANGE

By

George Edmond Bohannon

A DISSERTATION

Submitted to
Michigan State University
in partial fulfillment of the requirements
for the degree of

DOCTOR OF PHILOSOPHY

Department of Physics

1974

Physi
problem the wo
of work which
of physics.
of the authors
of some people

I owe
Signell, who s
encouragement
work in this
tion of this

I am
cussions abou
Edward Yen fo
particle phys
netic form fa
quark model h

Disc
in understand
tromagnetic i

ACKNOWLEDGEMENTS

Physics research involves focusing onto a specific problem the work of a large number of people. The diversity of work which can be so focused is a measure of the unity of physics. I have been influenced to some extent by each of the authors in the List of References. The contributions of some people should be specifically noted here.

I owe my sincerest gratitude to Professor Peter Signell, who suggested this problem and provided continued encouragement. His suggestions and remarks and his own work in this area have been valuable assets in the completion of this thesis.

I am grateful to Dr. Jon Pumplin for helpful discussions about particle physics. I am also grateful to Dr. Edward Yen for sharing with me some of his knowledge of particle physics. Their remarks regarding the electromagnetic form factors, vector-meson-dominance, quarks and the quark model have been particularly useful.

Discussions with Dr. Wayne Repko have been helpful in understanding the intricacies of field theory and electromagnetic interactions.

I al

Leon Heller re

the two-pion-e

cerning the re

Discu

aspects of the

I am

Stevens, Dr. G

the high energ

of the $N\bar{N}\to\pi\pi$ s

respectively.

The n

because of the

By qu

phase shift an

Wright made it

combinations o

uncertainties.

The a

results was ma

code, with son

graphs for thi

Final

National Scien

Public, for ma

I also appreciate a helpful discussion with Dr. Leon Heller regarding the calculation of a potential from the two-pion-exchange amplitude as well as his remarks concerning the reasons for generating such a potential.

Discussions with Dr. D.O. Riska concerning several aspects of the two-pion-exchange problem have been helpful.

I am grateful for communications with Dr. Paul Stevens, Dr. Geoffrey Epstein, and Dr. Graham Shaw regarding the high energy behavior of πN amplitudes, the evaluation of the $N\bar{N}\to\pi\pi$ s-wave amplitude, and the $I=J=0$ $\pi\pi$ phase shift, respectively.

The numerical calculations were much easier because of the expert advice of Dr. Jonas Holdeman.

By quickly responding to my request for the MAW-X phase shift analysis error matrix M.H. MacGregor and R.M. Wright made it possible to include in this thesis unpublished combinations of their published phase shifts with the correct uncertainties.

The accurate presentation of the calculational results was made possible by Rick Meyers, whose computer code, with some modifications, was used to draw most of the graphs for this thesis.

Finally and very importantly, I am grateful to the National Science Foundation and its supporters, the American Public, for making this research possible.

LIST OF TABLES

LIST OF FIGURE

INTRODUCTION.

Chapter

I. DISPERS

A. S

B. T

II. TWO-PI

A. T
B.
C.

III. EVALUA

A.

B.
C.

D.

E.

F.

G.

IV. THE NU

A.
B.
C.

TABLE OF CONTENTS

		Page
LIST OF TABLES		vi
LIST OF FIGURES		vii
INTRODUCTION		1
Chapter		
I.	DISPERSION RELATIONS	5
	A. Single Variable Dispersion Relations from Analyticity	5
	B. Two Dimensional Representation	11
II.	TWO-PION-EXCHANGE FORMALISM	22
	A. The Dispersion Theoretic Approach	22
	B. Inclusion of the $N\bar{N}\to\pi\pi$ Amplitudes	32
	C. Two Pion Exchange Potential	36
III.	EVALUATION OF THE $N\bar{N}\to\pi\pi$ AMPLITUDES	44
	A. Partial-Wave Dispersion Relations for $N\bar{N}\to\pi\pi$	44
	B. Pion-Pion Phase Shift Input	47
	C. Evaluation of $A^{(+)}$ and $\frac{\partial A^{(+)}}{\partial t}$ at s-u, t=0	57
	D. The $N\bar{N}\to\pi\pi$ s-Wave Amplitude: $A^{(+)}$ Fixed-ν Dispersion Relation	66
	E. The $N\bar{N}\to\pi\pi$ s-Wave Amplitude: Omnès Dispersion Relations	74
	F. The p-Wave $N\bar{N}\to\pi\pi$ Amplitudes and the Nucleon and Pion Electromagnetic Form Factors	78
	G. The $N\bar{N}\to\pi\pi$ d-Wave Helicity Amplitudes	94
IV.	THE NUCLEON-NUCLEON AMPLITUDE	98
	A. Phase Shifts	98
	B. Potentials	114
	C. Discussion	126

Chapter

LIST OF REFERE

APPENDICES

Appendix

A. THE HEI

B. POLE CO

C. PARTIAL

D. POTENTI

E. DIRAC

F. RHO-MES

G. OMEGA-

Chapter Page

LIST OF REFERENCES 130

APPENDICES

Appendix

A. THE HELICITY EXPANSION 138

B. POLE CONTRIBUTIONS TO THE $N\bar{N}\to\pi\pi$ AMPLITUDES. . 141

C. PARTIAL WAVE PROJECTIONS. 147

D. POTENTIAL EQUATIONS 154

E. DIRAC ALGEBRA 158

F. RHO-MESON COUPLING CONSTANTS 160

G. OMEGA-MESON COUPLING CONSTANTS. 164

Table

1. A compi
   deter

2. A compi
   deter

3. Results
   t=0.

4. Results

5. A compi
   minat

6. Contrib
   with

7. The p-w
   t=0.

8. Values
   evalu

9. Predict

LIST OF TABLES

Table

		Page
1.	A compilation of s-wave πN scattering length determinations	61
2.	A compilation of p-wave πN scattering length determinations	62
3.	Results for $A^{(+)}(0,t)$ and its derivative at t=0.	64
4.	Results of various authors for $A^{(+)}(0,0)$ . . .	64
5.	A compilation of πNN coupling constant determinations.	65
6.	Contributions to the s-wave dispersion relation with MS phase shift	77
7.	The p-wave $N\bar{N}\rightarrow\pi\pi$ amplitudes and derivatives at t=0.	82
8.	Values used as subtraction constants for the evaluation of the d-wave helicity amplitudes .	95
9.	Predictions for the omega coupling constants. .	171

Figure

1. The mome
   two-b

2. The doul
   scatt

3. Low ord

4. The πN
   regio

5. The Man
   scatt

6. Mandels
   scatt

7. The t-c

8. Singula
   $f^J_{\pm}(t)$

9. Single

10. The I=J
    exper

11. The I=J

12. The πN

13. Real pa

14. Imagina

15. The I=J
    calcu

LIST OF FIGURES

Figure		Page
1.	The momentum labels and scattering channels for two-body scattering	12
2.	The double spectral region for equal-mass scattering	14
3.	Low order πN scattering diagrams	19
4.	The πN physical regions and double spectral regions	20
5.	The Mandelstam diagram for pion-nucleon scattering	21
6.	Mandelstam diagram for nucleon-nucleon scattering	26
7.	The t-channel diagrams for $N\bar{N}\to\pi\pi\to N\bar{N}$	27
8.	Singularities of the $N\bar{N}\to\pi\pi$ helicity amplitudes $f^J_{+-}(t)$	45
9.	Single pion production and K_{e4} decay	48
10.	The I=J=0 $\pi\pi$ phase shift derived from experimental information	52
11.	The I=J=1 $\pi\pi$ phase shift	54
12.	The πN amplitude $A^{(+)}$ along s=u.	69
13.	Real part of the $N\bar{N}\to\pi\pi$ amplitude f^o_+	70
14.	Imaginary part of the $N\bar{N}\to\pi\pi$ amplitude f^o_+.	71
15.	The I=J=0 $\pi\pi$ phase shifts used in the calculations	73

Figure

16. The J=0

17. The pion

18. The J=1
dispe

19. The two-
of the

20. Fit to

21. Fit to

22. The $N\bar{N}$→

23. The $N\bar{N}$→

24. The $N\bar{N}$→

25. The $^1D_2$

26. The $^1G_4$

27. The $^3P_1$

28. The $^3\bar{P}_2$

29. The $^3\bar{F}_C$

30. The $^3\bar{F}_T$

31. The $^3\bar{F}_I$

32. The $^3\bar{F}_2$

33. The $^3F_3$

34. The $^3\bar{F}_4$

35. The $^1P_1$

36. The $^1F_3$

37. The $^3D_3$

38. The $^3\bar{D}_3$

39. The si

Figure

16. The J=0 spectral function 79

17. The pion form factor. 80

18. The J=1 $N\bar{N}\to\pi\pi$ amplitudes from twice subtracted dispersion relations 83

19. The two-pion contribution to the imaginary parts of the nucleon form factors. 85

20. Fit to the nucleon electric form factor . . . 88

21. Fit to the nucleon magnetic form factor . . . 89

22. The $N\bar{N}\to\pi\pi$ amplitude $q^{3/2}|\Gamma_1|$ 92

23. The $N\bar{N}\to\pi\pi$ amplitude $q^{3/2}|\Gamma_2|$ 93

24. The $N\bar{N}\to\pi\pi$ amplitude $q^{5/2}|f^2_{\pm}|$ 97

25. The $^1D_2$ phase shift 99

26. The $^1G_4$ phase shift 100

27. The $^3P_1$ phase shift 101

28. The $^3\bar{P}_2$ phase shift 102

29. The $^3\bar{F}_C$ phase shift 103

30. The $^3\bar{F}_T$ phase shift 104

31. The $^3\bar{F}_{LS}$ phase shift. 105

32. The $^3\bar{F}_2$ phase shift 106

33. The $^3F_3$ phase shift 107

34. The $^3\bar{F}_4$ phase shift 108

35. The $^1P_1$ phase shift 109

36. The $^1F_3$ phase shift 110

37. The $^3D_2$ phase shift 111

38. The $^3\bar{D}_3$ phase shift 112

39. The singlet even central potential 115

Figure

40. The trip

41. The T=1

42. The T=1

43. The lon

44. The sin

45. The trip

46. The T=0

47. The T=0

48. The lon

49. Imagina
reson

50. Meson-n

Figure Page

40. The triplet odd central potential 116

41. The T=1 tensor potential 117

42. The T=1 spin-orbit potential. 118

43. The long-range T=1 spin-orbit potential . . . 119

44. The singlet odd central potential 120

45. The triplet even central potential. 121

46. The T=0 tensor potential 122

47. The T=0 spin-orbit potential. 123

48. The long range T=0 spin-orbit potential . . . 124

49. Imaginary parts of the $N\bar{N}\to\pi\pi$ amplitudes Γ_i and resonance fits. 163

50. Meson-nucleon quark diagrams. 165

The de

nuclear force

physics resear

on expressions

better knowled

standing of nu

There

properties of

Although it is

determine the

a few paramet

introduce some

Phenomenologi

to isolate th

interest from

The t

interaction o

experimental

areas of part

enhance the k

INTRODUCTION

The desire to understand various aspects of the nuclear force is the motivation for a vast amount of physics research. Most nuclear physics calculations depend on expressions for the nucleon-nucleon interaction, and a better knowledge of this interaction may aid in the understanding of nuclei.

There have been many attempts to understand properties of the nuclear force from a fundamental approach. Although it is hoped that such an approach will eventually determine the nucleon-nucleon interaction in terms of only a few parameters, one is at present usually compelled to introduce some phenomenological content into a calculation. Phenomenological input to such calculations has been used to isolate the aspects of a problem which are of immediate interest from those not yet amenable to calculation.

The two-pion-exchange part of the nucleon-nucleon interaction offers an excellent opportunity to combine experimental information and theoretical ideas from several areas of particle physics. This unification will hopefully enhance the knowledge of each area.

Severa
order (in the
contribution
culation of th
Lomon[1] showed
Binstock[3] has
exchange poles
boson-exchang
culations is
except in the
ignored pion-
find that the
two-pion-exch

The d
lations of Am
amplitudes to
authors used
by which they
s-wave energy
scattering th
rescattering
p-wave ππ int
approach has
discussed by

Using
exchange Brow
in two respec

Several authors[1, 2] have calculated the fourth-order (in the πNN pseudoscalar interaction) perturbative contribution to nucleon-nucleon scattering. A recent calculation of the fourth-order potential by Partovi and Lomon[1] showed that this approach can be fairly successful. Binstock[3] has added the 4th-order amplitude to meson-exchange poles to obtain an improved version of the one-boson-exchange model. The obvious weakness of these calculations is that they ignored pion-pion interactions except in the sharp resonance approximation and usually ignored pion-nucleon rescattering. Nevertheless, we will find that the 4th-order contribution is the largest part of two-pion-exchange.

The dispersion-theoretic two-pion-exchange calculations of Amati, Leader, and Vitale[4] allowed the $N\bar{N}\to\pi\pi$ amplitudes to be included in a more realistic form. These authors used the Bowcock, Cottingham, Lurié[5] πN amplitudes, by which they included the fourth-order contribution, an s-wave energy-independent $\pi\pi$ interaction, and πN rescattering through (1) the Δ_{33} and (2) an effective rescattering constant. The calculations also included the p-wave $\pi\pi$ interaction via a rho-exchange pole. The ALV approach has also been used by Durso[6] and Kapadia,[7] and discussed by Signell.[8, 9]

Using the ALV dispersion treatment of two-pion-exchange Brown and Durso[10] have improved the calculation in two respects. First, they included a finite width

rho-exchange a

πNN coupling c

$N\bar{N}\to\pi\pi$ amplitu

In an

experimental

(NPP) continu

relations fro

region of the

amplitudes we

more reliable

mental determ

shift have sh

questionable.

has been used

exchange.[13,

Evalu

using the ππ

formed by Nie

Vinh Mau et a

use of these

of NPP appare

phase shift a

tudes were ca

I=J=0 ππ phas

phase shift i

ππ energy whe

exchange.

rho-exchange and, second, they introduced an axial-vector πNN coupling correction, consistent with PCAC,[11] into the $N\bar{N}\to\pi\pi$ amplitude.

In an attempt to determine the $N\bar{N}\to\pi\pi$ amplitudes from experimental input, Nielsen, Petersen, and Pietarien[12] (NPP) continued πN scattering amplitudes via dispersion relations from the πN physical region to the physical region of the two pions. As NPP pointed out, their p-wave amplitudes were in strong disagreement with the earlier, more reliable, results of Höhler et al. Recently, experimental determinations of the I=J=0 $\pi\pi$ scattering phase shift have shown that the s-wave $N\bar{N}\to\pi\pi$ NPP result is also questionable. Nevertheless, the NPP s-wave $N\bar{N}\to\pi\pi$ amplitude has been used in several recent calculations of two-pion-exchange.[13, 14]

Evaluations of the $N\bar{N}\to\pi\pi$ s- and p-wave amplitudes using the $\pi\pi$ phase shifts as input have recently been performed by Nielsen and Oades[15] and by Epstein and McKellar.[16] Vinh Mau et al.[14] and Epstein and McKellar[16] have shown that use of these newer $N\bar{N}\to\pi\pi$ s-wave amplitudes rather than that of NPP apparently results in somewhat poorer agreement with phase shift analysis. Both of these newer s-wave amplitudes were calculated using very similar forms for the I=J=0 $\pi\pi$ phase shift δ^{0}_{0} as input. As we shall see, this phase shift is not free of uncertainty, particularly at low $\pi\pi$ energy where it is of especial importance in two-pion-exchange.

In th

wave $N\bar{N}\to\pi\pi$ am

Omnès dispers

input, and us

begin with an

derived from

statements re

for fixed-t π

do not have k

from Mandelst

describe the

into the two-

describes the

discussion of

gives the res

and potential

Equat

units where $\hbar$

μ=1 and the r

required in M

the evaluatio

exchange we h

quoted masses

In this thesis we describe how the s-, p-, and d-wave $N\bar{N}\to\pi\pi$ amplitudes have been evaluated using subtracted Omnès dispersion relations with the $\pi\pi$ phase shifts as input, and used in the two-pion-exchange calculation. We begin with an elementary discussion of dispersion relations derived from analyticity assumptions followed by a few statements regarding the Mandelstam representation. Except for fixed-t πN dispersion relations, the relations we used do not have known field-theoretic proofs but all follow from Mandelstam analyticity. In the second chapter we describe the procedure for inputing the $N\bar{N}\to\pi\pi$ amplitudes into the two-pion-exchange calculation. The third chapter describes the evaluation of the $N\bar{N}\to\pi\pi$ amplitudes with a discussion of the $\pi\pi$ phase shift input. The fourth chapter gives the results for the two-pion-exchange phase shifts and potential. The appendices contain related matter.

Equations in this thesis are always written in units where $\hbar=c=1$. In most cases we also set the pion mass $\mu=1$ and the nucleon mass $m=6.7222$. Where the masses are required in MeV we used $\mu=139.576$ MeV, $m=938.259$ MeV. For the evaluation of the $N\bar{N}\to\pi\pi$ amplitudes and the NN two-pion-exchange we have assumed isospin invariance with the above quoted masses and $g^2_{\pi NN}/4\pi=14.6$.

A.

Apply

g(z) analytic

complex plane

If f(z) is a

no worse than

$$\left| \frac{f}{\prod_{k=1}^{N}} \right.$$

and, provided

contour can b

$$f(z)$$

$$\prod_{k=1}^{N} (z-$$

$$= \frac{1}{2}$$

I. DISPERSION RELATIONS

A. Single Variable Dispersion Relations from Analyticity

Applying Cauchy's integral theorem to a function g(z) analytic within a closed contour C in the upper half complex plane gives

$$g(z) = \frac{1}{2\pi i} \int_C \frac{g(z')}{z'-z}\, dz' . \qquad (I.1)$$

If f(z) is a function also analytic within C and diverging no worse than $|z|^{N-\eta}$ for positive N and η as $|z| \to \infty$ then

$$\left| \frac{f(z)}{\prod_{k=1}^{N} (z-z_k)} \right| \longrightarrow 0 \quad \text{as } |z| \to \infty , \qquad (I.2)$$

and, provided z_k are outside the original contour, the contour can be expanded to give

$$\frac{f(z)}{\prod_{k=1}^{N} (z-z_k)} = \frac{1}{2\pi i} \int_{-\infty}^{\infty} \frac{f(z')}{(z'-z)\prod_{k=1}^{N} (z'-z_k+i\delta)}\, dz'$$

$$= \frac{1}{2} \sum_r \frac{f(z_r)}{(z-z_r)\prod_{k\neq r}(z_r-z_k)} + \frac{1}{2\pi i} P \int_{-\infty}^{\infty} \frac{f(z')\,dz'}{(z'-z)\prod_{k=1}^{N} (z'-z_k)} , \qquad (I.3)$$

where the firs

on the real a

Now l

$z \to z+i\varepsilon$ and le

$$\frac{f(z)}{\prod_k (z-z_k)}$$

$$f(z) =$$

The real part

relation with

$$f(z) =$$

where the first term in the last line is a sum over poles on the real axis.

Now letting z approach the real axis by writing $z \to z+i\varepsilon$ and letting $\varepsilon \to 0+$ we obtain

$$\frac{f(z)}{\prod_k (z-z_k)} = \frac{1}{2}\sum_r \frac{f(z_r)}{(z-z_r)\prod_{k\neq r}(z_r-z_k)} + \frac{1}{2}\frac{f(z)}{\prod_k (z-z_k)}$$

$$+ \frac{1}{2\pi i} P\int_{-\infty}^{\infty} \frac{f(z')}{(z'-z)\prod_k (z'-z_k)}\, dz' , \qquad \text{(I.4)}$$

$$f(z) = \sum_r \frac{\prod_{k\neq r}(z-z_k)}{\prod_{k\neq r}(z_r-z_k)} f(z_r)$$

$$+ \frac{\prod_k (z-z_k)}{\pi i}\int_{-\infty}^{\infty} \frac{f(z')\,dz'}{(z'-z)\prod_k (z'-z_k)} . \qquad \text{(I.5)}$$

The real part of this equation gives the usual dispersion relation with N subtractions:

$$f(z) = \sum_r \frac{\prod_{k\neq r}(z-z_k)}{\prod_{k\neq r}(z_r-z_k)} f(z_r)$$

$$+ \frac{\prod_k (z-z_k)}{\pi}\int_{-\infty}^{\infty} \frac{\mathrm{Im}\, f(z')\, dz'}{(z'-z)\prod_k (z'-z_k)} . \qquad \text{(I.6)}$$

For N=

axis the dispe

$$f(z)$$

$$+$$

Letti

of the twice

$$f(z) = f($$

$$+ \frac{(z}{}$$

In (I.6, 7,

integrand de

to properly

following po

1. It w

parts of f(z

upper half p

2. Anal

plane.

3. It w

real axis.

For N=2 with both subtraction points on the real axis the dispersion relation takes the form

$$f(z) = \frac{(z-z_2)}{(z_1-z_2)} f(z_1) + \frac{(z-z_1)}{(z_2-z_1)} f(z_2)$$

$$+ \frac{(z-z_1)(z-z_2)}{\pi} \int_{-\infty}^{\infty} \frac{Im\, f(z')\, dz'}{(z'-z)(z'-z_1)(z'-z_2)} . \quad (I.7)$$

Letting z_2 approach z_1 gives a commonly used form of the twice subtracted relation:

$$f(z) = f(z_1) + (z-z_1) \frac{\partial}{\partial z'} f(z') \Big|_{z'=z_1}$$

$$+ \frac{(z-z_1)^2}{\pi} \int_{-\infty}^{\infty} \frac{Im\, f(z')\, dz'}{(z'-z)(z'-z_1)^2} . \quad (I.8)$$

In (I.6, 7, 8) it is understood that each factor in the integrand denominators has a small negative imaginary part to properly reproduce the imaginary part of f(z). The following points are emphasized:

1. It was necessary that both the real and imaginary parts of f(z) behave no worse than $|z|^{N-\eta}$ as $|z| \to \infty$ in the upper half plane.

2. Analyticity was assumed only in the upper half plane.

3. It was not actually necessary to let z approach the real axis. Thus, the dispersion relation (I.6) can be used

to continue f

sider the uns

$$f(z) =$$

The real part

$$\operatorname{Re} f(z) =$$

Because the

upper half p

$$\frac{1}{2\pi}\int_{-\infty}^{\infty}$$

Combining wi

$$\operatorname{Re} f(z)$$

As in (I.11)

to continue f(z) into the complex plane. For example, consider the unsubtracted version of (I.3).

$$f(z) = \frac{1}{2\pi i} \int_{-\infty}^{\infty} \frac{f(z')}{(z'-z)} \, dz' \, . \qquad \text{(I.9)}$$

The real part of f(z) is

$$\mathrm{Re}\, f(z) = \frac{1}{2\pi} \int_{-\infty}^{\infty} \frac{\mathrm{Im}\, f(z')(z'-\mathrm{Re}\, z) + \mathrm{Re}\, f(z')\, \mathrm{Im}\, z}{(z'-z)(z'-z^*)} \, dz' \, . \qquad \text{(I.10)}$$

Because the integration can be considered as around the upper half plane, the last term in the numerator gives

$$\frac{1}{2\pi} \int_{-\infty}^{\infty} \frac{\mathrm{Re}\, f(z')\, \mathrm{Im}\, z}{(z'-z)(z'-z^*)} \, dz' = \frac{1}{2} \mathrm{Re}\, f(z) \, . \qquad \text{(I.11)}$$

Combining with (I.10) we find

$$\mathrm{Re}\, f(z) = \frac{1}{\pi} \int_{-\infty}^{\infty} \frac{\mathrm{Im}\, f(z')\, \mathrm{Im}\, z}{(z'-z)(z'-z^*)} \, dz' \, . \qquad \text{(I.12)}$$

As in (I.11) one can show that

$\mathrm{Im}\, f(z) =$

Adding (I.12)

version of (I

$$f(z)$$

In pr

discontinuiti

provided the

rapidly one r

singularities

dispersion in

$$\frac{\prod_{k=1}^{N} (z-$$

$$\pi$$

If L is much

z_k then we m

$$\mathrm{Im}\, f(z) = \frac{1}{\pi}\int_{-\infty}^{\infty} \frac{\mathrm{Im}\, f(z')\, \mathrm{Im}\, z}{(z'-z)(z'-z^*)}\, dz' . \qquad \text{(I.13)}$$

Adding (I.12) and i times (I.1e) gives the unsubtracted version of (I.6):

$$f(z) = \frac{1}{\pi}\int_{-\infty}^{\infty} \frac{\mathrm{Im}\, f(z')}{z'-z}\, dz' . \qquad \text{(I.14)}$$

In practical calculations ones knowledge about the discontinuities, 2Imf(z), is limited. Nevertheless, provided the dispersion integral converges sufficiently rapidly one may find it useful to include only the "nearby" singularities. Consider the large z' contribution to the dispersion integral in (I.6),

$$\frac{\prod_{k=1}^{N}(z-z_k)}{\pi}\int_{L}^{\infty} \frac{\mathrm{Im}\, f(z')\, dz'}{(z'-z)\prod_{k=1}^{N}(z'-z_k)} . \qquad \text{(I.15)}$$

If L is much greater than z and all the subtraction points z_k then we may expand (I.15) as follows:

$$\frac{\prod(z-z_k}{\pi}$$

$$= \frac{\prod(z-z}{\pi}$$

Applying (I.

Im f

where f_o is

For L<z<L' w

Im f

where f_1 is

An u

$$\frac{\prod_{k=1}^{N}(z-z_k}{\pi}$$

Thus, the do
dispersion
polynomial.

The
later is ba

$$\frac{\Pi(z-z_k)}{\pi}\int_L^\infty \frac{Im\, f(z')\, dz'}{(z')^{N+1}\left(1-\frac{z}{z'}\right)\Pi\left(1-\frac{z_k}{z'}\right)}$$

$$= \frac{\Pi(z-z_k)}{\pi}\int_L^\infty \frac{Im\, f(z')}{(z')^{N+1}}\left\{1+\frac{z+\Sigma z_k}{z'}+\cdots\right\}dz'. \quad \text{(I.16)}$$

Applying (I.2) for $z \geq L'$, where $L' \geq L$, we have

$$Im\, f(z) \leq f_o\, z^{N-\eta} \quad , z \geq L' \quad \text{(I.17)}$$

where f_o is a constant.

For $L<z<L'$ we define an upper bound on Imf(z) as

$$Im\, f(z) \leq f_1 \quad , L < z < L' \quad \text{(I.18)}$$

where f_1 is a constant.

An upper limit to (I.15) is, therefore,

$$\frac{\prod_{k=1}^{N}(z-z_k)}{\pi}\left\{\frac{f_o}{\eta L^\eta}+\frac{f_1}{NL^N}\left[1-\left(\frac{L}{L'}\right)^N\right]+O\left(\frac{z+\Sigma z_k}{L}\right)\right\} \quad \text{(I.19)}$$

Thus, the dominant contribution neglected by terminating the dispersion integral at $z'=L$ is, for $L>>z,z_k$, an Nth order polynomial.

The two-pion-exchange calculation to be described later is based on an unsubtracted dispersion relation where

the variable

contribution

expected to b

primarily to

B

The t

Mandelstam[17]

than the one

discussed.

We ma

Then the vari

are the baryo

channels, re

Mand

in s, t, and

required by

relation has

required

the variable of integration is the momentum transfer. The contribution from the neglected distant singularities is expected to be approximately constant and to contribute primarily to the low NN partial waves.

B. Two Dimensional Representation

The two dimensional representation introduced by Mandelstam[17] in 1958, provides considerably more information than the one dimensional dispersion relations which we have discussed.

We may consider the 2→2 process shown in Figure 1. Then the variables

$$s = -(p_1 - n_1)^2 ,$$

$$t = -(p_1 - p_2)^2 , \qquad \text{(I.20)}$$

$$u = -(p_1 - n_2)^2$$

are the barycentric energies squared in the s-, t-, u-channels, respectively.

Mandlestam postulated that the only singularities in s, t, and u of a properly chosen amplitude are those required by unitarity. The two-dimensional dispersion relation has the following form if no subtractions are required

t-channel →

Figure

channels

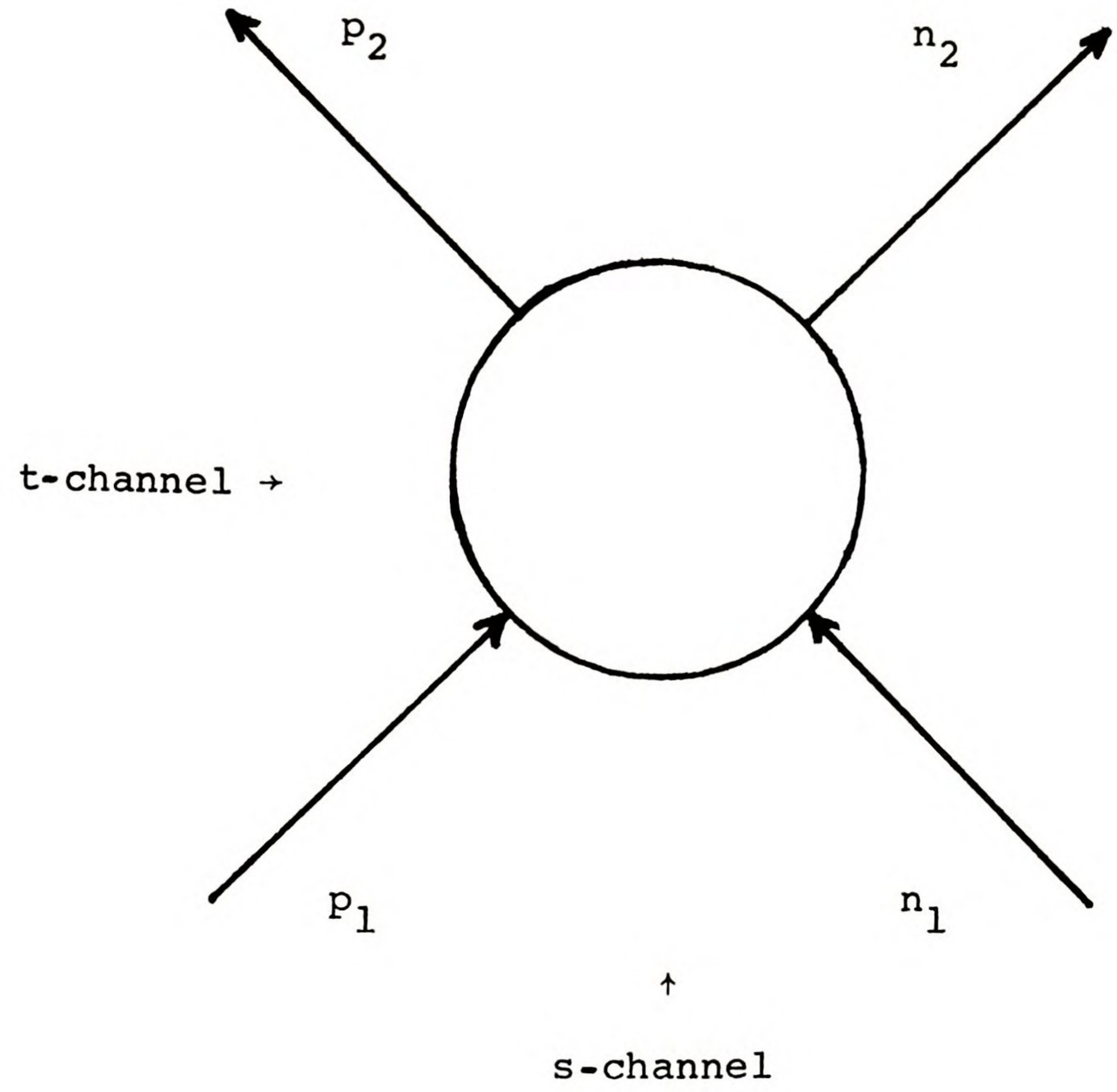

Figure 1. The momentum labels and scattering channels for two-body scattering.

$$A(s,t,u) = \frac{1}{\pi}$$

$$+ \frac{1}{\pi}$$

$$+ \frac{1}{\pi}$$

$$+ \frac{1}{\pi}$$

It is unders
small negati
real and the
are at least
realizable s

As a
particles of
$\rho_{st}(st)$ is n
s and t are

The
obtained by
lowest mass
The boundary

$$A(s,t,u) = \frac{1}{\pi}\int ds' \frac{\rho_s(s')}{s'-s} + \frac{1}{\pi}\int dt' \frac{\rho_t(t')}{t'-t}$$

$$+ \frac{1}{\pi}\int du' \frac{\rho_u(u')}{u'-u}$$

$$+ \frac{1}{\pi^2}\int ds' \int dt' \frac{\rho_{st}(s't')}{(s'-s)(t'-t)}$$

$$+ \frac{1}{\pi^2}\int ds' \int du' \frac{\rho_{su}(s'u')}{(s'-s)(u'-u)}$$

$$+ \frac{1}{\pi^2}\int dt' \int du' \frac{\rho(t'u')}{(t'-t)(u'-u)} \quad . \qquad \text{(I.21)}$$

It is understood that each factor in the denominators has a small negative imaginary part. The spectral functions are real and they are nonvanishing only when their arguments are at least as large as the mass squared of a physically realizable system.

As an example consider the scattering of two particles of equal mass. The double spectral function $\rho_{st}(st)$ is nonvanishing only in a restricted region where s and t are both greater than $(2m)^2$.

The boundary of the double spectral region is obtained by considering the Feynman diagram involving the lowest mass intermediate states in the s and t channels. The boundary (Figure 2) is found to be $st-4m^2(s+t)+4m^4=0$.

Figu

equa

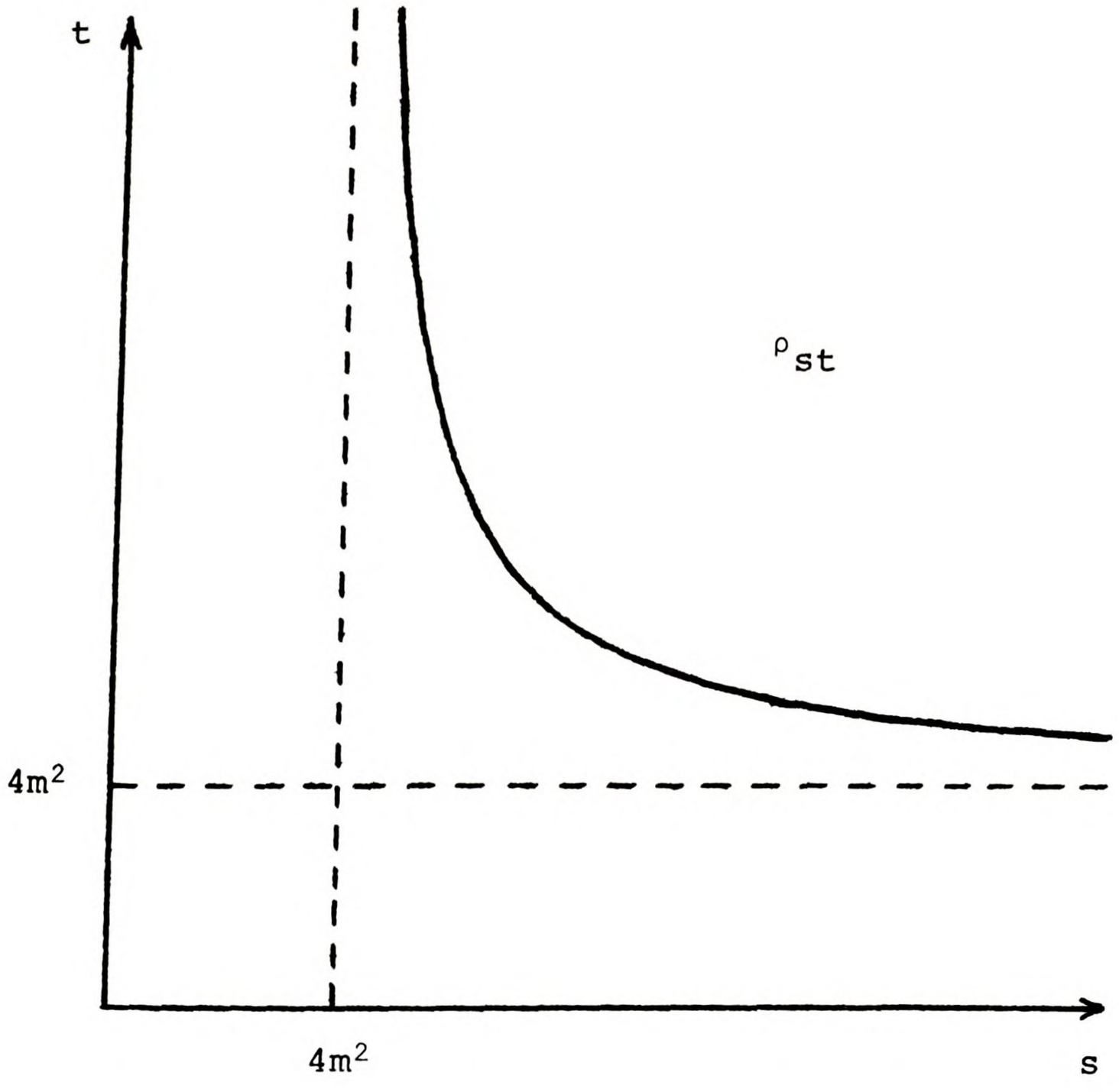

Figure 2. The double spectral region for equal-mass scattering.

The double sp
singularity a
identicle bos
and the three

The M
valid for an
ities, which
intermediate
because it ca
of analyticit
However, the
theory for ar
Mandelstam,[17]
representatio
sional repres
approximation

We ma
only the doub
In particular
or u. The s-
imaginary par
denominator s

$$\frac{1}{s'-s-i\varepsilon} \to P \frac{1}{s'-s} + i\pi\delta(s'-s)$$

absorptive pa

The double spectral function ρ_{st} has an inverse square root singularity along this boundary. If the two particles are identicle bosons the amplitude is symmetric in s, t, and u and the three double spectral functions are identical.

The Mandelstam representation is expected to be valid for an amplitude which has only dynamical singularities, which are due to the presence of real, on-mass-shell intermediate states. The representation is very attractive because it can incorporate the important physical principles of analyticity, crossing symmetry and Lorentz covariance. However, the representation has not been proven from field theory for any process. It has been shown, originally by Mandelstam,[17] that the 4th-order diagrams do satisfy the representation. Furthermore, all uses of the two dimensional representation have been in a "nearest singularities" approximation.

We may now reduce equation (I.21) (we shall consider only the double-spectral distributions) to one-dimension. In particular we may write down relations for fixed s, t, or u. The s-channel absorptive part is defined by the imaginary part of A(s,t,u) in the s-channel where only the denominator s'-s may vanish. Then with the prescription $\frac{1}{s'-s-i\varepsilon} \to P\,\frac{1}{s'-s} + i\pi\delta(s'-s)$ we write the s-channel absorptive part as

$$A_s(s,t,u)$$

Similarly th

$$A_t(s,t,u) =$$

$$A_u(s,t,u) =$$

The

have the fol

$$A(s$$

A(

A(

$$A_s(s,t,u) = \frac{1}{\pi}\int_{t_s} dt' \frac{\rho_{st}(s\,t')}{t'-t} + \frac{1}{\pi}\int_{u_s} du' \frac{\rho_{su}(s\,u')}{u'-u} . \quad \text{(I.22a)}$$

Similarly the t- and u-channel absorptive parts are

$$A_t(s,t,u) = \frac{1}{\pi}\int_{s_t} ds' \frac{\rho_{st}(s't)}{s'-s} + \frac{1}{\pi}\int_{u_t} du' \frac{\rho_{tu}(t\,u')}{u'-u} , \quad \text{(I.22b)}$$

$$A_u(s,t,u) = \frac{1}{\pi}\int_{s_u} ds' \frac{\rho_{su}(s'u)}{s'-s} + \frac{1}{\pi}\int_{t_u} dt' \frac{\rho_{tu}(t'u)}{t'-t} . \quad \text{(I.22c)}$$

The fixed s, t, and u dispersion relations then have the following forms:

$$A(s,t,u) = \frac{1}{\pi}\int_{t_s} dt' \frac{A_t(s,t',u''(s,t'))}{t'-t} + \frac{1}{\pi}\int_{u_s} du' \frac{A_u(s,t''(s,u'),u')}{u'-u} , \quad \text{(I.23a)}$$

$$A(s,t,u) = \frac{1}{\pi}\int_{s_t} ds' \frac{A_s(s',t,u''(s',t))}{s'-s} + \frac{1}{\pi}\int_{u_t} du' \frac{A_u(s''(t,u'),t,u')}{u'-u} , \quad \text{(I.23b)}$$

$$A(s,t,u) = \frac{1}{\pi}\int_{s_u} ds' \frac{A_s(s',t''(s',u),u)}{s'-s} + \frac{1}{\pi}\int_{t_u} dt' \frac{A_t(s''(t',u),t',u)}{t'-t} . \quad \text{(I.23c)}$$

we have intro

In va

distinguish b

the first cas

$$\frac{1}{s'-s}$$

leads quickly

The

be surprisin

ables. The

integration

we merely re

-dt" and tha

$$A(s,t,u)$$

The lower li

s. These tw

cuts of A as

As a

cases be sim

have seen is

$$\pm A_u(u,t,s),$$

we have introduced the notation $u''(s,t') \equiv \Sigma m_i^2 - s - t'$, etc.

In varifying these relations one must be careful to distinguish between primed and unprimed arguments. Then in the first case, for example, the identity

$$\frac{1}{s'-s}\left[\frac{1}{t'-t}+\frac{1}{u'-u}\right] = \frac{-1}{(t'-t)(u'-u)}$$

leads quickly back to equation (I.21).

The form of the one-dimensional representations may be surprising in that each involves two integration variables. The equations may, however, easily be cast in one integration variable. For the fixed-s dispersion relation we merely realize that $t''(s,u') = \Sigma m_i^2 - s - u'$ implies $du' = -dt''$ and that $u'-u = -(t''-t)$. Then we can write

$$A(s,t,u) = \frac{1}{\pi}\int_{t_s}^{\infty} dt' \; \frac{A_t(s,t',u''(s,t'))}{t'-t}$$

$$+ \frac{1}{\pi}\int_{t(s,u_s)}^{-\infty} dt' \; \frac{A_u(s,t',u''(s,t'))}{t'-t} \quad . \tag{I.24}$$

The lower limit of the second integral is now a function of s. These two terms correspond to the right- and left-hand cuts of A as a function of t at fixed s.

As already mentioned the forms (I.23) may in some cases be simplified by crossing symmetry. An example we have seen is πN scattering where one may write $A_s(s,t,u) = \pm A_u(u,t,s)$, the sign depending on the isospin state being

considered.

written

$$A(s,t,u) =$$

The

spectral req

scalar natur

only an odd

similarly fo

Figure 3. T

$s=(m+2\mu)^2$, t

at $s=(m+\mu)^2$

in Figure 4

5.

considered. The fixed-t dispersion relation can then be written

$$A(s,t,u) = \frac{1}{\pi}\int_{(m+\mu)^2}^{\infty} ds' \, A_s(s',t,u''(s',t))\left[\frac{1}{s'-s} \pm \frac{1}{s'-u}\right] .$$

The diagrams determining the πN scattering double spectral region boundaries are complicated by the pseudoscalar nature of the pion, which disallows vertices having only an odd number of pions. The boundary for ρ_{st} and similarly for ρ_{ut} is determined by the two diagrams in Figure 3. The diagram in Figure 3a has branch cuts at $s=(m+2\mu)^2$, $t=4\mu^2$ while the diagram in Figure 3b has cuts at $s=(m+\mu)^2$, $t=16\mu^2$. The double spectral regions are shown in Figure 4 and dynamical singularities are shown in Figure 5.

Figu

N

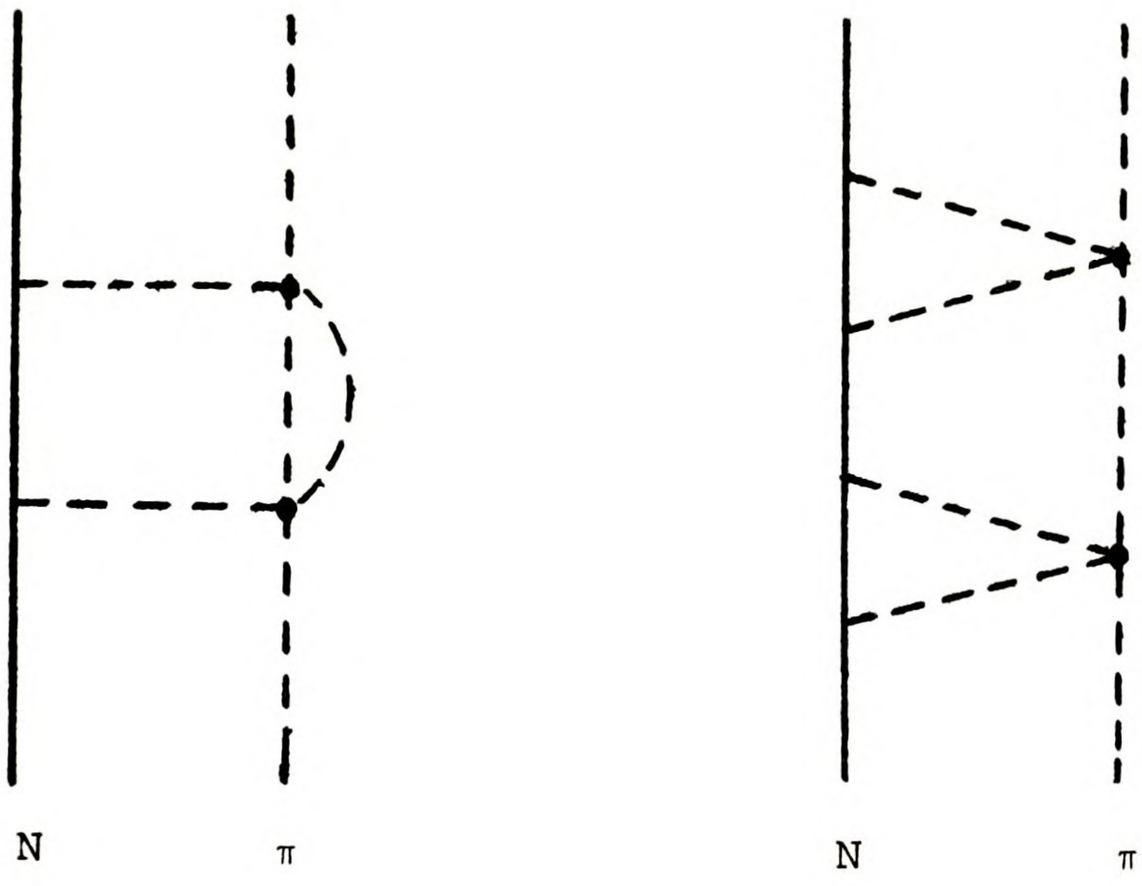

(a) (b)

Figure 3. Low order πN scattering diagrams.

Figure
spectr

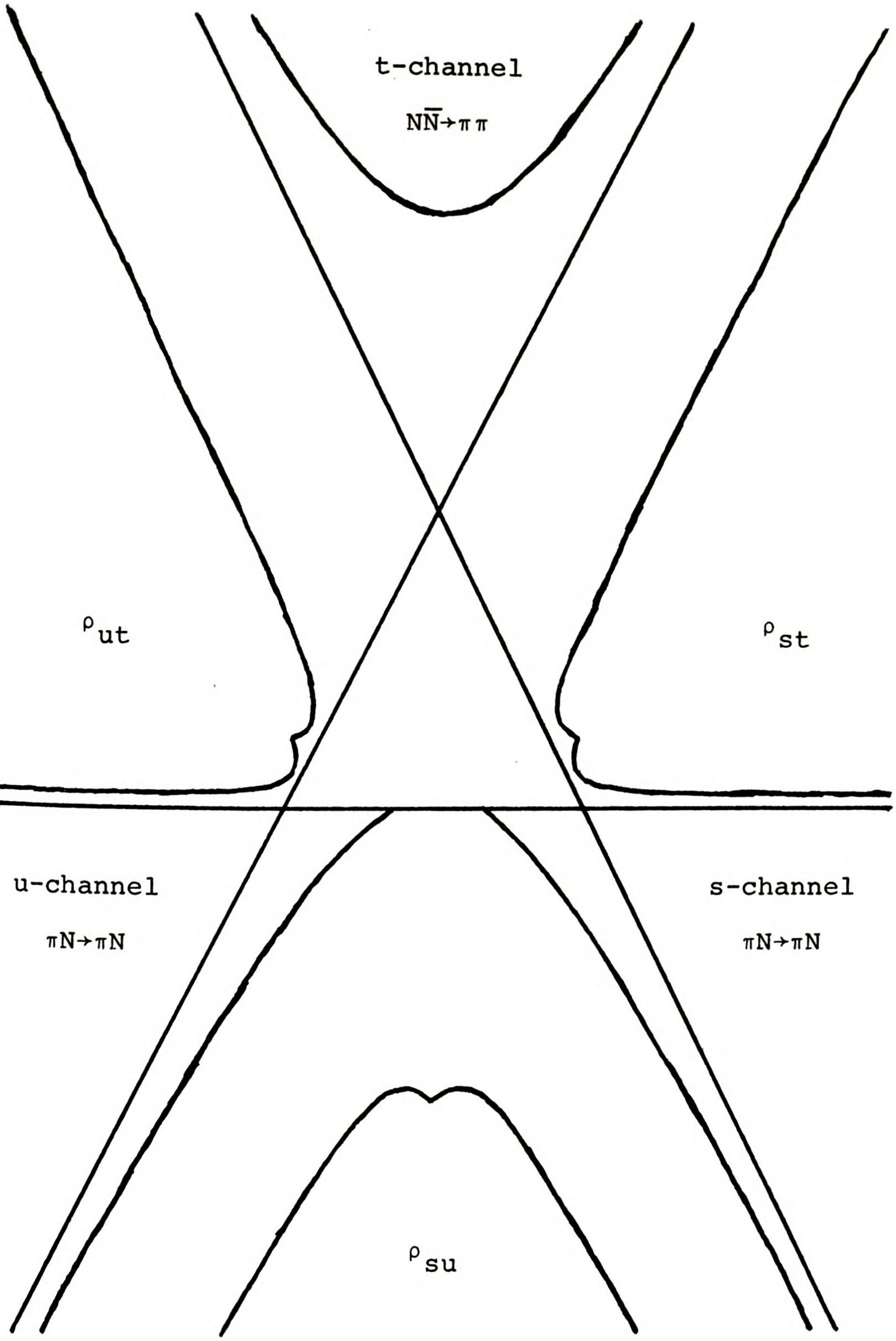

Figure 4. The πN physical regions and double spectral regions.

Figure 5.

scatterin

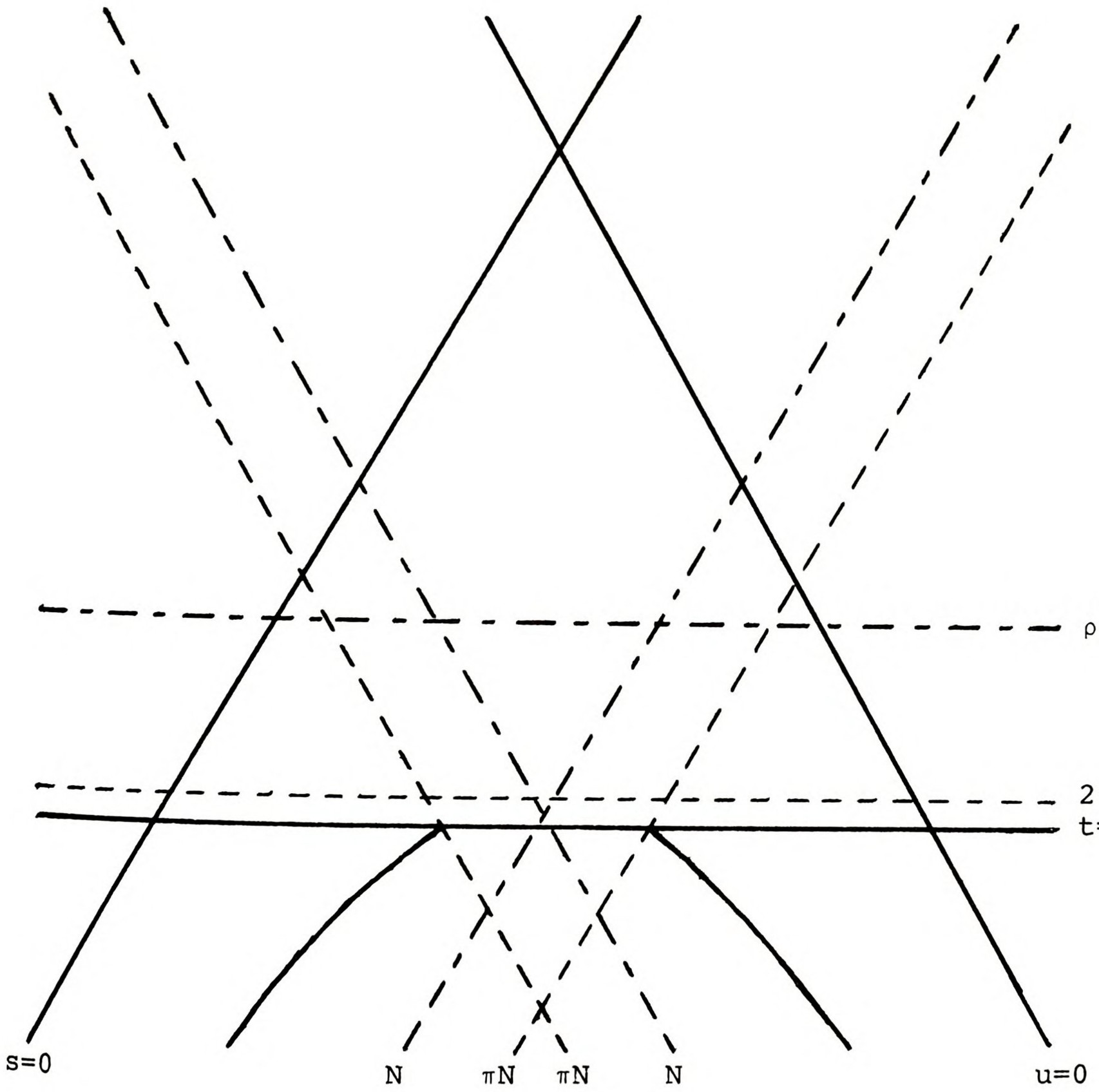

Figure 5. The Mandelstam diagram for pion-nucleon scattering.

Th

pion-excha

For comple

nology the

including

Th

Figure 1.

which are

angle θ, e

II. TWO-PION-EXCHANGE FORMALISM

A. The Dispersion Theoretic Approach

The basic dispersion theoretic treatment of two-pion-exchange is described in the literature.[4,7,8,9,13,14] For completeness and to establish the notation and terminology the formalism is repeated here. The procedure for including the $N\bar{N}\to\pi\pi$ d-wave amplitudes is also introduced.

The nucleon four-momenta are labelled as in Figure 1. The Mandelstam variables are defined by

$$w = -(p_1+n_1)^2 \ ,$$

$$t = -(n_1-n_2)^2 \ , \qquad \text{(II.1)}$$

$$\bar{t} = -(p_1-n_2)^2 \ ,$$

which are written in terms of the center of mass scattering angle θ, energy per particle E, and momentum p as

$$w = 4E^2 = 4(p^2+m^2) \ ,$$

$$t = -2p^2(1-\cos\theta) \ , \qquad \text{(II.2)}$$

$$\bar{t} = -2p^2(1+\cos\theta) \ .$$

As usual,

the sum of

We define

and the se

which have

As usual, the sum of the Mandelstam variables is equal to the sum of the squares of the external masses.

$$w+t+\bar{t} = 4m^2 \qquad \text{(II.3)}$$

We define the four-vectors

$$\begin{aligned} N &= (n_1+n_2)/2 \ , \\ P &= (p_1+p_2)/2 \ , \\ \Delta &= (p_2-p_1) = (n_1-n_2) \ , \end{aligned} \qquad \text{(II.4)}$$

and the set of orthogonal four vectors

$$\begin{aligned} M &= N+P \ , \\ K &= N-P \ , \\ &\Delta \ , \\ L_\lambda &= \varepsilon_{\lambda\mu\nu\rho} M_\mu K_\nu \Delta_\rho \ , \end{aligned} \qquad \text{(II.5)}$$

which have moduli given by

$$\begin{aligned} N^2 &= P^2 = -1/4(w+\bar{t}) \ , \\ M^2 &= -w \ , \\ K^2 &= -\bar{t} \\ \Delta^2 &= -t \ , \\ L^2 &= -wt\bar{t} \ . \end{aligned} \qquad \text{(II.6)}$$

Th

terms of

$$S_{fi} =$$

Th

$$\mathcal{M}_{fi} =$$

M_{fi} is a

The Dirac

Th

expressed

$$P$$
$$P$$
$$P$$
$$P$$
$$P$$

and the p

Then

$$\mathcal{M}$$

Now the l

satisfy t

The invariant amplitude M_{fi} for NN→NN is defined in terms of the S-matrix by

$$S_{fi} = \delta_{fi} + i\,\delta^4(p_2+n_2-p_1-n_1)\left[\frac{m^4}{(2\pi)^4 E_{p_1}E_{n_1}E_{p_2}E_{n_2}}\right]^{1/2}\mathcal{M}_{fi}\,. \tag{II.7}$$

The amplitude M is defined by

$$\mathcal{M}_{fi} = \bar{u}(p_2)\,\bar{u}(n_2)\,\mathcal{M}\,u(p_1)\,u(n_1)\,. \tag{II.8}$$

M_{fi} is a matrix in the isospin space of the two nucleons. The Dirac algebra is defined in Appendix E.

The spin and isospin structure of M is conveniently expressed in terms of the spin operators

$$\begin{aligned} P_1 &= 1\,,\\ P_2 &= i\left(\gamma^{(2)}\cdot P + \gamma^{(1)}\cdot N\right),\\ P_3 &= -\gamma^{(1)}\cdot N\,\gamma^{(2)}\cdot P\,,\\ P_4 &= \gamma^{(1)}\cdot\gamma^{(2)}\,,\\ P_5 &= \gamma_5^{(1)}\,\gamma_5^{(2)}\,, \end{aligned} \tag{II.9}$$

and the Pauli isospin matrices.

Then

$$\mathcal{M} = \sum_{k=1}^{5}\left[3p_k^+(wt\bar{t}) + 2p_k^-(wt\bar{t})\,\tau^{(1)}\cdot\tau^{(2)}\right]P_k\,. \tag{II.10}$$

Now the longer range contributions to p_k^+ are assumed to satisfy the dispersion relation

$P_k^+(wt\bar{t}$

where the

$P_k^+(OPE)$

Th

branch cut

Figure 6.

sponding t

the other

we will la

amplitude

Th

cuts in (

process NN

two pions

and illus

$$P_k^{\pm}(wt\bar{t}) = P_k^{\pm}(OPE) + \frac{1}{\pi}\int_4^{\infty} dt' \, \frac{\rho_k'^{\pm}(wt'\bar{t})}{t'-t} \, , \qquad \text{(II.11)}$$

where the one-pion-exchange contribution is

$$P_k^{+}(OPE) = 0 \quad , \quad P_k^{-}(OPE) = \frac{g^2}{2(t-1)} \delta_{k5} \, . \qquad \text{(II.12)}$$

The integration in (II.11) begins at the two pion branch cut, clearly seen in the Mandelstam diagram in Figure 6. One sees that there are in fact two cuts corresponding to the two pion state, one beginning at t=4 and the other at $\bar{t}$=4. For now we include only the cut in t but we will later retrieve the other by antisymmetrizing the amplitude.

The two pion cut is isolated from the more distant cuts in (II.11) by applying unitarity for the t-channel process $N\bar{N} \to N\bar{N}$ and restricting the intermediate states to two pions. The kinematics in the $N\bar{N}$ channel are defined by

$$p = p^2 \, ,$$

$$p' = -p_1 \, ,$$

$$n = n_1 \, , \qquad \text{(II.13)}$$

$$n' = -n_2 \, ,$$

$$Q = (q-q')/2 \qquad \text{(II.14)}$$

and illustrated in Figure 7.

ρ

2π

t-channel

$N\bar{N}\to N\bar{N}$

Figure 6.

scattering

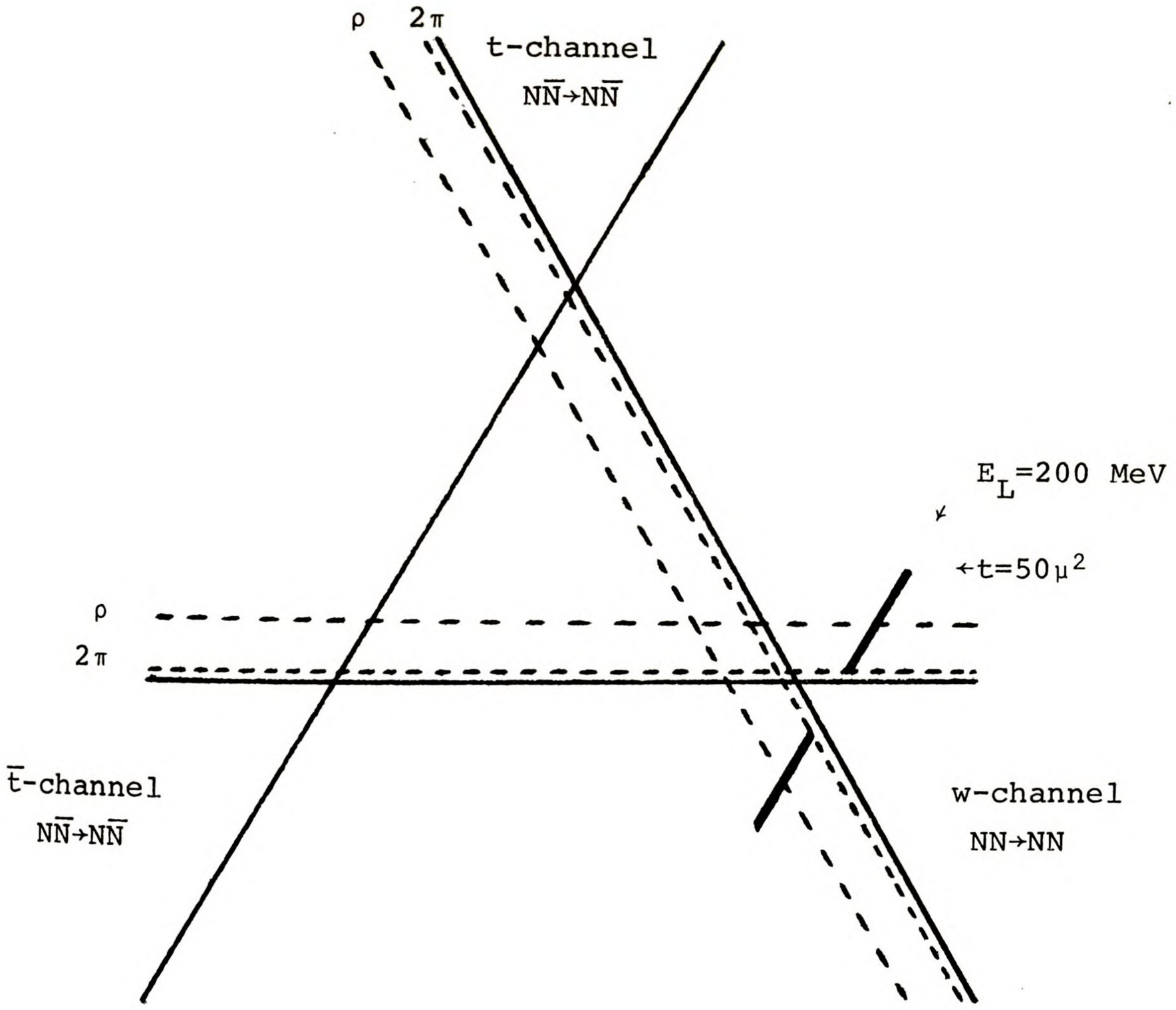

Figure 6. Mandelstam diagram for nucleon-nucleon scattering.

Figure

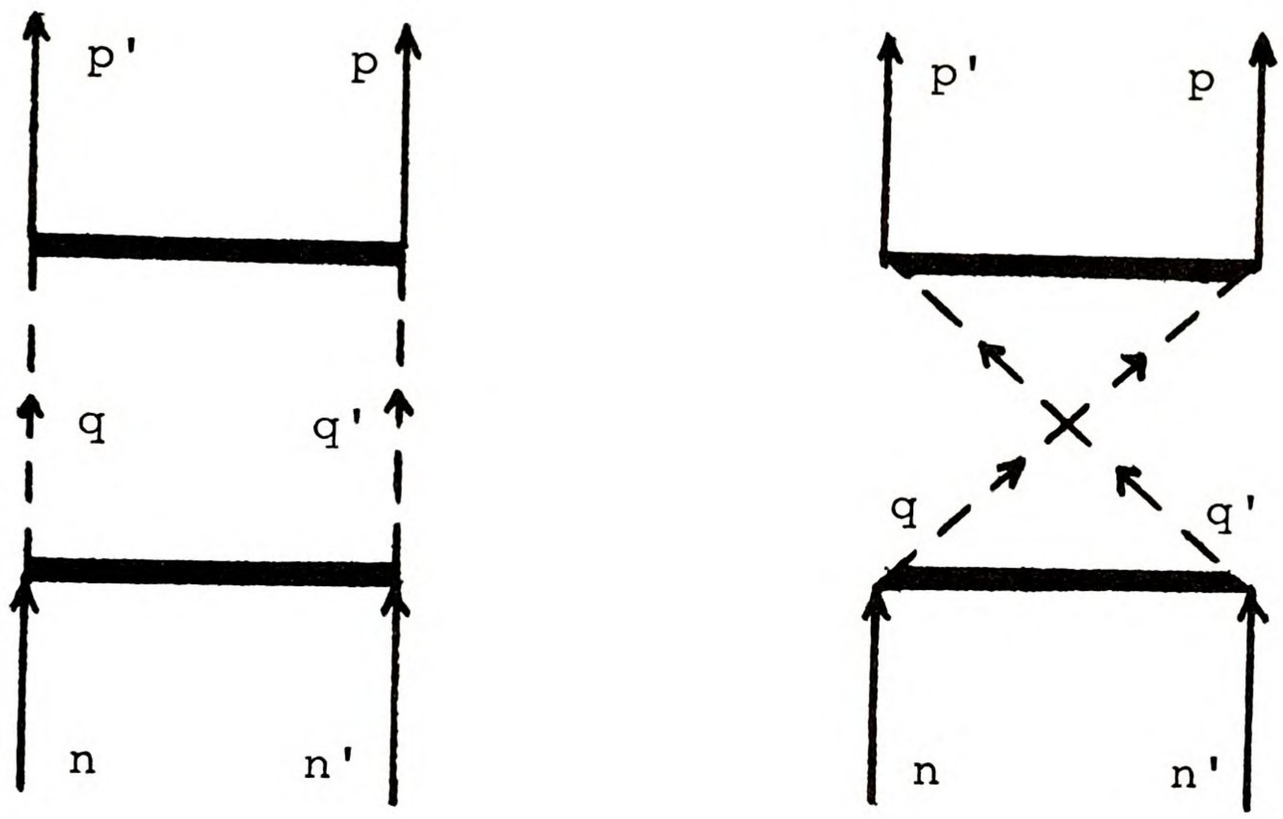

(a) (b)

Figure 7. The t-channel diagrams for $N\bar{N}\to\pi\pi\to N\bar{N}$.

Th

momenta a

notation.

Th

$$:[m$$

$$\frac{1}{\sigma}$$

where n_j

ω_j and $\prod_{(n}$

particles

volume, a

counting

(conventi

is

$$i < N\bar{N}$$

x

x

where α,β

T

of the $N\bar{N}$

far belo

continua

The nucleons have momenta n,p while the antinucleon momenta are n',p'. Note the minor deviation from the ALV notation.

The unitarity relation for M reads[19]

$$i[\mathcal{M}^{\dagger}_{fi} - \mathcal{M}_{fi}] =$$

$$\frac{1}{\sigma}\sum_{(n)}(2\pi)^4\delta^4(P_f - P_n)\left(\prod_{(n)}\frac{n_j}{V}\right)\mathcal{M}^{\dagger}_{fn}\,\mathcal{M}_{ni}, \qquad \text{(II.15)}$$

where $n_j = \frac{1}{2\omega_j}$ for intermediate state bosons with energy ω_j and $\prod_{(n)}\frac{n_j}{V}$ means to include only the intermediate state particles in the product. Of course V is the quantization volume, and σ is a statistical factor to avoid multiple counting in the sum. Designating the $N\bar{N}\to\pi\pi$ amplitude by T (convention), the two-pion intermediate state contribution is

$$i\langle N\bar{N}|\mathcal{M}^{\dagger}-\mathcal{M}|N\bar{N}\rangle = \frac{1}{2}\sum_{\alpha,\beta}\frac{1}{(2\pi)^2 t}\int d^3q\int d^3q'$$

$$\times\langle N\bar{N}|T^{\dagger}|\pi_\alpha(q)\pi_\beta(q')\rangle\langle\pi_\alpha(q)\pi_\beta(q')|T|N\bar{N}\rangle$$

$$\times\,\delta^4(n+n'-q-q'). \qquad \text{(II.16)}$$

where α,β are the pion isospin indices.

The usefulness of (II.16) depends on a continuation of the $N\bar{N}\to N\bar{N}$ unitarity relation from the physical region to far below physical threshold.[9] The possibility of such a continuation follows from the assumption of Mandelstam

analyticit

indicates

to be rela

points bel

of the dou

Th

tude is g

$\langle \pi_\alpha \pi$

and T

The ampli

variables

In the $N\bar{N}$

momenta a

analyticity. Furthermore, the Mandelstam representation indicates how the quantities $\langle\pi\pi|T|N\bar{N}\rangle$ and $\langle N\bar{N}|T^{\dagger}|\pi\pi\rangle$ are to be related after continuing across the various branch points below the $N\bar{N}$ threshold, provided one remains outside of the double spectral regions.

The spin and isospin structure of the $N\bar{N}\to\pi\pi$ amplitude is given by CGLN[20]:

$$\langle\pi_\alpha\pi_\beta|T|N\bar{N}\rangle = \delta_{\alpha\beta}T^{(+)} + \tfrac{1}{2}[\tau_\beta,\tau_\alpha]T^{(-)} \qquad \text{(II.17)}$$

and

$$T^{(\pm)} = -A^{(\pm)} + i\gamma\cdot Q\,B^{(\pm)} . \qquad \text{(II.18)}$$

The amplitudes $A^{(\pm)}$ and $B^{(\pm)}$ are functions of the Mandelstam variables for πN scattering defined as

$$\begin{aligned} s_n &= -(n-q)^2 , \\ u_n &= -(n-q')^2 , \\ s_p &= -(p-q')^2 , \\ u_p &= -(p-q)^2 , \\ t_p &= t_n = t = -(n+n')^2 = -(p+p')^2 . \end{aligned} \qquad \text{(II.19)}$$

In the $N\bar{N}$ c.m. frame the magnitudes of the nucleon and pion momenta are given by

$$\begin{aligned} p^2 &= t/4-m^2 , \\ q^2 &= t/4-1 . \end{aligned} \qquad \text{(II.20)}$$

The c.m.

so that

will make

apparent

From (II.

The c.m. frame scattering angles are

$$\cos\theta_n = \frac{s_n - u_n}{4pq_b}, \qquad \cos\theta_p = \frac{s_p - u_p}{4pq_b}, \tag{II.21}$$

so that

$$\begin{aligned} s_n &= -(p^2+q_b^2-2pq_b\cos\theta_n), \\ u_n &= -(p^2+q_b^2+2pq_b\cos\theta_n), \\ s_p &= -(p^2+q_b^2-2pq_b\cos\theta_p), \\ u_p &= -(p^2+q_b^2+2pq_b\cos\theta_p), \\ t &= 4(p^2+m^2) = 4(q_b^2+1). \end{aligned} \tag{II.22}$$

Before introducing these variables into (II.16) we will make the inclusion of both diagrams in Figure 7 more apparent by writing

$$\rho_k'^{(t)}(wt\bar{t}) = \rho_k^{(t)}(wt') \mp (-1)^k \rho_k^{(t)}(\bar{t}\,t'). \tag{II.23}$$

From (II.10, 11) we find

$$\begin{aligned} i\langle N\bar{N}|\mathcal{M}^\dagger - \mathcal{M}|N\bar{N}\rangle = \\ \sum_{k=1}^{5}\Big[3\{\rho_k^{(+)}(wt) - (-1)^k\rho_k^{(+)}(\bar{t}\,t)\} \\ + 2\{\rho_k^{(-)}(wt) + (-1)^k\rho_k^{(-)}(\bar{t}\,t)\}\tau^{(1)}\cdot\tau^{(2)}\Big]P_k. \end{aligned} \tag{II.24}$$

Collectin

where Ω_Q

Expressin

gives the

amplitude

Collecting (II.16, 17, 18, 24) we can write

$$\sum_{k=1}^{5} \left[\rho_k^{(\pm)}(wt') \mp (-1)^k \rho_k^{(\pm)}(\bar{t}t') \right] P_k =$$

$$\frac{1}{128\pi^2} \sqrt{\frac{t'-4}{t'}} \int d\Omega_Q \left[-A^{(\pm)*}(s_p t') + i\gamma^{(p)}\cdot Q\, B^{(\pm)*}(s_p t') \right]$$

$$\times \left[-A^{(\pm)}(s_n t') + i\gamma^{(n)}\cdot Q\, B^{(\pm)}(s_n t') \right], \qquad \text{(II.25)}$$

where Ω_Q is the $\pi\pi$ solid angle in the $N\bar{N}$ c.m. frame. Expressing the right side of (II.25) in terms of the P_k gives the spectral functions $\rho_k^{(\pm)}$ in terms of the $N\bar{N}\to\pi\pi$ amplitudes.

$$8\pi^2 t \left[\rho_k^{(\pm)}(wt') \mp (-1)^k \rho_k^{(\pm)}(\bar{t}t') \right] =$$

$$\begin{cases} (a + 2mc + m^2 e) & k=1 \\ -(b + md) & k=2 \\ e & k=3 \\ -f & k=4 \\ 0 & k=5 \end{cases} \qquad \text{(II.26)}$$

a = 4

b = 4

c = 4

d = 5

e = 1

f =

N =

to calcu

$N\bar{N} \to \pi\pi$ am

separate

defined

$$a = 4\pi^2 tN \int A^{(\pm)*}(s_p t')\, A^{(\pm)}(s_n t')\, d\Omega_Q ,$$

$$b = 4\pi^2 tN \int Re\left[B^{(\pm)*}(s_p t')\, A^{(\pm)}(s_n t')\right]\left[\frac{Q\cdot M}{M^2} + \frac{Q\cdot k}{k^2}\right] d\Omega_Q ,$$

$$c = 4\pi^2 tN \int Re\left[B^{(\pm)*}(s_p t')\, A^{(\pm)}(s_n t')\right]\left[\frac{Q\cdot M}{M^2} - \frac{Q\cdot k}{k^2}\right] d\Omega_Q ,$$

$$d = \frac{4\pi^2 tN}{M^2 k^2} \int B^{(\pm)*}(s_p t')\, B^{(\pm)}(s_n t') \left[\frac{(Q\cdot M)^2}{M^2}(2k^2+M^2)\right.$$

$$\left. + \frac{(Q\cdot k)^2}{k^2}(k^2+2M^2) - Q^2(k^2+M^2)\right] d\Omega_Q ,$$

$$e = \frac{4\pi^2 tN}{M^2 k^2} \int B^{(\pm)*}(s_p t')\, B^{(\pm)}(s_n t') \left[\frac{(Q\cdot M)^2}{M^2}(2k^2-M^2)\right.$$

$$\left. + \frac{(Q\cdot k)^2}{k^2}(k^2-2M^2) + Q^2(M^2-k^2)\right] d\Omega_Q ,$$

$$f = 4\pi^2 tN \int B^{(\pm)*}(s_p t')\, B^{(\pm)}(s_n t') \left[Q^2 - \frac{(Q\cdot M)^2}{M^2} - \frac{(Q\cdot k)^2}{k^2}\right] d\Omega_Q ,$$

$$N = \frac{1}{64\pi^2}\sqrt{\frac{t'-4}{t'}} \,. \qquad \text{(II.27)}$$

B. Inclusion of the $N\bar{N}\to\pi\pi$ Amplitudes

The formalism of the preceeding section allows one to calculate the two-pion-exchange NN amplitude given the $N\bar{N}\to\pi\pi$ amplitudes $A^{(\pm)}$, $B^{(\pm)}$. The amplitude $B^{(\pm)}$ is separated into Born and non-Born parts (the Born terms are defined by pseudoscalar coupling theory):

$= (7)W$

are easil

Recall th

Inserting

the nucle

T

are easil

$$B^{(\pm)} = B_B^{(\pm)} + \tilde{B}^{(\pm)}, \qquad \text{(II.28)}$$

$$B_B^{(\pm)} = g^2\left[\frac{1}{m^2-s} \mp \frac{1}{m^2-u}\right]. \qquad \text{(II.29)}$$

Recall that there is no Born contribution to $A^{(\pm)}$:

$$A_B^{(\pm)} = 0 . \qquad \text{(II.30)}$$

Inserting (II.29, 30) for $A^{(\pm)}$, $B^{(\pm)}$ into (II.26) produces the nucleon-box two-pion-exchange spectral functions.

The results for the nucleon-box spectral functions are easily written in terms of the following functions.

$$h = \frac{t-2}{4pq}, \qquad \text{(II.31)}$$

$$\phi = \left(\frac{t-2}{2}\right)^2 - q^2(w-\bar{t}), \qquad \text{(II.32a)}$$

$$\chi = wq^2\left[4q^2\bar{t} - (t-2)^2\right], \qquad \text{(II.32b)}$$

$$I_0(t) = \frac{2\pi}{\chi}\,\mathrm{Log}\left[\frac{\phi+\sqrt{\chi}}{\phi-\sqrt{\chi}}\right] \quad \text{for } \chi>0,$$

$$= \frac{4\pi}{\phi} \quad \text{for } \chi=0,$$

$$= \frac{4\pi}{\sqrt{-\chi}}\,\arctan\frac{\sqrt{-\chi}}{\phi} \quad \text{for } \chi<0, \qquad \text{(II.33)}$$

$$X(t) = \frac{\pi w}{p^2}\left(1 - h\arctan\frac{1}{h}\right), \qquad \text{(II.34a)}$$

$$M(t) = X(t) + 4\pi\left(1-2h\arctan\frac{1}{h}\right) + \left(\frac{t-2}{2}\right)^2 I_0(t), \qquad \text{(II.34b)}$$

Re $\rho_1^{(\pm)}$

+

Re $\rho_2^{(\pm)}$

Re $\rho_3^{(\pm)}$

Re $\rho_4^{(\pm)}$

$\rho_5^{(\pm)}$ (w

The more

given by

one must

momentum

momentum

duced vi

channel

write

$$N = \frac{1}{64\pi^2}\sqrt{\frac{t-4}{4}} \,. \qquad \text{(II.35)}$$

$$\text{Re}\,\rho_1^{(\pm)}(wt) = \pm \frac{m^2 N g^4}{w\bar{t}}\left[\frac{3w+4p^2}{\bar{t}} M(t)\right.$$

$$\left. + \frac{3w+8p^2}{w} X(t) + g^2(w-\bar{t})\, I_0(t)\right], \qquad \text{(II.36a)}$$

$$\text{Re}\,\rho_2^{(\pm)}(wt) = \pm \frac{mNg^4}{w\bar{t}}\left[\frac{2w+\bar{t}}{\bar{t}} M(t)\right.$$

$$\left. + \frac{w+2\bar{t}}{w} X(t) - 4p^2 g^2\, I_0(t)\right], \qquad \text{(II.36b)}$$

$$\text{Re}\,\rho_3^{(\pm)}(wt) = \frac{1}{m^2}\,\text{Re}\,\rho_1^{(\pm)}(wt)\,, \qquad \text{(II.36c)}$$

$$\text{Re}\,\rho_4^{(\pm)}(wt) = \pm Ng^4\left[\frac{1}{\bar{t}} M(t) + \frac{1}{w} X(t)\right.$$

$$\left. + g^2\, I_0(t)\right], \qquad \text{(II.36d)}$$

$$\rho_5^{(\pm)}(wt) = 0\,. \qquad \text{(II.36e)}$$

The more general expressions for other box diagrams were given by ALV[4]. When using the general expressions of ALV one must remember that ALV used the t-channel nucleon momentum rather than the conventionally chosen antinucleon momentum as the quantization axis.

The non-Born contributions $A^{(\pm)}$, $B^{(\pm)}$ are introduced via the helicity expansion (A.3). Because the t-channel partial waves in (II.27) do not interfere, we may write

$\rho_k^{(\pm)}$ (v

where $\rho_k^{(\pm)}$

with the

from (A.3

Born appr

T

We write

$A^{(+)}$

$A^{(-)}$

$B^{(+}$

$B^{(-}$

where th

momentum

$\rho_1^{(+)}$

$$\rho_k^{(\pm)}(wt') = \rho_{k;B}^{(\pm)}(wt) + \rho_{k;spd}^{(\pm)}(wt) - \rho_{k;Bspd}^{(\pm)}(wt), \qquad \text{(II.37)}$$

where $\rho_{k;B}^{(\pm)}$ is derived from (II.29, 30), $\rho_{k;spd}$ from (A.3) with the first three partial waves included, and $\rho_{k;Bspd}$ from (A.3) with the first three partial waves included in Born approximation.

The partial wave contributions are summerized here. We write the expansion (A.3) more conveniently as

$$A^{(+)} = \alpha_0 + \alpha_{21} + \alpha_{22}\left(\frac{s-u}{4}\right)^2 + (J \geq 4), \qquad \text{(II.38a)}$$

$$A^{(-)} = \alpha_1\left(\frac{s-u}{4}\right) + (J \geq 3), \qquad \text{(II.38b)}$$

$$B^{(+)} = \beta_2\left(\frac{s-u}{4}\right) + (J \geq 4), \qquad \text{(II.38c)}$$

$$B^{(-)} = \beta_1 + (J \geq 3), \qquad \text{(II.38d)}$$

where the first subscript on each term denotes the angular momentum J. From (II.27) we find the J=0,1,2 contributions

$$\rho_1^{(+)}(wt') = N\pi\left[|\alpha_0|^2 + |\alpha_{21}|^2 + \frac{2}{3}mq_b^2\,Re(\beta_2^*\alpha_{21}) - \frac{w}{3}q_b^2\,Re(\alpha_{21}^*\alpha_{22}) - \frac{w}{15}mq_b^4\,Re(\beta_2^*\alpha_{22}) + \frac{w}{40}q_b^4|\alpha_{22}|^2(w-\tfrac{1}{3}\bar{t}) + \frac{m^2}{15}q_b^4|\beta_2|^2\right], \qquad \text{(II.39a)}$$

the calc

procedur

discusse

$M_{fi} \equiv M$

unitari-

$\rho_3^{(-)}$ (

$\rho_4^{(-)}$ (

$\rho_5^{(+)}$ (

$\rho_2^{(-)}$ (

$\rho_1^{(-)}$ (

$\rho_4^{(+)}$ (

$\rho_3^{(+)}$ (

$\rho_2^{(+)}$ (

$$\rho_2^{(+)}(wt') = N\pi \frac{w}{15} q^4 \, Re(\beta_2^* \alpha_{22}), \tag{II.39b}$$

$$\rho_3^{(+)}(wt') = N\pi \frac{1}{15} q^4 |\beta_2|^2, \tag{II.39c}$$

$$\rho_4^{(+)}(wt') = N\pi \frac{w}{30} q^4 |\beta_2|^2, \tag{II.39d}$$

$$\rho_1^{(-)}(wt') = -N\pi \frac{w}{6} q^2 |\alpha_1|^2, \tag{II.39e}$$

$$\rho_2^{(-)}(wt') = -N\pi \frac{1}{3} q^2 \, Re(\alpha_1^* \beta_1), \tag{II.39f}$$

$$\rho_3^{(-)}(wt') = 0, \tag{II.39g}$$

$$\rho_4^{(-)}(wt') = -N\pi \frac{1}{3} q^2 |\beta_1|^2, \tag{II.39h}$$

$$\rho_5^{(t)}(wt') = 0. \tag{II.39i}$$

Evaluation of the $J=0,1,2$ $N\bar{N}\to\pi\pi$ amplitudes completes the calculation of the two-pion-exchange amplitude. The procedure for projecting out partial-wave amplitudes is discussed in Appendix C.

C. Two-Pion Exchange Potential

Recall from Equation (II.7) the definition of $M_{fi} \equiv M((\underline{p}_1-\underline{p}_2)/2, (\underline{n}_1-\underline{n}_2)/2)$ which has the NN elastic unitarity relation[21] in the c.m. frame:

$m^{\dagger}(k',k$

where E =

T

Lippmann-

$T(k',k$

satisfie

$T^{\dagger}(k',$

Using k^2

$T^{\dagger}(k',$

Thus, th

T

$V_{\pi}(k',$

where M_T

$$\mathcal{M}^{\dagger}(k',k)-\mathcal{M}(k',k)=\frac{-im^2}{(2\pi)^2E^2}\int d^3q\,\mathcal{M}^{\dagger}(k',q)\mathcal{M}(q,k)\,\delta(2E_q-2E). \tag{II.40}$$

where $E = (k^2+m^2)^{1/2}$ and $E_q = (q^2+m^2)^{1/2}$.

The scattering amplitude T(k',k) occurring in the Lippmann-Schwinger equation

$$T(k',k)=V(k',k)-\frac{m}{(2\pi)^3}\int d^3q\,V(k',q)\frac{1}{E_q^2-E^2-i\epsilon}\,T(q,k) \tag{II.41}$$

satisfies the unitarity relation

$$T^{\dagger}(k',k)-T(k',k)=\frac{i}{(2\pi)^2}\int d^3q\,T^{\dagger}(k',q)\,T(q,k)\,\delta\left(\frac{q^2}{m}-\frac{k^2}{m}\right). \tag{II.42}$$

Using $k^2=k'^2 = E^2-m^2$ (II.42) becomes[21]

$$T^{\dagger}(k',k)-T(k',k)=\frac{im}{(2\pi)^2E}\int d^3q\,T^{\dagger}(k',q)T(q,k)\,\delta(2E_q-2E). \tag{II.43}$$

Thus, the relation between M and T is

$$T(q,k) = -\left(\frac{m^2}{E_q\,E_k}\right)^{1/2}\mathcal{M}(q,k). \tag{II.44}$$

The one-pion-exchange potential is defined by

$$V_{\pi}(k',k)=-\left(\frac{m^2}{E_{k'}\,E_k}\right)^{1/2}\bar{u}_p(\underline{k}')\,\bar{u}_n(-\underline{k}')\,\mathcal{M}_{\pi}\,u_p(\underline{k})\,u_n(-\underline{k}), \tag{II.45}$$

where M_{π} is the one-pion-exchange amplitude

and t =

Explicit

$V_\pi($

The coor

$V(r'$

If $V(\underline{k}';\underline{k}$

$\underline{k}'-\underline{k}$ the

where $\underline{\Delta}$

not loca

one-meso

factor

an expa

exchang

exchang

$$\mathcal{M}_\pi = \tau_p \cdot \tau_n \; \gamma_5^p \gamma_5^n \frac{g^2}{\mu^2 - t} , \qquad \text{(II.46)}$$

and $t = -(\underline{k}' - \underline{k})^2$.

Explicitly, the potential is

$$V_\pi(k',k) = \left(\frac{m^2}{E_{k'} E_k}\right)^{1/2} \chi_p^\dagger \chi_n \; \tau_p \cdot \tau_n \; \frac{g^2}{4m^2(t-\mu^2)}$$

$$\times \; \underset{\sim}{\sigma}_p \cdot (\underset{\sim}{k}' - \underset{\sim}{k}) \; \underset{\sim}{\sigma}_n \cdot (\underset{\sim}{k}' - \underset{\sim}{k}) \; \chi_p \chi_n \; . \qquad \text{(II.47)}$$

The coordinate space potential is the Fourier transform

$$V(r',r) = \frac{1}{(2\pi)^6} \int e^{i\underset{\sim}{k}\cdot\underset{\sim}{r}} \, e^{-i\underset{\sim}{k}'\cdot\underset{\sim}{r}'} \, V(k',k) \, d^3k \, d^3k' . \qquad \text{(II.48)}$$

If $V(\underline{k}';\underline{k})$ is a function of only the momentum transfer $\underline{k}' - \underline{k}$ then $V(\underline{r}', \underline{r})$ is local and $V(\underline{r}', \underline{r}) = V(r) \; \delta^3(\underline{r}' - \underline{r})$,

$$V(r) = \frac{1}{(2\pi)^3} \int e^{-i\underset{\sim}{\Delta}\cdot\underset{\sim}{r}} \, V(\Delta) \, d^3\Delta \qquad \text{(II.49)}$$

where $\underline{\Delta} = \underline{k}' - \underline{k}$.

The one-pion-exchange potential (II.47) is clearly not local. Partovi and Lomon[1] have shown how to calculate one-meson-exchange potentials by expanding the square-root factor in (II.47) in powers of $\underline{P} = 1/2(\underline{k}' + \underline{k})$ while avoiding an expansion in $\underline{\Delta}$. Their treatment is useful for massive exchanges ($m_{meson} \approx m_{nucleon}$) but unnecessary for π-exchange. The one-pion-exchange potential is obtained by

nonrelat

(II.47)

$V_\pi(\Delta$

and the

$V_\pi(r)$

The tens

$V_{2\pi}($

where M

iterate

nonrelativistically reducing the square-root factor in (II.47) to unity.

The momentum-space potential is then

$$V_\pi(\Delta) = -\chi_p^\dagger \chi_n^\dagger \tau_p\cdot\tau_n \frac{g^2}{4m^2(\Delta^2+\mu^2)} \times \underset{\sim}{\sigma}_p\cdot\underset{\sim}{\Delta}\ \underset{\sim}{\sigma}_n\cdot\underset{\sim}{\Delta}\ \chi_p\chi_n \qquad \text{(II.50)}$$

and the coordinate space potential is

$$V_\pi(r) = \chi_p^\dagger\chi_n^\dagger \tau_p\cdot\tau_n \frac{g^2}{4\pi}\frac{1}{(2m)^2}\underset{\sim}{\sigma}_p\cdot\underset{\sim}{\nabla}\,\underset{\sim}{\sigma}_n\cdot\underset{\sim}{\nabla}\frac{e^{-\mu r}}{r}\chi_p\chi_n$$

$$= \chi_p^\dagger\chi_n^\dagger \tau_p\cdot\tau_n \frac{g^2}{4\pi}\left(\frac{\mu}{2m}\right)^2\left\{\frac{1}{3}\underset{\sim}{\sigma}_p\cdot\underset{\sim}{\sigma}_n + \left[\frac{1}{(\mu r)^2}+\frac{1}{\mu r}+\frac{1}{3}\right]S_{12}\right\}\frac{e^{-\mu r}}{r}\chi_p\chi_n. \qquad \text{(II.51)}$$

The tensor operator is

$$S_{12} = 3\,\underset{\sim}{\sigma}_p\cdot\hat{r}\ \underset{\sim}{\sigma}_n\cdot\hat{r} - \underset{\sim}{\sigma}_p\cdot\underset{\sim}{\sigma}_n\ .$$

The two-pion-exchange potential is defined by

$$V_{2\pi}(k',k) = -\left(\frac{m^2}{E_{k'}E_k}\right)^{1/2}\bar{u}_p(\underset{\sim}{k}')\,u_n(-\underset{\sim}{k}')\,\mathcal{M}_{2\pi}\,u_p(\underset{\sim}{k})\,u_n(-\underset{\sim}{k}) - T_{\pi 2}(k',k) \qquad \text{(II.52)}$$

where $M_{2\pi}$ is the two-pion-exchange amplitude and $T_{\pi 2}$ is the iterated one-pion-exchange,

$T_{\pi 2}$ (

unity.

factor i

The reas

(II.53)

tic redu

(II.44)

wave fun

V

T

We find

T_{π}

Blankenb

which wa

$$T_{\pi 2}(k',k) = \frac{-m}{(2\pi)^3} \sum_{\substack{\text{interm.}\\ \text{spin}}} \int d^3q\, V_\pi(k',q) \frac{1}{E_q^2 - E^2 - i\epsilon} V_\pi(q,k). \tag{II.53}$$

We may reduce the square-root factor in (II.52) to unity. However, it is necessary to retain the square-root factor in V_π, using (II.47) rather than (II.50) in (II.53). The reason is clear: the intermediate state integral in (II.53) involves a large momentum q so that a nonrelativistic reduction of V_π is inappropriate.

It has been pointed out by Leon Heller[22] that (II.44) is (except for the sign) merely a change in the wave function normalization. Defining

$$V_\pi(q,k) = -\left(\frac{m^2}{E_q E_k}\right)^{1/2} \mathcal{V}_\pi(q-k), \tag{II.54}$$

$$T_{\pi 2}(q,k) = -\left(\frac{m^2}{E_q E_k}\right)^{1/2} \mathcal{T}_{\pi 2}(q,k), \tag{II.55}$$

we find

$$\mathcal{T}_{\pi 2}(k',k) = \frac{m^2}{(2\pi)^3} \sum_{\substack{\text{interm}\\ \text{spin}}} \int \frac{d^3q}{E_q} \mathcal{V}_\pi(k'-q) \times \frac{1}{E_q^2 - E^2 - i\epsilon} \mathcal{V}_\pi(q-k). \tag{II.56}$$

Equation (II.56) also follows directly from the Blankenbecler-Sugar-Logunov-Tavkhelidze[23,24] equation, which was used by Chemtob, Durso, and Riska[13] to obtain

the iter

(Appendi

for $T_{\pi 2}$

space we

the foll

for $\tilde{\Omega}_{SO}$

set of

the iterated one-pion-exchange contribution to $V_{2\pi}$ (Appendix D). It is most convenient to discuss the results for $T_{\pi 2}$ along with the complete potential $V_{2\pi}$.

Before transforming the potential to coordinate space we shall rewrite the amplitude (II.10) in terms of the following set of spin operators:

$$\begin{aligned}
\tilde{\Omega}_c &= 1 \\
\tilde{\Omega}_{so} &= \tfrac{1}{2} i (\underset{\sim}{\sigma}_p + \underset{\sim}{\sigma}_n) \cdot (\underset{\sim}{k}' \times \underset{\sim}{k}) \\
\tilde{\Omega}_T &= \Delta^2 \underset{\sim}{\sigma}_p \cdot \underset{\sim}{\sigma}_n - 3 \underset{\sim}{\sigma}_p \cdot \underset{\sim}{\Delta}\, \underset{\sim}{\sigma}_n \cdot \underset{\sim}{\Delta} \\
\tilde{\Omega}_{ss} &= \Delta^2 \underset{\sim}{\sigma}_p \cdot \underset{\sim}{\sigma}_n \\
\tilde{\Omega}_{so2} &= \underset{\sim}{\sigma}_p \cdot (\underset{\sim}{k}' \times \underset{\sim}{k})\, \underset{\sim}{\sigma}_n \cdot (\underset{\sim}{k}' \times \underset{\sim}{k}) \quad .
\end{aligned} \tag{II.57}$$

These operators are of convenience because, except for $\tilde{\Omega}_{SO2}$, they Fourier transform directly into the following set of operators:

$$\begin{aligned}
\Omega_c &= 1 \\
\Omega_{so} &= \tfrac{1}{2} (\underset{\sim}{\sigma}_p + \underset{\sim}{\sigma}_n) \cdot \underset{\sim}{L} \\
\Omega_T &= S_{12} = 3 \underset{\sim}{\sigma}_p \cdot \hat{r}\, \underset{\sim}{\sigma}_n \cdot \hat{r} - \underset{\sim}{\sigma}_p \cdot \underset{\sim}{\sigma}_n \\
\Omega_{ss} &= \underset{\sim}{\sigma}_p \cdot \underset{\sim}{\sigma}_n \\
\Omega_{so2} &= \tfrac{1}{2} (\underset{\sim}{\sigma}_p \cdot \underset{\sim}{L}\, \underset{\sim}{\sigma}_n \cdot \underset{\sim}{L} + \underset{\sim}{\sigma}_n \cdot \underset{\sim}{L}\, \underset{\sim}{\sigma}_p \cdot \underset{\sim}{L}) \quad .
\end{aligned} \tag{II.58}$$

We there

$$\sum_k \rho$$

The tran

$$V(r';r)$$

$$\times$$

where $\underline{P}$

exchange

$4m^2-w-\Delta^2$

functior

A simila

Appendix

As in Ap

$\bar{t}=0$. As

dependen

vidually

Furtherm

at long

then con

operato

We therefore write

$$\sum_k \rho_k'^{(\pm)}(wt'\underline{r})\,P_k = \sum_\alpha \bar{\bar{\rho}}_\alpha'^{(\pm)}(wt'\underline{r})\,\tilde{\Omega}_\alpha$$

The transformation from ρ_k' to $\bar{\bar{\rho}}_\alpha'$ is given in Appendix D.

The coordinate space potential is now

$$V(r';r) = \frac{-1}{(2\pi)^6}\sum_\alpha \iint d^3P\, d^3\Delta\; e^{i\underline{P}\cdot\left(\frac{\underline{r}-\underline{r}'}{2}\right)}\; e^{-i\underline{\Delta}\cdot\left(\frac{\underline{r}+\underline{r}'}{2}\right)}$$

$$\times \frac{1}{\pi}\int dt'\;\frac{\bar{\bar{\rho}}_\alpha'(wt'\underline{r}) + \bar{\bar{\eta}}_\alpha(wt'\underline{r})}{t'+\Delta^2}\;\tilde{\Omega}_\alpha$$

where $\underline{P} = 1/2(\underline{k}'+\underline{k})$. The $\bar{\bar{\eta}}_\alpha$ form the iterated one-pion-exchange contribution (Appendix D). The presence of $\bar{t} = 4m^2-w-\Delta^2$ and $w=\Delta^2+4P^2+4m^2$ in the arguments of the spectral functions complicates the Fourier transforms in (II.60). A similar problem with the $\bar{t}$ dependence is encountered in Appendix C where partial-wave amplitudes are projected out. As in Appendix C, and with the same justification, we set $\bar{t}=0$. As for the w dependence, the sum $\bar{\bar{\rho}}_\alpha'+\bar{\bar{\eta}}_\alpha$ is only mildly dependent on w when $|k'|=|k|$, although $\bar{\bar{\rho}}_\alpha'$ and $\bar{\bar{\eta}}_\alpha$ are individually strongly w dependent.[13] We therefore set $w=4m^2$. Furthermore, the dependence on $\underline{P}\cdot\underline{\Delta}$ is expected to be weak at long range[1] and it is neglected. The only nonlocality then comes from the $\tilde{\Omega}_\alpha$.

Expanding the coordinate space potential in the operators (II.58) and simplifying the notation gives

$$\sum_{\alpha}$$

where $\tilde{\Omega}$

can be e

$$V_{\alpha}^{(\pm)}(r)$$

where x

$$\sum_\alpha V_\alpha(r)\,\Omega_\alpha = -\frac{1}{(2\pi)^3}\sum_\alpha \int d^3\Delta\; e^{-i\underline{\Delta}\cdot\underline{r}}$$

$$\times\ \frac{1}{\pi}\int_1^\infty dt'\ \ \frac{\bar{\bar{\rho}}_\alpha'(t') + \bar{\bar{\eta}}_\alpha(t')}{t'+\Delta^2}\ \tilde{\Omega}_\alpha' \qquad \text{(II.61)}$$

where $\tilde{\Omega}_\alpha'$ have been integrated over $\underline{P}$. The Fourier transform can be easily performed to give

$$V_\alpha^{(\pm)}(r) = -\frac{1}{(2\pi)^2}\int_1^\infty dt' \left[\bar{\bar{\rho}}_\alpha'^{(\pm)}(t') + \bar{\bar{\eta}}_\alpha^{(\pm)}(t')\right] R_\alpha(x)\,\frac{e^{-x}}{r}\,, \qquad \text{(II.62)}$$

where $x = \sqrt{t'}\,r$ and

$$R_c = 1\,,$$

$$R_{so} = -\frac{t'}{x}\left(1+\tfrac{1}{x}\right),$$

$$R_T = t'\left(1+\tfrac{3}{x}+\tfrac{3}{x^2}\right),$$

$$R_{ss} = -t'\,,$$

$$R_{so2} \approx -\frac{t'^2}{x^2}\left(1+\tfrac{3}{x}+\tfrac{3}{x^2}\right)\,. \qquad \text{(II.63)}$$

amplitud

branch c

intermed

correspo

left cu

(πN sca

by the

t=0 the

mediate

require

I

where δ

other w

π. Alt

t=16 it

scatter

III. EVALUATION OF THE $N\bar{N}\to\pi\pi$ AMPLITUDES

A. Partial-Wave Dispersion Relations for $N\bar{N}\to\pi\pi$

The analyticity structure of the $N\bar{N}\to\pi\pi$ helicity amplitudes[25] $f^J_{+-}(t)$ is shown in Figure 8. The right-hand branch cut begins at t=4 and corresponds to the two-pion intermediate state. Further branch points lie on this cut corresponding to 4, 8, ... pion intermediate states. The left cut is produced by the s- and u-channel reactions (πN scattering). The branch point at $t=4-1/m^2\equiv a$ is caused by the partial-wave projection of the nucleon pole. At t=0 the πN states produce an additional branch point.

Since for $4<t<16$ the only t-channel physical intermediate state is two pions, the unitarity condition requires that

$$\mathrm{Im}\, f^J_{\pm}(t) = f^{J*}_{\pm}(t)\, e^{i\delta^I_J} \sin\delta^I_J , \qquad \text{(III.1)}$$

where δ^T_J is the appropriate $\pi\pi$ scattering phase shift. In other words, the phase of f^J_{+-} is the $\pi\pi$ phase shift, modulo π. Although this relation is strictly valid only below t=16 it is expected to be useful as long as the pion scattering for angular momentum J is essentially elastic.

Figur

ampli

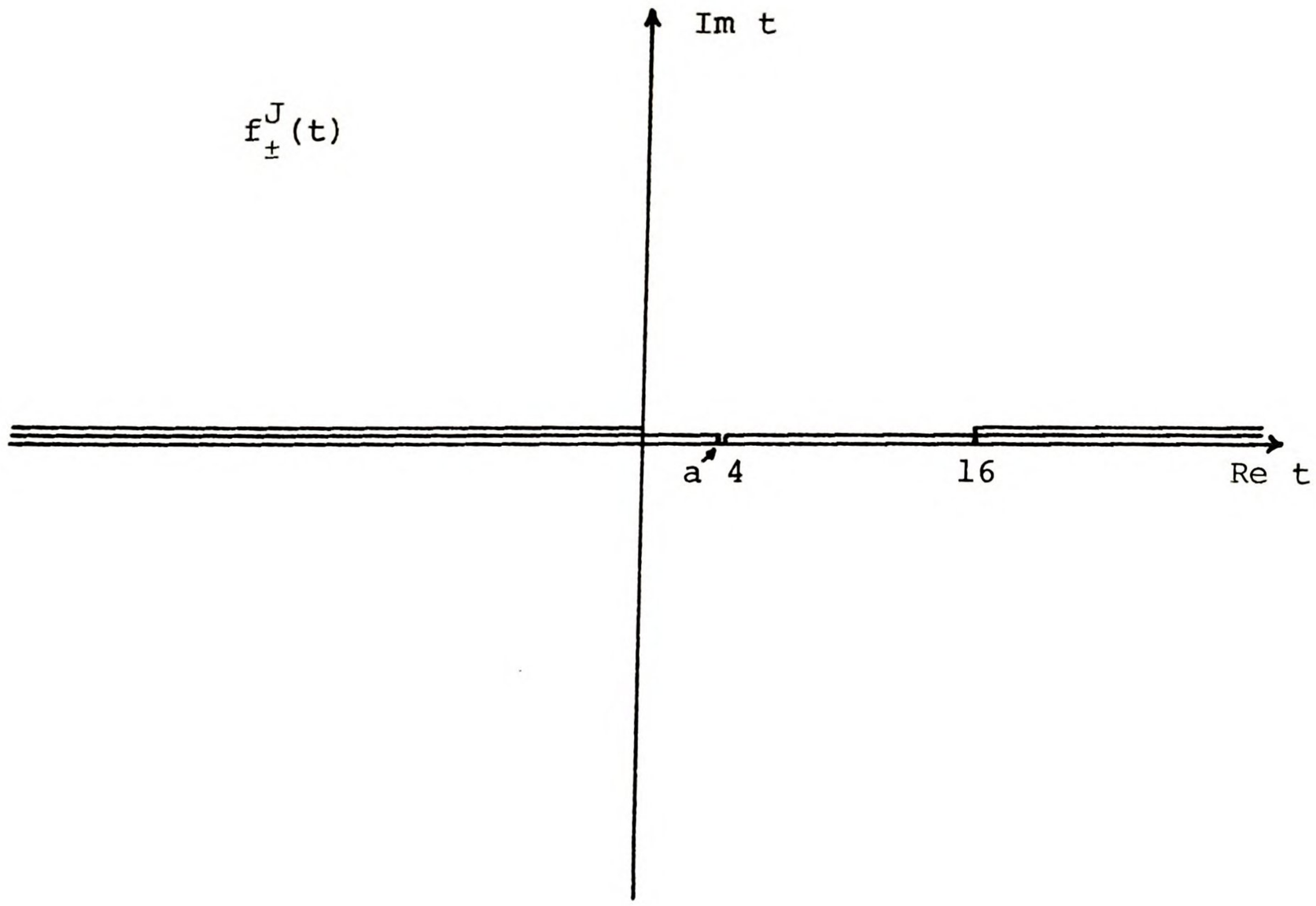

Figure 8. Singularities of the $N\bar{N}\to\pi\pi$ helicity amplitudes $f_{\pm}^{J}(t)$.

is an ar

extendi

that the

$t<4-1/m^2$

inelast

followi

subtrac

T

The J=0

may wri

D

Nielser

(III.3)

by Nie

By int

effect

The Omnès function,[26] defined as

$$D_J(t) = \exp\left[\frac{-t}{\pi}\int_4^\infty \frac{\delta_J^I(t')}{t'(t'-t-i\epsilon)}\,dt'\right] \qquad \text{(III.2)}$$

is an analytic function except for a cut beginning at t=4 extending to t=∞. The phase of $D_J(t)$ along this cut is such that the product $D_J(t)\ f_{\pm}^J(t)$ has only a left cut at $t<4-1/m^2$ and a right cut where J-wave ππ scattering becomes inelastic. With this knowledge of the analyticity the following dispersion relation can be written, assuming no subtractions are required:

$$D_J(t)\,f_\pm^J(t) = \frac{1}{\pi}\int_{-\infty}^{a} \frac{D_J(t')\ \mathrm{Im}\,f_\pm^J(t')}{t'-t}\,dt' \quad . \qquad \text{(III.3)}$$

The J=0 amplitude has a kinematical zero[25] at $t=4m^2$ so we may write

$$\frac{D_0(t)\,f_+^0(t)}{t-4m^2} = \frac{1}{\pi}\int_{-\infty}^{a} \frac{D_0(t')\ \mathrm{Im}\,f_+^0(t')}{(t'-4m^2)(t'-t)}\,dt'$$

The helicity amplitudes f_+^0 and $f_{\pm}^1$ were evaluated by Nielsen and Oades[15] in 1972. Their procedure was based on (III.3) with the discontinuity on the left cut determined by Nielsen[27] from $A'^{(+)}$, $B^{(+)}$ fixed-t dispersion relations. By introducing the Omnès function (III.2) the right cut was effectively moved out to t ≃ 50. Nielsen and Oades could

then ex

unsubtr

from t<

with se

and Oad

but onl

shown h

relatio

$N\bar{N}\to\pi\pi$ a

states

equalit

shifts

of the

Much o

ferenc

signif

center

angle

$a_2(\omega,t$

and t

dipion

$\pi\pi\to\pi\pi$.

then extrapolate a discrepancy $(D_o f_+^o/(t-4m^2)$ minus the unsubtracted Omnès relation (III.4)) by conformal mapping, from $t<4$ to $4\leq t<50$. The s-wave amplitude f_+^o was evaluated with several different s-wave $\pi\pi$ phase shifts δ_o^o. Nielsen and Oades preferred a δ_o^o with a negative scattering length but only their solution using the Morgan-Shaw[28] δ_o^o will be shown here.

B. Pion-Pion Phase Shift Input

As pointed out in the discussion of the Omnès relation, generalized unitarity equates the phases of the $N\bar{N}\to\pi\pi$ and $\pi\pi\to\pi\pi$ amplitudes in the same angular momentum states as long as the $\pi\pi$ waves are elastic. For this equality to be useful, an accurate knowledge of the phase shifts for $\pi\pi$ scattering is required.

There have been a very large number of analyses[29] of the reaction $\pi N\to\pi\pi N$ to determine the $\pi\pi$ phase shifts. Much of the early work relied on measuring the s-p interference in the $\pi\pi$ system.[30] If only s, p, and d-waves are significant, then the angular distribution in the dipion center of mass can be written in terms of the $\pi\pi$ scattering angle as approximately $W(\omega,t,\cos\theta) = a_o(\omega,t)+a_1(\omega,t)\cos\theta+ a_2(\omega,t)\cos^2\theta$. In this expression ω is the dipion energy and t is the negative mementum transfer squared to the dipion. Figure 9a depicts the relation between $\pi N\to\pi\pi N$ and $\pi\pi\to\pi\pi$.

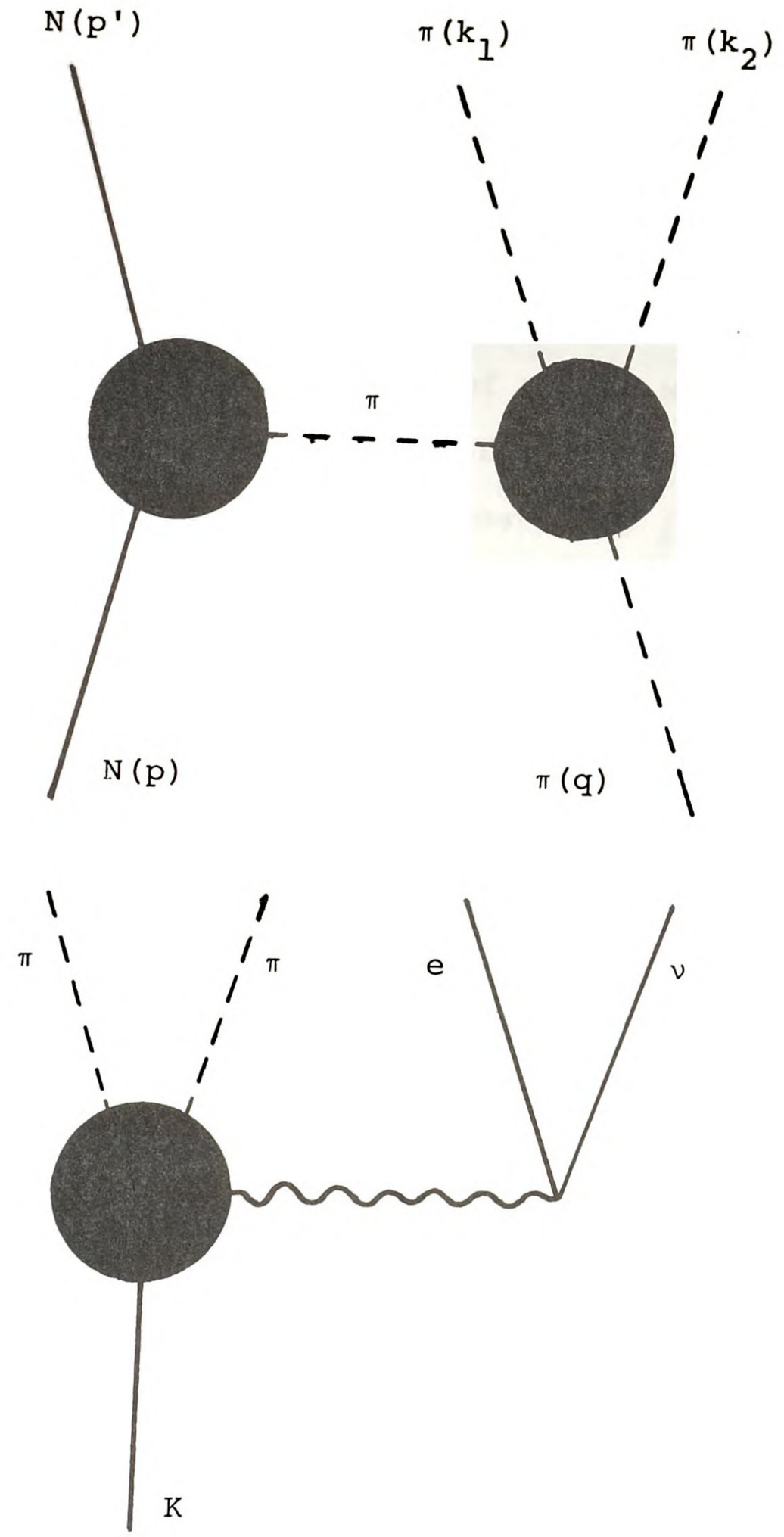

Figure 9. Single pion production and K_{e4} decay.

The int

an asym

(forwar

and B a

respect

be writ

The asy

the pic

in term

procedu

extract

additio

the $\pi\pi$

amplitu

amplitu

proces

produc

The variables ω and t are defined as

$$\omega^2 = -(k_1+k_2)^2$$

$$t = -(p-p')^2$$

The interference among the different partial waves causes an asymmetry between the number of events with $\cos\theta>0$ (forward, F) and those with $\cos\theta<0$ (backward, B). Since F and B are proportional to $\int_0^1 W\, d(\cos\theta)$ and $\int_{-1}^0 W\, d(\cos\theta)$, respectively, the asymmetry defined by g = (F-B)/(F+B) can be written as

$$g = \frac{A_1}{2/3\ A_2+2A_0} \quad .$$

The asymmetry can be smoothly extrapolated to $t = \mu^2$ where the pion scattering is on-mass-shell and g can be written in terms of the s, p, and d-wave phase shifts. The procedure requires a knowledge of the p-wave phase shift to extract the less well known s-wave phase shift. In addition, there is a two-fold ambiguity $\delta_0^0 \to \pi/2 - (\delta_0^0 - \delta_1^1)$.

Similarly, one may concentrate on the minimum in the $\pi\pi$ angular distribution and determine the s-wave amplitude which will interfere with the input p-wave amplitude to produce such a minimum.[31]

An alternate procedure involves assuming that the process in Figure 9a dominates the physical single pion production at small |t| (nearest the pion pole).[30] This

treatme

evaluat

the sug

polate

$(t=\mu^2)$

extrapo

pansion

mapping

increas

have be

δ^0_0 abov

resolve

popescu

effect

analysi

The Ber

analysi

larger

resolve

below

treatment allows, with a sufficient number of events, the evaluation of all of the relevant phase shifts.

The latter procedure has been improved by following the suggestion of Goebel[32] and of Chew and Low[33] to extrapolate the $\pi\pi$ differential cross-section to the pion pole ($t=\mu^2$) where the phase shift analysis is performed. The extrapolation has been performed[34-36] by polynomial expansion in both t and in a variable obtained by conformally mapping the t-plane such that the domain of convergence is increased.

Analyses based on extrapolated $\pi\pi$ cross-sections have been plagued by an ambiguity in the I=J=0 phase shift δ^o_o above the rho mass. This ambiguity has recently been resolved in large part by the Berkeley analysis of Protopopescu et al.[36] The authors included, approximately, the effect of the $K\bar{K}$ threshold in a dipion energy dependent analysis of the reactions

$$\pi^+ p \rightarrow \pi^+\pi^- \Delta^{++}$$

$$\pi^+ p \rightarrow K^+ K^- \Delta^{++} .$$

The Berkeley group also performed an energy independent analysis and found a similar but slightly larger δ^o_o with larger uncertainty.

The CERN-Munich[37] energy independent analysis resolved the ambiguity (their two solutions also differed below the rho) by comparing the predicted $\pi^o\pi^o$ mass

spectru

the exp

below 8

Berkele

also su

CERN-Mu

thus gi

shifts

wave δ^{o}_{o}

MeV alt

about +

particu

energy

situati

higher

down ar

due to

exchan

smooth

energy

spectrum, which involves only even partial waves, with the experimental spectrum. However, the preferred solution below 800 MeV is consistently about 11° higher than the Berkeley energy dependent solution (Figure 10).

Other experiments[38] to determine the $\pi^\circ\pi^\circ$ spectrum also support the preferred solutions of the Berkeley and CERN-Munich analyses.

The vast experimental effort on the $\pi\pi$ problem has thus given a good qualitative picture of the $\pi\pi$ phase shifts between 450 MeV and 1 GeV. Quantitatively, the s-wave δ_o^o is uncertain by about 15° between 450 MeV and 770 MeV although individual analyses quote error limits of about $\pm$4° and less.

A look at the Omnès function (III-2), regarding in particular its once-subtracted form, reveals that the low energy $\pi\pi$ phase shift is very important. The experimental situation below 500 MeV is at least as uncertain as at higher energy because of the emphasis on resolving the up-down ambiguity and the large total number of events required due to the presence of the Δ_{33} and ρ.

The early analysis of Jones et al.[30] by one-pion-exchange dominance and of Walker et al.[31] indicated a smooth continuation of δ_o^o from higher energy to threshold.

The phase shift δ_o^o has been studied[39,40] at low $\pi\pi$ energy via K_{e4} decay (Figure 9b)

$$K^+ \to e^+\nu\pi^+\pi^- \ .$$

DEGREES

Fi
ex

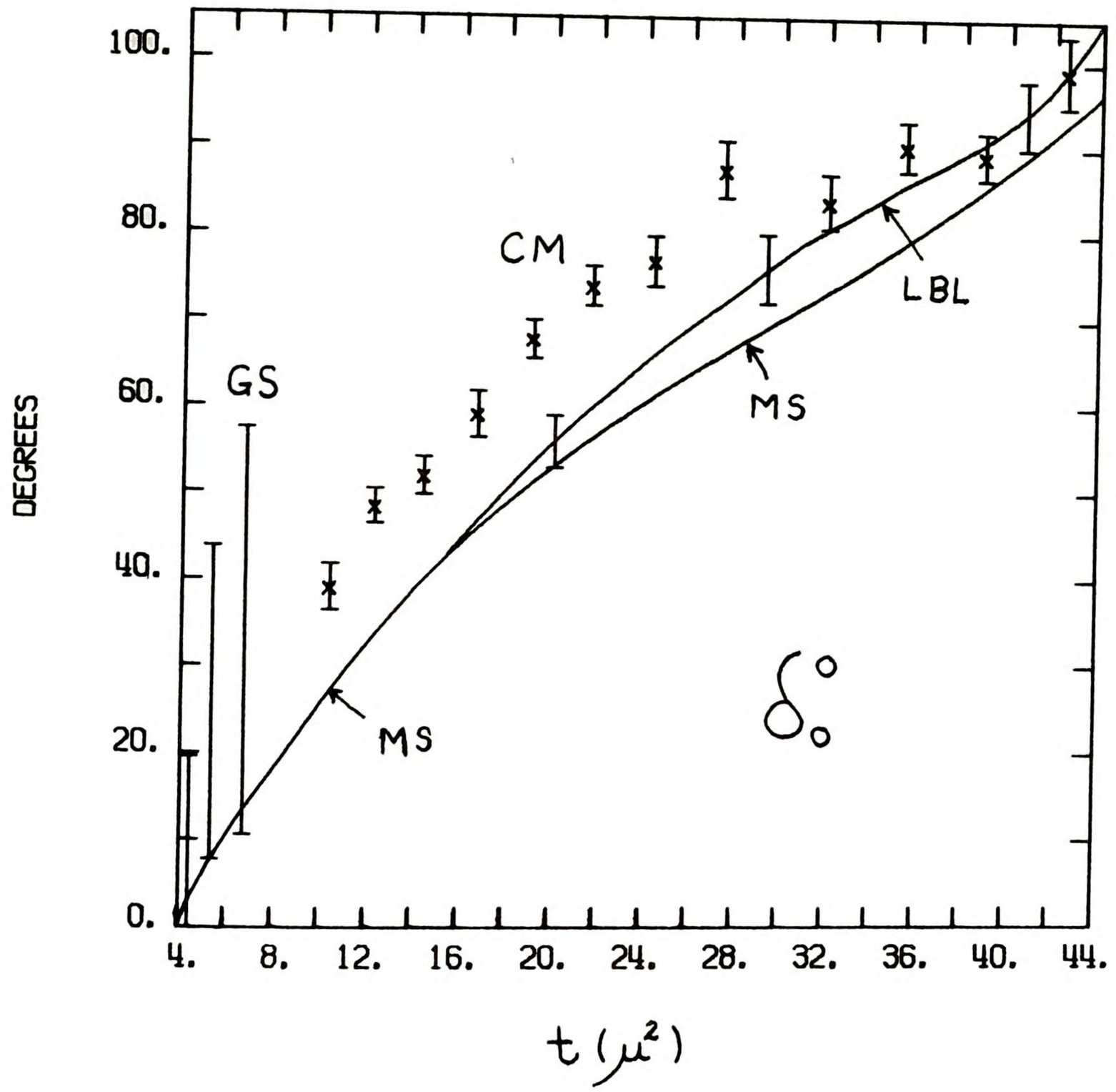

Figure 10. The I=J=0 ππ phase shift derived from experimental information.

The Gene

phase sh

of a_0 =

as 0.2,

Pennsyl

two of

δ_0^0 resu

a_0/a_2 w

results

Geneva-

the π-p

CERN-Mu

ever, w

length

value o

Penning

newer e

becaus

shift a

shown a

This i

parame

The Geneva-Saclay collaboration[39] found a rather large phase shift at low energy, and preferred a scattering length of $a_o = 0.6 \pm 0.25$. They will not rule out a value as small as 0.2, however. A similar experiment was performed by the Pennsylvania group[40] who obtained very similar results at two of the three $\pi\pi$ energy bands.

Morgan and Shaw[28] had earlier combined experimental δ_o^o results and the ratio of I=0 to I=2 scattering lengths a_o/a_2 with $\pi\pi$ dispersion relations to determine δ_o^o. Their results for δ_o^o at low energy are considerably below the Geneva-Scalay[39] K_{e4} decay results and somewhat lower than the π-production experiment results from Berkeley,[36] and CERN-Munich[37] (Figure 10). The latter two analyses, however, were for energies above about 500 MeV. The scattering length found by Morgan and Shaw is $a_o = 0.16\ \mu^{-1}$. This value of a_o is strongly supported by the results of Pennington and Protopopescu[41] who combined analyticity with newer experimental results.

The p-wave phase shift δ_1^1 is much better known because of the strong ρ-resonance. In Figure 11 this phase shift as found by the Berkeley[36] experimental analysis is shown along with two parameterizations of the form

$$\sqrt{\frac{\nu+1}{\nu}}\ \cot \delta_1^1 = \frac{(1-a\nu)(1+b\nu)}{c\nu} . \qquad \text{(III.4)}$$

This is the form used by Morgan and Shaw[28] where the parameters were found to be

(DEGREES)

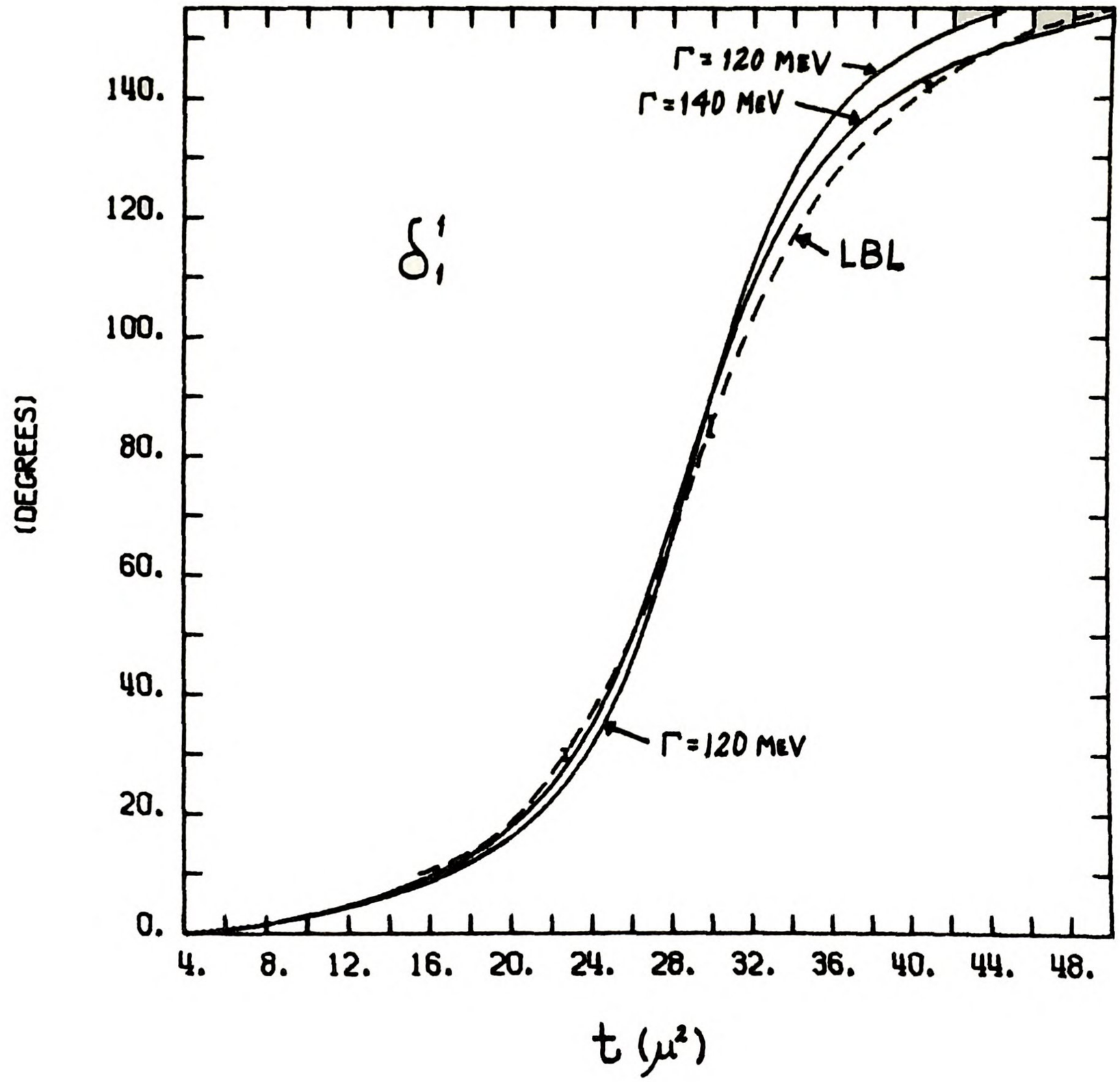

Figure 11. The I=J=1 $\pi\pi$ phase shift.

These p

resonan

($\Gamma_\rho \Xi$-m

Thus,

(m_π =

Nielse

has a

c as

Γ = l

agreem

prima

resul

for t

$$a = 0.1536 ,$$

$$b = 0.028 , \qquad \text{(III.5)}$$

$$c = 0.035 .$$

These parameters are related to the scattering length a_1, resonant mass m_ρ (where $\delta_1^1 = 90°$) and resonant width ($\Gamma_\rho \equiv -m_\rho \frac{\partial}{\partial s} \cot\delta_1^1$) by

$$a_1 = c$$

$$m_\rho = 2\sqrt{\frac{a+1}{a}} \qquad \text{(III.6)}$$

$$\Gamma_\rho = \frac{2c}{\sqrt{a}(a+1)(a+b)} \quad .$$

Thus, the Morgan-Shaw δ_1^1 has a resonant mass of 765 MeV (m_π = 139.576 MeV) and width of 119 MeV.

Another form for δ_1^1 given by Olsson[42] and used by Nielsen and Oades[15] is completely equivalent to (III.4) and has a width of 120 MeV. and scattering length 0.035.

The second curve in Figure 11 is (III.4) with a and c as in Morgan and Shaw but with b changed to 0.00076, or Γ = 140 MeV. This second curve is in considerably better agreement with the experimental phase shift. However, of primary importance to us is the Omnès function which results from this phase shift. This subject is reserved for the section on the p-wave $N\bar{N}\to\pi\pi$ amplitudes.

However
unimpor
is that

which
Munich

The CE
inelas
4π dec
Γ(4π)/
expres
degree

(III.
become
consi
ρ mas
the e
the n
MeV w
analy
elast
The p
1 GeV

The d-wave phase shift is rather poorly known. However, we shall see that its precise value is rather unimportant because of its small size. The form used here is that of Morgan and Shaw[28]

$$\sqrt{\frac{\nu}{\nu+1}}\ \cot\delta_2^0 = \frac{(1-0.0524\nu)(1+0.204\nu+0.0015\nu^2)}{0.0015\,\nu^2}, \qquad \text{(III.7)}$$

which exhibits a resonance at the f° mass, t=80. The CERN-Munich[37] $\pi\pi$ analysis found the d-wave resonance at t=83. The CERN-Munich analysis, however, found considerable inelasticity, $\eta \simeq 0.6$, at resonance. The situation regarding 4π decay of the f° is still hazy, but the branching ratio $\Gamma(4\pi)/\Gamma(2\pi)$ is generally agreed to be very small.[43] The expression (III.7) indicates that δ_2^0 reaches about eight degrees at 1 GeV.

A meaningful application of the unitarity relation (III.1) requires that we know where the $\pi\pi$ amplitudes become appreciably inelastic. All analyses have been consistent with elastic s- and p-wave amplitudes below the ρ mass. Baton et al.[34] analyzed the data with and without the elasticity constraint on the s-wave δ_0^0 and found that the now-preferred down solution remains elastic up to 800 MeV where inelasticity gradually sets in. More recent analyses[36,37] have found the s-wave amplitude essentially elastic to 1 GeV where it becomes very strongly inelastic. The p-wave δ_1^1 also appears to be essentially elastic to 1 GeV.

6π bra

that t

(t=50)

consta

Omnès

isospi

t=0.

relati

field

able ν

subtra

scatte

$A^{(+)}$ c

A

These results indicate that the 4π and possibly the 6π branch cuts in the $N\bar{N}\to\pi\pi$ helicity amplitudes are weak so that the unitarity relation may be useful to about 1 GeV ($t\simeq 50$).

C. Evaluation of $A^{(+)}$ and $\partial A^{(+)}/\partial t$ at $s=u$, $t=0$

In preparation for determining the subtraction constants to be used in a J=0 twice subtracted form of the Omnès dispersion relation (III.3) we first evaluated the isospin-even πN amplitude $A^{(+)}$ and its derivative at $s=u$, $t=0$. The evaluation was performed via πN fixed-t dispersion relations, which have been rigorously proven in quantum field theory.[44]

The dispersion relations were written in the variable $\nu = \frac{s-u}{4m}$ and subtracted once at $\nu_c = 1+\frac{t}{4m}$ where the subtraction terms could be written in terms of the πN scattering lengths.

The amplitude $A^{(+)}$ satisfies the relation

$$A^{(+)}(\nu,t) = A^{(+)}(\nu_c,t) + \frac{2(\nu^2-\nu_c^2)}{\pi}\int_{\nu_c}^{\infty} \frac{\nu' \,\mathrm{Im}\, A^{(+)}(\nu',t)}{(\nu'^2-\nu_c^2)(\nu'^2-\nu^2)}\, d\nu'. \quad \text{(III.8)}$$

It is necessary to define

$$A'^{(+)}(\nu,t) = A^{(+)}(\nu,t) + \frac{\nu}{1+t/(4m^2)} B^{(+)}(\nu,t). \quad \text{(III.9)}$$

which

(III.8

tudes

The am

$1+\frac{t}{4m}$ a

includ

A

B

A

which also satisfies a dispersion relation of the form (III.8).

The scattering lengths for the isospin even amplitudes are written in the following notation:

$a_0^{(+)}$ s-wave ,

$a_{1\pm}^{(+)}$ p-wave with $J=1\pm 1/2$,

$a_{2\pm}^{(+)}$ d-wave with $J=2\pm 1/2$.

The amplitudes $A^{(+)}$ and $A'^{(+)}$ can be written for $\nu=\nu_c=1+\frac{t}{4m}$ as follows. For completeness the expression $B^{(+)}$ is included.

$$A^{(+)}(\nu_c,t) = 8\pi\left[\frac{2m+1}{4m}\left(a_0^{(+)}+\frac{3}{2}a_{1+}^{(+)}t\right) - m\left(a_{1-}^{(+)}-a_{1+}^{(+)}+\frac{3}{2}(a_{2-}^{(+)}-a_{2+}^{(+)})t\right)\right] \quad \text{(III.10a)}$$

$$B^{(+)}(\nu_c,t) = 8\pi\left[\frac{1}{4m}\left(a_0^{(+)}+\frac{3}{2}a_{1+}^{(+)}t\right) + m\left(a_{1-}^{(+)}-a_{1+}^{(+)}+\frac{3}{2}(a_{2-}^{(+)}-a_{2+}^{(+)})t\right)\right] \quad \text{(III.10b)}$$

$$A'^{(+)}(\nu_c,t) = 4\pi\,\frac{m+1}{m}\left[a_0+\left(\frac{a_0^{(+)}}{8m^2}+\frac{1}{2}a_{1-}^{(+)}+a_{1+}^{(+)}\right)t+O(t^2)\right] \quad \text{(III.10c)}$$

$a_{1+}^{(+)}$

its p

for s

the i

$A^{(+)}(v$

we not

tract

The presence of the d-wave scattering lengths makes $A^{(+)}(\nu_c,t)$ useful only for t=0. To determine the derivative we note that at $\nu=0$ crossing symmetry implies that

$$\frac{\partial}{\partial t} A'^{(+)}(\nu,t)\Big|_{\text{fixed }\nu} = \frac{\partial}{\partial t} A'^{(+)}(\nu,t)\Big|_{\text{fixed s.}} \qquad \text{(III.11)}$$

The following expressions are the necessary subtraction terms.

$$A^{(+)}(1,0) = 8\pi m\left[\frac{2m+1}{4m^2}\, a_0^{(+)} + a_{1+}^{(+)} - a_{1-}^{(+)}\right] \qquad \text{(III.12a)}$$

$$\simeq 8\pi m\left[\,0.08\, a_0^{(+)} + a_{1+}^{(+)} - a_{1-}^{(+)}\right]$$

$$\frac{\partial}{\partial t} A'^{(+)}(\nu,t)\Big|_{\substack{t=0\\ \text{fixed s}}} = 4\pi\,\frac{m+1}{m}\left[\frac{a_0^{(+)}}{4m^2} + \frac{1}{2}\, a_{1-}^{(+)} + a_{1+}^{(+)}\right] \qquad \text{(III.12b)}$$

$$\simeq 4\pi\,\frac{m+1}{m}\left[0.0028\, a_0^{(+)} + \frac{1}{2} a_{1-}^{(+)} + a_{1+}^{(+)}\right].$$

As we shall see, $a_0^{(+)}$ is quite small compared to $a_{1+}^{(+)}$ and the subtraction terms are only weakly dependent on its precise value.

In terms of the scattering lengths a_{2T} and $a_{2T,2J}$ for s- and p-waves of definite isospin and angular momentum, the isospin-even combinations are

$$a_0^{(+)} = \tfrac{1}{3}(a_1 + 2a_3),$$

$$a_{1-}^{(+)} = \tfrac{1}{3}(a_{11} + 2a_{31}),$$

poorly

We use

Carter

althou

larges

in Tab

$(a_{13}+2$

have

binati

and o

limit

$(a_{13}+$

for d

$B^{(+)}$

finit

lengt

uncer

and

$$a_{1+}^{(+)} = \frac{1}{3}(a_{13}+2a_{33}) \quad . \qquad \text{(III.13)}$$

The s-wave scattering length $a_o^{(+)}$ is particularly poorly known. A partial compilation is given in Table 1. We used the value found recently by Bugg, Carter, and Carter[45] from forward πN dispersion relations.

The isospin even p-wave scattering lengths, although much better known than the s-wave, produced the largest uncertainty in our results. A compilation is given in Table 2. It is seen that the relevant combinations $(a_{13}+2a_{33}) - (a_{11}+2a_{31})$ and $(a_{13}+2a_{33}) + 1/2\ (a_{11}+2a_{31})$ have just less than a 3% variation. In the latter combination, however, the results of Hamilton and Woolcock[46] and of Höhler et al.[47] are about identical. The 0.7% error limit given by Bugg et al.[45] for the p-wave combination $(a_{13}+2a_{33}) - (a_{11}+2a_{31})$ is remarkably small. Their method for determining this combination involves evaluating the $B^{(+)}$ dispersion relation at threshold using the f^2 found at finite energies. However, the quoted p-wave scattering-length uncertainty is smaller than that produced by their uncertainty in f^2 alone. We have used the values

$$(a_{13}+2a_{33})-(a_{11}+2a_{31}) = 0.571 \pm 0.010 \qquad \text{(III.14a)}$$

and

$$(a_{13}+2a_{33})+\tfrac{1}{2}(a_{11}+2a_{31}) = 0.310 \pm 0.010 \quad . \qquad \text{(III.14b)}$$

Table

a.
0.055
-.002
-.005
-.014
+.003
-.023
-.073
-.021
-.070
-.088

diffe
-.006

Table 1.--A compilation of s-wave πN scattering length determinations.

a_1+2a_3	First Author (Ref.)	Method
$0.0557 \pm .0155$[a]	Lovelace (56)	backward d.r.
$-.002 \pm .008$	Hamilton (57)	low energy $\pi^{\pm}$ p data
$-.005 \pm .009$[b]	Hamilton (46)	forward d.r. and sum rule + Pan. ratio
$-.014 \pm .005$	Bugg (45)	forward d.r.
$+.0031 \pm .008$	Samaranake (58)	forward d.r.
$-.023 \pm .015$	Hald (59)	forward d.r.
$-.073$[c]	Engels (55)	forward d.r.
-.021	Höhler (47)	partial wave d.r.

[a]Values quoted are $a_1 = 0.1957 \pm .0111$ and $a_3 = -.0700 \pm .0054$.

[b]Values quoted are $a_1 = 0.171 \pm .005$ and $a_3 = -.088 \pm .004$.

[c]Several values quoted in reference corresponding to different applications of forward d.r. Values range from -.006 to -.073.

Table

a_{11}
-.177
-.168
-.173

The r

a

with

a_{2T} 2 error

Table 2.--A compilation of p-wave πN scattering length determinations.

$a_{11} + 2a_{31}$	$a_{13} + 2a_{33}$	First Author (Ref.)	Method
$-.177 \pm .012^a$	$0.401 \pm .011^a$	Hamilton (46)	forward d.r. + sum rule + Pan. ratio
$-.168 \pm .02^a$	$0.396 \pm .02^a$	Höhler (47)	partial wave d.r.
$-.173 \begin{smallmatrix}+.009\\-.014\end{smallmatrix}$	$0.390 \begin{smallmatrix}+.014\\-.016\end{smallmatrix}$	Engels (55)	forward d.r.

The result of Bugg (45)

$$a_{11} + 2a_{31} - (a_{13} + 2a_{33}) = -.570 \pm .004$$ is consistent with the values above.

[a]Values quoted by authors are for individual $a_{2T,2J}$. Errors given here assume no correlation in quoted errors and therefore may be inaccurate.

which

by the

shift

These

severa

its t-

were

set.

exten

energy

Barge

dispe

input

sets.

The v

Table

et al

deter

inclu

which are consistent with all values in Table 2.

The imaginary parts of the πN amplitudes required by the dispersion relations were calculated from phase shift solutions as supplied by the Particle Data Group.[48] These included Glasgow A and B,[49] Saclay,[50] Roper,[51] and several CERN[52] solutions. The results for both $A^{(+)}$ and its t-derivative are dominated by the subtraction terms and were rather insensitive to the choice of πN phase shift set. Except for the Roper solution, these phase shifts extend to about 2 GeV center-of-mass energy. Above this energy we have used the two-Pomeron pole parameterization of Barger and Phillips.[53] However, the once subtracted dispersion integrals were insensitive to this high energy input. Table 3 gives the results for several phase shift sets. The following values summerize this work.

$$A^{(+)}(s=u, t=o) = 25.9 \pm 0.5 \qquad \text{(III.15a)}$$

$$\frac{\partial}{\partial t} A^{(+)}(s=u, t)\Big|_{t=o} = 1.16 \pm 0.05 \qquad \text{(III.15b)}$$

The value of $A^{(+)}$ is compared to other determinations in Table 4. The slope is consistent with that of Höhler et al.[54] (1.15 ± 0.1), Engels,[55] and Nielsen.[27]

Since in many cases the πNN coupling constant was determined along with the scattering lengths, we have included in Table 5 a compilation of the f^2 results.

Table

CERN	
CERN	
Roper	
Roper	

Table

First
Samar
Höhle
Engel
Niels
Adler
This

Calcu

Table 3.--Results for $A^{(+)}(0,t)$ and its derivative at t=0.

Phase Shifts	$A^{(+)}(s=u,t=0)$	$\frac{\partial}{\partial t}A^{(+)}(s=u,t)\,\vert\,t=0$
CERN EXP (Kirsopp or Wagner)	25.9	1.16
CERN (Almehed, Lovelace)	25.8	1.16
Roper + Glasgow A	25.9	
Roper + Saclay min. path	25.8	

Table 4.--Results of various authors for $A^{(+)}(0,0)$.

First Author (Ref.)	$A^{(+)}(s=u,t=0)$
Samaranayake[a] (60)	24.6 $\pm$ 0.4
Höhler (54)	26.1 $\pm$ 0.3
Engels (55)	26.0
Nielsen (27)	26.1
Adler (11)	26.15 $\pm$ 0.2
This work	25.9 $\pm$ 0.5

[a]See Ref. 58 for comments on the input to this calculation.

Table

0.078
0.076
0.078
0.077
0.076
0.076
0.081
0.079
0.081
0.083
0.074
0.080

value

this

Table 5.--A compilation of πNN coupling constant determinations.

f^2	First Author (Ref.)	Method
$0.0787 \pm .0034$[a]	MacGregor (61)	N.N. Scatt., no dist. for $\pi\pm$, $\pi°$
$0.076 \pm .005$	Bilen'kaya (62)	Same
0.078[b]	Cutkosky (63)	analytic approx theory 350 MeV
0.077[c]	Cutkosky (63)	400 MeV n-p data w/ Form Factor
$0.0763 \pm .002$	Samaranake (58)	forward d.r. for lab. amp.
$0.0816 \pm .0029$	Hald (59)	forward d.r. for lab. amp.
$0.0790 \pm .0010$	Bugg (45)	d.r. for $B^{(\pm)}$
$0.081 \pm .002$	Hamilton (46)	forward d.r. + sum rule $\pm$ Pan. ratio
$0.083 \pm .005$	Höhler (47)	d.r. for $B^{(+)}$, CERN forw. amps
$0.074 \pm .01$	Höhler (47)	d.r. for $F^{(-)}$, CERN forw. amps, CEX forward cross sections
$0.0803 \pm .0010$[d]	Lichard (64)	analytic continuation of $F^{(-)}(\omega)/\omega$

[a]Value uses $\pi°$ mass. Charged pion mass raises value by 7%.

[b]Quoted as $g^2/4\pi = 14.1\ (+1.4,-0.8)$.

[c]Quoted as $g^2/4\pi = 13.9\ (+1.6,-1.7)$.

[d]See Ref. 58 regarding the uncertainty quoted in this result.

An ex

Pilku

$A^{(+)}$.

tribu

where

t=0,

dispe

As wa

we in

for D

at t>

ampli

J>4 p

the n

J>2-w

mate

parts

An extensive compilation of πN parameters was given by H. Pilkuhn et al., Nucl. Phys. B65, 460 (1973).

D. The $N\bar{N}\to\pi\pi$ s-Wave Amplitude: $A^{(+)}$ Fixed-ν Dispersion Relation

The $N\bar{N}\to\pi\pi$ s-wave amplitude contributes only to $A^{(+)}$. In terms of the helicity amplitude f_+^o this contribution is

$$A^{(+)}_{J=0}(\nu,t) = \frac{4\pi}{p_-^2} f_+^o(t) , \qquad \text{(III.16)}$$

where $p_-^2 = m^2 - t/4$.

The values (III.15) of $A^{(+)}(0,0)$ and $\frac{\partial}{\partial t} A^{(+)}(0,t)\,|_{t=0}$, previously discussed, have been used in a fixed-ν dispersion relation for $A^{(+)}$ to determine the low-t $f_+^o(t)$. As was the case for the partial-wave Omnès relation (III.3), we introduced the s-wave Omnès function $D_o(t)$ and dispersed for $D_o(t)\ A^{(+)}(0,t)$. This function maintains the right cut at t>4 which can, however, be evaluated with the d-wave amplitudes f_+^2 yet to be described. We assumed that all $J\geq 4$ partial wave amplitudes are adequately represented by the nucleon pole (Born) amplitude. The smallness of the $J\geq 2$-wave ππ phase shifts allowed us to accurately approximate the $J\geq 2$ partial wave amplitudes f_+^J by their real parts. The twice subtracted dispersion relation reads

D

where

4mμ~-

for 0

two s

for a

depen

that

intro

negat

conti

where

Then

$$D_0(t)A^{(+)}(0,t) = A^{(+)}(0,0) + t\frac{\partial}{\partial t'}\left[D_0(t')A^{(+)}(0,t')\right]_{t'=0}$$

$$+I_L + \frac{t^2}{\pi}\int_4^\infty \frac{|D_0(t')|\mathrm{Re}\left[e^{-i\delta_0^0(t')}A^{(+)}_{J\geq 2}(0,t')\right]\sin\delta_0^0(t')}{(t')^2(t'-t)}\,dt', \tag{III.17}$$

where

$$A^{(+)}_{J\geq 2} = A^{(+)} - \frac{4\pi}{p^2}f_+^0 .$$

The contribution from the left cut beginning at $t = 4m_\mu \simeq -27$ is represented by I_L. This contribution is small for $0 \leq t \leq 4$ because of the distance of the left cut and the two subtractions in (III.17). Nevertheless, I_L is necessary for an accurate evaluation of f_+^0. Because of the weak dependence on the left cut discontinuity and the expectation that only its leading edge ($t \simeq -4m_\mu$) will be important, we introduced a simple parameterization and extrapolated from negative to positive t. We represented the left cut discontinuity by

$$D_0(t)\,\mathrm{Abs}\,A^{(+)}(0,t) = \alpha\sqrt{-t-b}, \tag{III.18}$$

where $b = 4m_\mu$ and $t \leq -b$.

Then

$$I_L = \alpha\frac{t^2}{\pi}\int_{-\infty}^{-b}\frac{\sqrt{-t'-b}\;dt'}{(t')^2(t'-t)}$$

$$= \alpha\left(\sqrt{b+t} - \sqrt{b} - \frac{t}{2\sqrt{b}}\right). \tag{III.19}$$

To de

fixed

With

Figur

$A^{(+)}_{J\geq 2}$

the

evalu

in a

dispe

sens

of f

mina

To determine α equation (III.17) was compared with the fixed-t dispersion results of Nielsen at t=-5 and -10. With the Morgan-Shaw[28] δ_o^o we found $\alpha \simeq 29\mu^{-2}$.

Results for $A^{(+)}(0,t)$ and $f_+^o(t)$ are shown in Figures 12, 13, 14. For $t>4$ f_+^o was obtained by subtracting $A^{(+)}_{J\geq 2}$ from $A^{(+)}$. We have used t=80 for the upper limit in the integrand (III.17).

An important product of this calculation was the evaluation of $A^{(+)}(0,4) = \frac{16\pi}{m^2-1} f_+^o(4)$, which will be used in a second calculation of $f_+^o(t)$. The s-wave Omnès dispersion relation subtracted at t=0 and t=4 is very sensitive to the value at t=4 so an accurate determination of $f_+^o(4)$ is required. We list the input to the determination of $f_+^o(4)$:

a. s-wave $\pi\pi$ phase shift δ_o^o. The Morgan-Shaw preferred solution is used to $t \simeq 50$ where δ_o^o is turned downward and extended to ∞ as 1/t.

b. Subtraction constants $A^{(+)}(0,0) = 25.9$ and $\frac{\partial}{\partial t} A^{(+)}(0,t)\big|_{t=0} = 1.16$.

c. Left cut discontinuity approximated as described above.

d. The higher partial wave amplitudes $A^{(+)}_{J\geq 2}$ from partial wave Omnès relation (J=2) and the nucleon pole ($J \geq 4$). The value $\tilde{f}_+^2(24)$ was used for $\tilde{f}_+^2(t \geq 24)$.

ر-ر

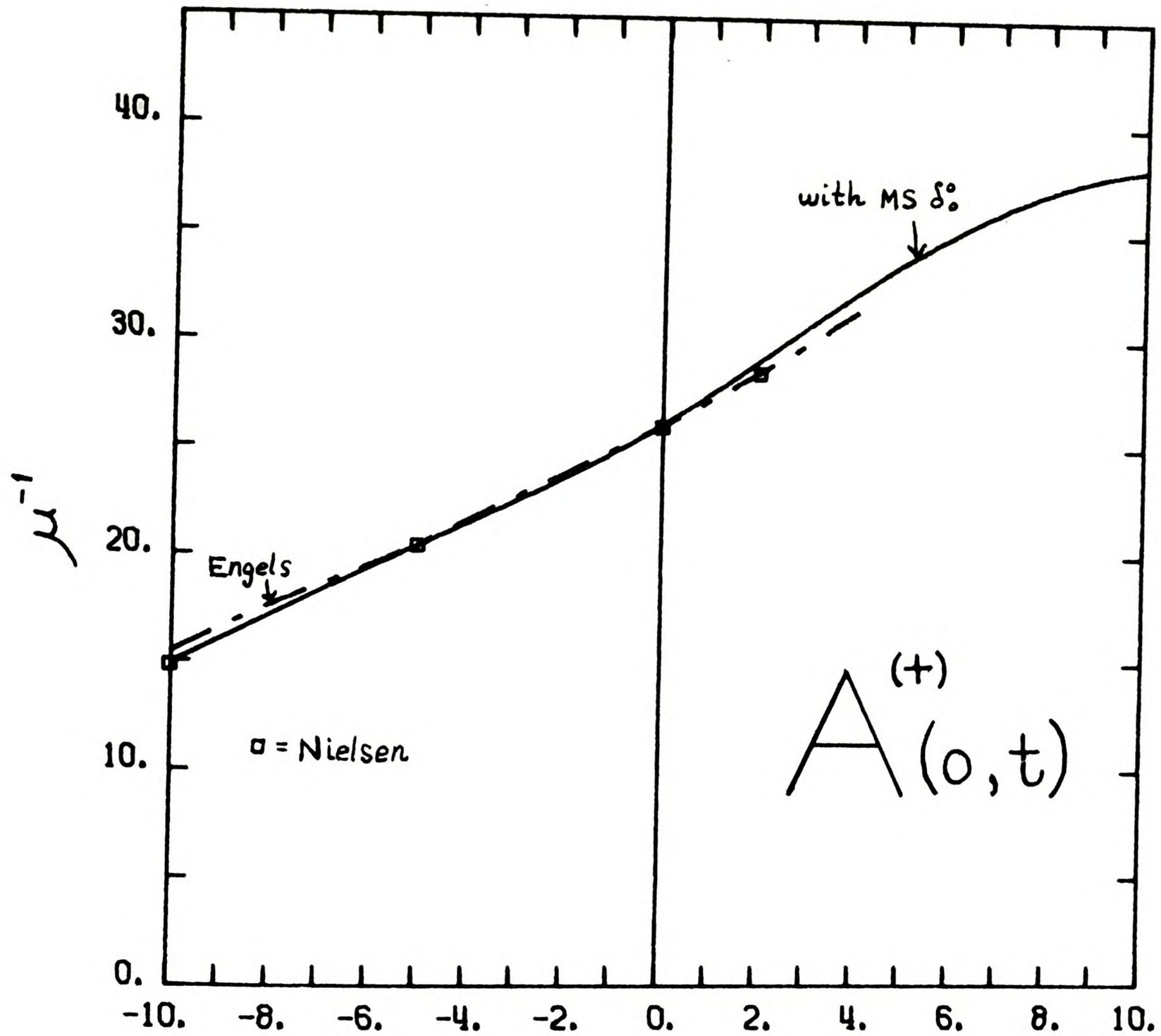

Figure 12. The πN amplitude $A^{(+)}$ along s=u.

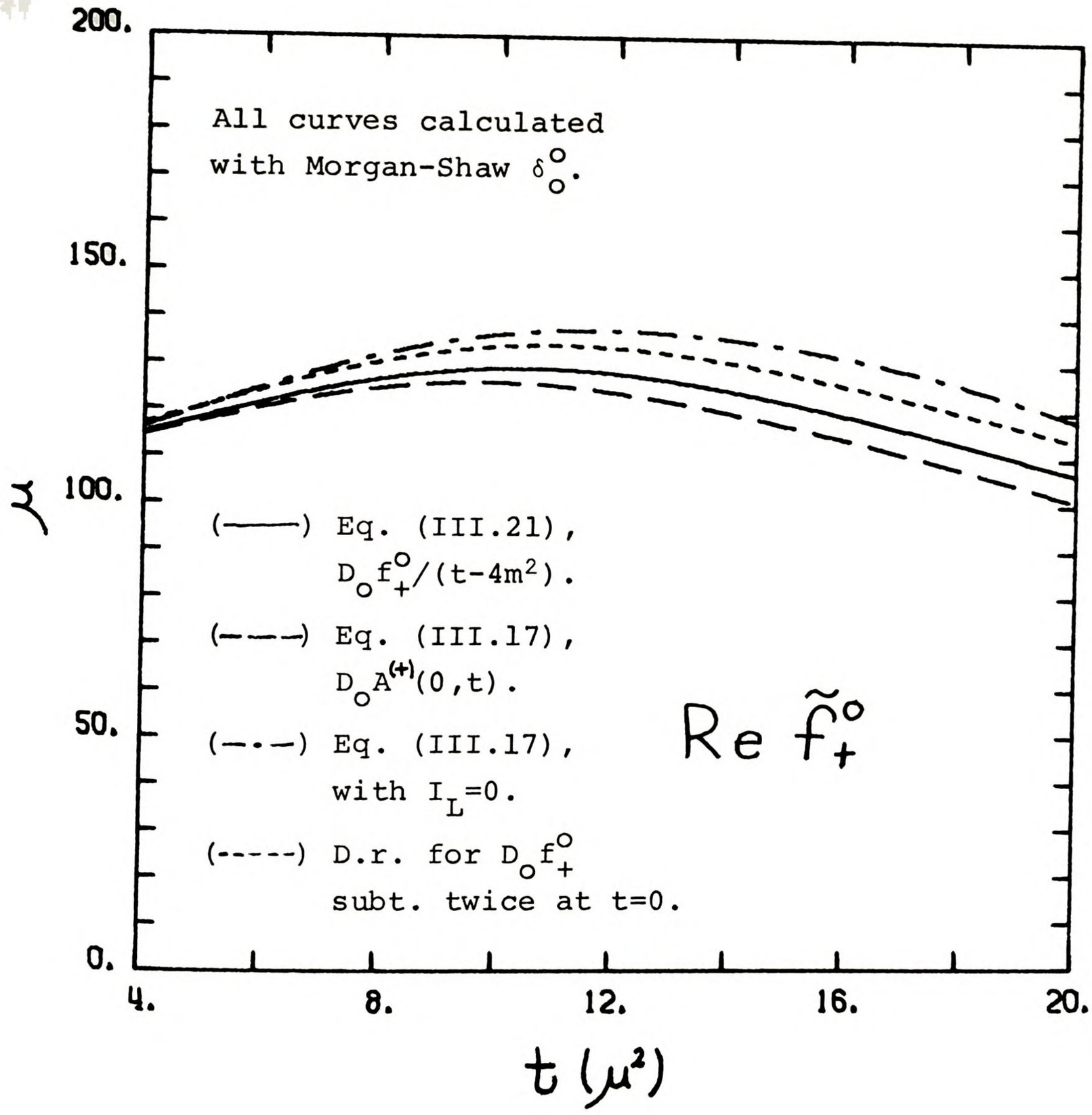

Figure 13. Real part of the $N\bar{N}\to\pi\pi$ amplitude f^0_+.

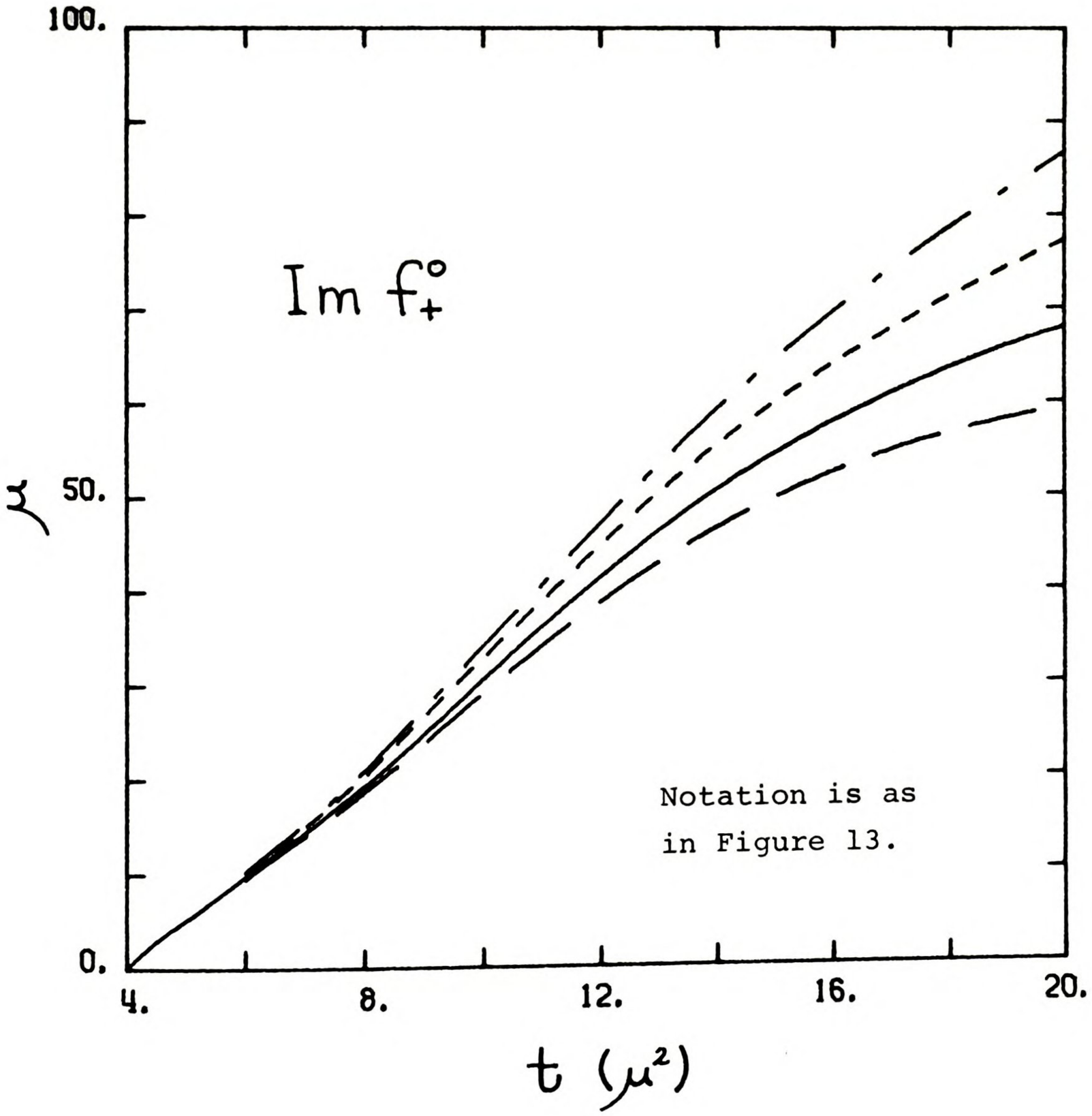

Figure 14. Imaginary part of the $N\bar{N}\to\pi\pi$ amplitude f_+^0.

e

The

abov

we h

t=15

the

Figu

f_+^o(4

cula

plet

Usir

f_+^o(4

agre

smo

at

pha

det

and

lli

e. The analyticity structure of $A^{(+)}(0,t)$ and $f_+^{o,2}(t)$. Mandelstam analyticity is sufficient. With this input we found

$$f_+^0(4) = 114. \pm 2. \qquad \text{(III.20a)}$$

The error limit is intended to include uncertainty in the above inputs (b) through (d). As an alternate phase shift we have used the Berkeley[36] energy dependent results above t=15 appended to the low energy phase shift predicted by the Morgan-Shaw[65] model. This phase shift is shown in Figure 15. The result with otherwise the same input was $f_+^o(4) = 115$. On the other hand, extrapolating the calculated $\tilde{f}_+^2$ linearly to t=80 reduced $f_+^o(4)$ to 113. Completely neglecting the left cut in (III.1) gave $f_+^o(4) = 116$. Using the Morgan-Shaw δ_o^o extended beyond t=50 as $1/t^3$ gave $f_+^o(4) = 113$.

In Figures 10, 15 we have shown a δ_o^o constructed to agree with the Geneva-Saclay[39] K_{e4} decay results and join smoothly with the Berkeley[36] energy dependent phase shift at t=20. With otherwise the same input as for (III.20) this phase shift, designated GS+LBL, gave $\alpha=29$ and

$$f_+^o(4) = 118. \pm 2. \qquad \text{(III.20b)}$$

The values (III.20) of $f_+^o(4)$ can be compared to determinations by fixed-t dispersion relations. Engels[55] and Höhler et al.[47] each obtained $A^{(+)}(0,4) = 31.5$, $f_+^o(4) = 111$. Nielsen's[27] tables can be extrapolated by hand to

DEGREES

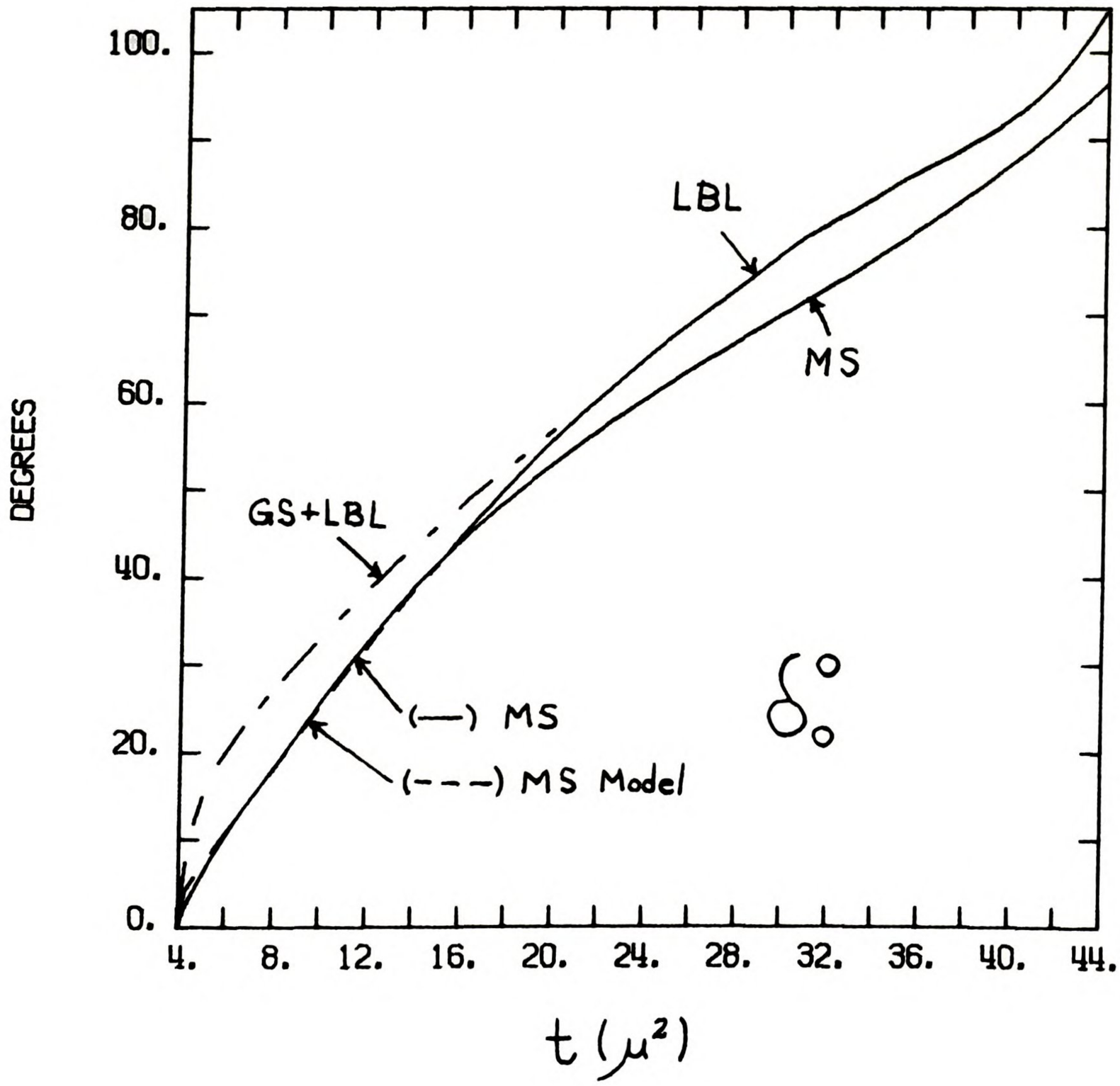

Figure 15. The I=J=0 $\pi\pi$ phase shifts used in the calculations.

imply
are o
of πN
Niels
and Z
ampli
optim
extra
one a
erro
the
GS+L
are
Howe
The
sign
mor
sho
pse
cal
kin
wri

imply $A^{(+)}(0,4) = 31.6$, $f_+^o(4) = 111$. However, such values are of questionable accuracy since they involve continuation of πN amplitudes by Legendre polynomials to the branch cut. Nielsen appropriately terminated his tables at t=3. Chao and Zia[66] have studied the problem of continuing πN amplitudes to the ππ cut. They found that using an optimized expansion they could place an upper bound on the extrapolation error. The upper bound rises very sharply as one approaches the cut. With a Legendre expansion the error bound may be smoother and probably larger than for the optimized expansion.

That we found the same α for both the MS and GS+LBL phase shifts means that the results for $A^{(+)}(0,t<0)$ are very weakly dependent on the s-wave ππ interaction. However, we note the nonlinearity of $A^{(+)}(0,t)$ for $0<t<4$. The 4% change in $f_+^o(4)$ resulting from the change in δ_o^o is significant for the NN two-pion-exchange problem.

E. The $N\bar{N}\to\pi\pi$ s-Wave Amplitude: Omnès Dispersion Relations

The partial wave Omnès relation provides a second, more conventional, way to obtain $f_+^o(t)$. The left cut, as shown in Figure 8, begins at $t=a\equiv 4-1/m^2\approx 3.97$, very near the pseudophysical threshold, but the discontinuity can be calculated for $t>-26$ from πN phase shifts. Because of a kinematical zero[25] at $t=4m^2$ the dispersion relation may be written for $D_o f_+^o$ or for $D_o f_+^o/(t-4m^2)$. The latter is

(II

con

The

a I

f°_{+}

and

sub

tra

Re

wh

Ni

(I

t=

pa

In

exp

rel

expected to converge more rapidly on the left cut. The relevant disperion relation is

$$\frac{D_0(t)\, f_+^0(t)}{t-4m^2} = \frac{(t-4)\, f_+^0(0)}{16m^2} + \frac{t\, D_0(4)\, f_+^0(4)}{4(4-m^2)}$$

$$+ \frac{t(t-4)}{\pi}\int_{-\infty}^{a} \frac{D_0(t')\, \mathrm{Im} f_+^0(t')}{t'(t'-4)(t'-4m^2)(t'-t)}\, dt' \quad . \qquad \text{(III.21)}$$

Twice subtracted dispersion relations such as (III.21) are quite sensitive to error in the subtraction constants because of the multipliers proportional to t. The large size of $f_+^0(4)$ produces a particular problem where a 1% uncertainty in $f_+^0(4)$ produces about 10% uncertainty in $|f_+^0(20)|^2$. The value of $f_+^0(0)=-2.8$ was found by Furuichi and Watanabe[67] using the partial wave projection of a once-subtracted fixed t dispersion relation for $A^{(+)}$. The subtraction constant in that calculation, $A^{(+)}(0,0)$, taken from Reference 60, can be replaced by the value (II.15a) to give

$$f_+^0(0) = -2.4 \qquad \text{(III.22)}$$

which was used in all of our evaluations of (III.21).

The imaginary part of $\tilde{f}_+^0(t<a)$ was obtained from Nielsen's[27] tables. We have cut off the integral in (III.21) at t'=-35, extrapolating Im $\tilde{f}_+^0(t)$ by hand from t=-25 to t=-35. This extrapolation is a reasonable compromise between cut off error and uncertainty in Im $\tilde{f}_+^0(t<-25)$.

the pha

the dis

are sho

Figures

with th

labelle

118. W

t>20.

$f_+^0(4)$,

among t

three t

of $f_+^0(4$

a calcu

$D_0(t)f_+^0$

calcula

extrapo

and the

we used

The results from (III.21) are somewhat sensitive to the phase of $f_+^o(t>50)$ which is unknown. We have evaluated the dispersion relation with t>50 phases of the form

$$\delta(t) = (50/t)^n \, \delta(50).$$

The results for the s-wave spectral function

$$\rho_o^{(+)} = 8\pi \sqrt{\frac{t-4}{t}} \left| \frac{f_+^o(t)}{4m^2-t} \right|^2$$

are shown in Figure 16. We have also shown results in Figures 13, 14. The curves labelled S1 have been calculated with the Morgan-Shaw phase shift δ_o^o and $f_+^o(4)=114$. Those labelled S2 were calculated with the GS$\pm$LBL δ_o^o and $f_+^o(4)=118$. We see that the t>50 phase affects $|f_+^o(t)|$ mostly at t>20. Although the GS$\pm$LBL phase shift gave a larger $f_+^o(4)$, it gives a smaller $|f_+^o(t>5.7)|$.

There is a considerable amount of cancellation among the three terms of (III.21). Table 6 shows these three terms at various values of t. We see the importance of $f_+^o(4)$ and the relative unimportance of $\mathrm{Re}f_+^o(0)$.

In Figures 13, 14 we have also shown the results of a calculation using a dispersion relation written for $D_o(t)f_+^o(t)$ subtracted twice at t=0. The input to this calculation included the M-S δ_o^o, Nielsen's[27] $\mathrm{Im}\tilde{f}_+^o(t<a)$ extrapolated to t=-45, $\mathrm{Re}f_+^o(0)=-2.4$ as discussed previously, and the derivative of $\mathrm{Re}f_+^o(t)$ at t=0. For the derivative we used

which wa

the t>50

smoothly

Table 6.

t	Su
5	
10	
20	
30	

than tha

value 2

$f_+^0(4)=1$

-2.8, th

$A^{(+)}(0,$

$f_+^0(4)=1$

(III.17

$$\frac{\partial}{\partial t}\mathrm{Re}\ f_+^o(t)\big|_{t=0} = 3.2\ ,$$

which was obtained from the tables of Reference 27. For the $t>50$ f_+^o phase we used n=1 but allowed the phase to turn smoothly over at t=50.

Table 6.--Contributions to the s-wave dispersion relation with MS phase shift.

t	t=0 Subtraction	t=4 Subtraction	Disperion Integral	Total
5	-102.5	-19487.	13110.	-6480.
10	-580.7	-36788.	29103.	-8266.
20	-1372.	-65212.	55427.	-11157.
30	-1961.	-86027.	75355.	-12633.

The derivative value quoted above is much larger than that used by Epstein and McKellar[16] who found the value 2.0 by forcing the disperion relation to give $f_+^o(4)=111$. In addition, Epstein and McKellar used $\mathrm{Re}f_+^o(0)=-2.8$, the value found by Furuichi and Watanabe[67] using $A^{(+)}(0,0)$ from Reference 60.

With our calculation, derivative=3.2, we found $f_+^o(4)=117$, somewhat larger than we found from Equation (III.17) with the MS δ_o^o.

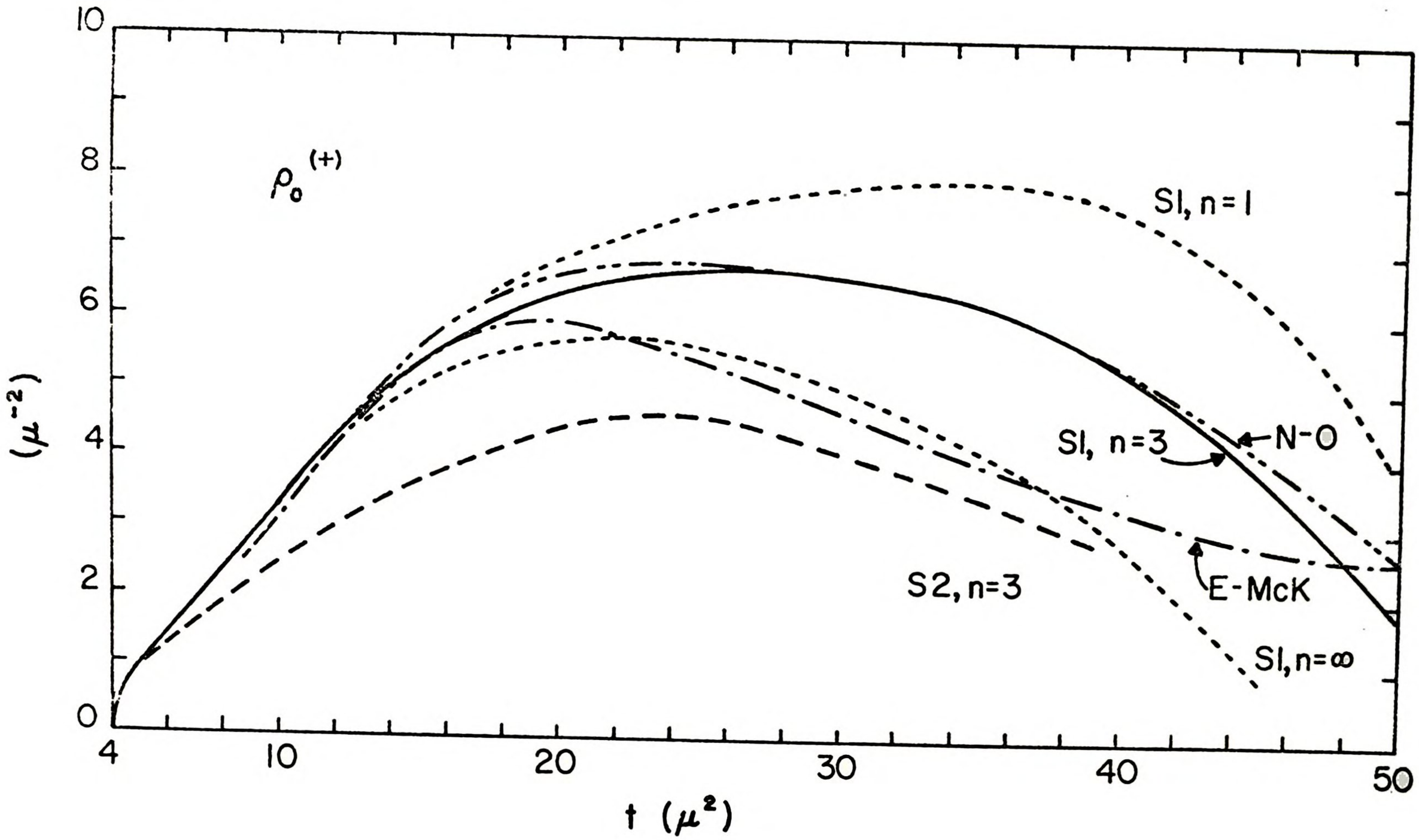

Figure 16. The J=0 spectral function.

siderati

They are

the nucl

the inve

The pea

shift δ

differe

are the

Orsay[69]

by Niel

Morgan

already

approx.

form f

t=50.

neglec

unitar

followi

F. The p-Wave $N\bar{N}\to\pi\pi$ Amplitudes and the Nucleon and Pion Electromagnetic Form-Factors

The p-wave $N\bar{N}\to\pi\pi$ amplitudes require special consideration because of the presence of the strong ρ resonance. They are of special interest because of their relation to the nucleon electromagnetic form factors.

The p-wave Omnès function $D_1(t)$ is approximately the inverse of the pion electromagnetic form factor F_π.[68]

$$F_\pi(t) \simeq \exp\left[\frac{t}{\pi}\int_4^\infty \frac{\delta_1'(t')}{t'(t'-t)}\,dt'\right] \qquad \text{(III.23)}$$

The peak of F_π near the ρ mass is sensitive to the phase shift δ_1^1. In Figure 17 we show $|F_\pi|$ evaluated with two different rho widths in the expression (III.4). Also shown are the results of the colliding e^+e^- beam experiments at Orsay[69] and Novosibirsk.[70] The value Γ = 120 MeV was used by Nielsen and Oades[15] and is very close to that found by Morgan and Shaw.[28] We used the value Γ = 140 MeV. We have already noted that a rho width of 140 MeV gives a good approximation to the experimental δ_1^1 for $t\leq 50$. The $t>25$ form factor, however, is sensitive to the phase shift above $t=50$. We also note that (III.23) is approximate in that it neglects all but the 2π intermediate state in the $\pi\pi\to\gamma$ unitarity relation.

The amplitudes $f_\pm^1$ were assumed to satisfy the following twice subtracted Omnès dispersion relation.

Fig.

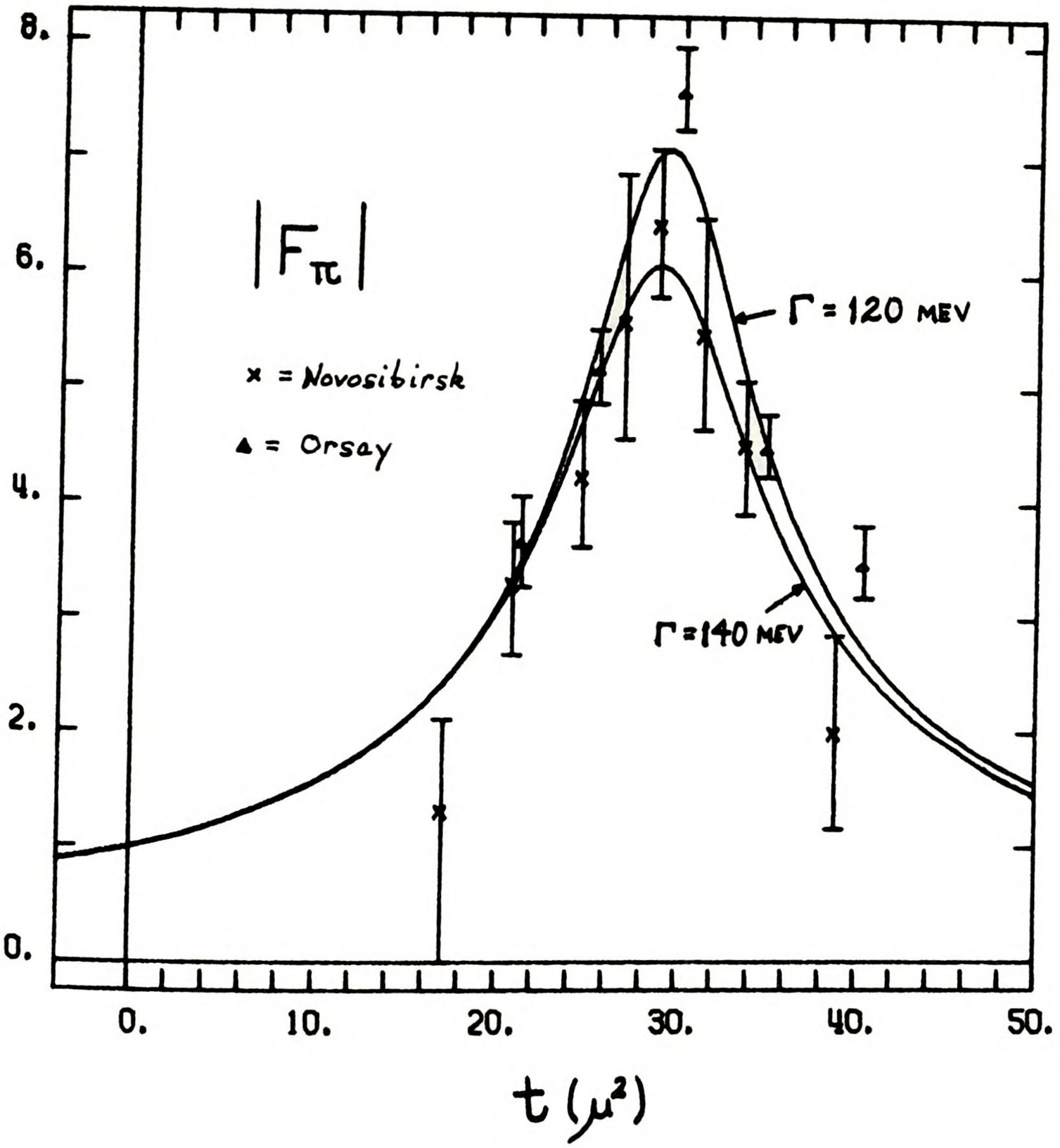

Figure 17. The pion form factor.

$D_1(t)$ -

From Fi

the ρ m

180. I

subtrac

present

fact ha

the p-w

These a

relati

t<10 u

The no

Nielse

the ex

of t=-

(simil

Imf_-^1 a

$$D_1(t) f_\pm^1(t) = f_\pm^1(0) + t\left[\frac{\partial}{\partial t'} D_1(t') f_\pm^1(t')\right]_{t'=0}$$

$$+ \frac{t^2}{\pi}\int_{-\infty}^{a} \frac{D_1(t')\, Im\, f_\pm^1(t')}{(t')^2(t'-t)}\, dt' \quad . \qquad \text{(III.24)}$$

From Figure 17 we see that $D(30) = 1/|F_\pi(30)| \approx 6$ so that at the ρ mass the error in $\frac{\partial}{\partial t} f_\pm^1|_{t=0}$ is amplified by $tD_1(30) \approx 180$. In fact we found that the J=1 dispersion relations subtracted twice at t=0 are not useful above t=10 with presently known values of the subtraction constants. This fact has also been noted by Epstein.[16] When considering the p-wave amplitudes it is convenient to define[25,5]

$$\Gamma_1(t) = \frac{m}{p^2}\left(f_+^1(t) - \frac{t}{4\sqrt{2}m} f_-^1(t)\right) , \qquad \text{(III.25a)}$$

$$\Gamma_2(t) = \frac{1}{2p^2}\left(-f_+^1(t) + \frac{m}{\sqrt{2}} f_-^1(t)\right) . \qquad \text{(III.25b)}$$

These amplitudes are also expected to satisfy dispersion relations of the form (III.24).

From (III.20) we have calculated Γ_2 and f_-^1 for $t<10$ using as subtraction constants the values in Table 7. The non-Born entries were found by interpolation of Nielsen's[27] tables and the Born terms were calculated from the expressions in Appendix B. We have used a lower limit of t=-45 in (III.24) and let $Imf_-^1(t) = Imf_-^1(-25)$ for $-45<t<-25$ (similarly for $Im\Gamma_2(t)$). This lack of knowledge about Imf_-^1 and $Im\Gamma_2$ below t=-25 is a second reason that (III.24)

This f

becaus

near t

tracti

Γ_B

fails f

Figure

tudes

relatio

$D_{,q}$

Table 7

$\mathrm{Re}\ \Gamma_2(0$	
$\mathrm{Re}\ f_-^1(0$	
$\mathrm{Re}\ \frac{\partial}{\partial t}\ \Gamma$	
$\mathrm{Re}\ \frac{\partial}{\partial t}\ f$	fail

Table 7.--The p-wave $N\bar{N}\to\pi\pi$ amplitudes and derivatives at t=0.

	Born	Non-Born	Complete
Re $\Gamma_2(0)$	0.02394	-.0185	0.0054
Re $f_-^1(0)$	-.2280	0.328	0.100
Re $\frac{\partial}{\partial t}\Gamma_2(0)$	-.00566	-.0004	-.0061
Re $\frac{\partial}{\partial t} f_-^1(0)$	0.0554	0.001	0.056

fails for $t\geq 10$. The results for $t<10$ are shown in Figure 18.

A more satisfactory approach to the p-wave amplitudes is to subtract at t=0 and m_ρ^2. The dispersion relation for Γ_i takes the form

$$D_1(t)\Gamma_i(t) = \frac{t_0-t}{t_0}\Gamma_i(0) + \frac{t}{t_0}D_1(t_0)\Gamma_i(t_0) + \frac{t(t-t_0)}{\pi}\int_{-\infty}^{a}\frac{D_1(t')\,\mathrm{Im}\,\Gamma_i(t')}{t'(t'-t_0)(t'-t)}\,dt'. \quad \text{(III.26)}$$

This form of the dispersion relation is difficult to use because the Born contribution to $\mathrm{Im}\Gamma_2$ is rapidly varying near t=a. This rapid variation can be suppressed by subtracting a similar relation for Γ_{Bi}, the Born amplitude,

$$\Gamma_{Bi} = \frac{t_0-t}{t_0}\Gamma_{Bi}(0) + \frac{t}{t_0}\Gamma_{Bi}(t_0) + \frac{t(t-t_0)}{\pi}\int_{-\infty}^{a}\frac{\mathrm{Im}\,\Gamma_{Bi}(t')}{t'(t'-t_0)(t'-t)}\,dt'. \quad \text{(III.27)}$$

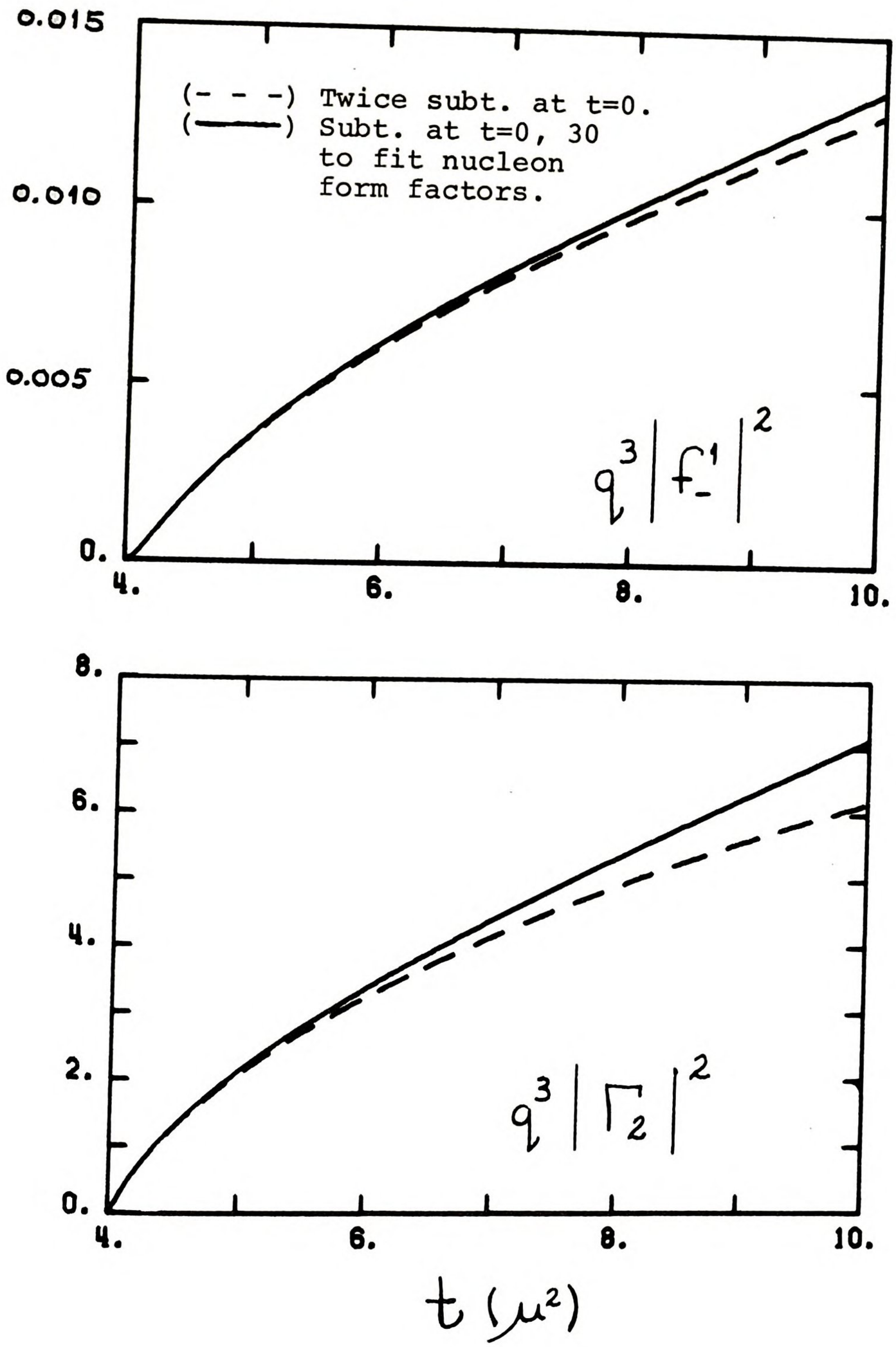

Figure 18. The J=1 $N\bar{N}\to\pi\pi$ amplitudes from twice subtracted dispersion relations.

The res

$D_1($

+

In prac

constar

becaus

Previou

small

maliza-

at pos

by uni-

pion i

factor

pions

two pi

nucleo

The resulting dispersion relation is

$$D_1(t)\,\Gamma_i(t) = \Gamma_{Bi}(t) + \frac{t}{t_o}\left[D_1(t_o)\Gamma_i(t_o) - \Gamma_{Bi}(t_o)\right]$$

$$+ \frac{t_o - t}{t_o}\,\tilde{\Gamma}_i(o)$$

$$+ \frac{t(t-t_o)}{\pi}\int_{-\infty}^{a} \frac{D_1(t')\,\mathrm{Im}\tilde{\Gamma}(t') + [D_1(t')-1]\,\mathrm{Im}\,\Gamma_{Bi}(t')}{t'\,(t'-t_o)\,(t'-t)}\,dt'. \qquad \text{(III.28)}$$

In practice we used $t_o=30$. To determine the subtraction constants at t_o we turned to the nucleon form factors.

The nucleon electromagnetic form factors are useful because the photon isolates the $J=1$ $N\bar{N}\to\pi\pi$ amplitudes. Previous work[5,71,72] has supported the postulate that for small $|t|$ the form factors are determined by their normalization at $t=0$ and the nearest part of their branch cut at positive t. The discontinuity along this cut is given by unitarity as depicted in Figure 19 where only the two-pion intermediate state is shown. The $I=1$ (isovector) form factor can have contributions only from an even number of pions in the intermediate state. We assumed that only the two pion state is important.

The form factors are defined in terms of the nucleon electromagnetic current j_μ by[73]

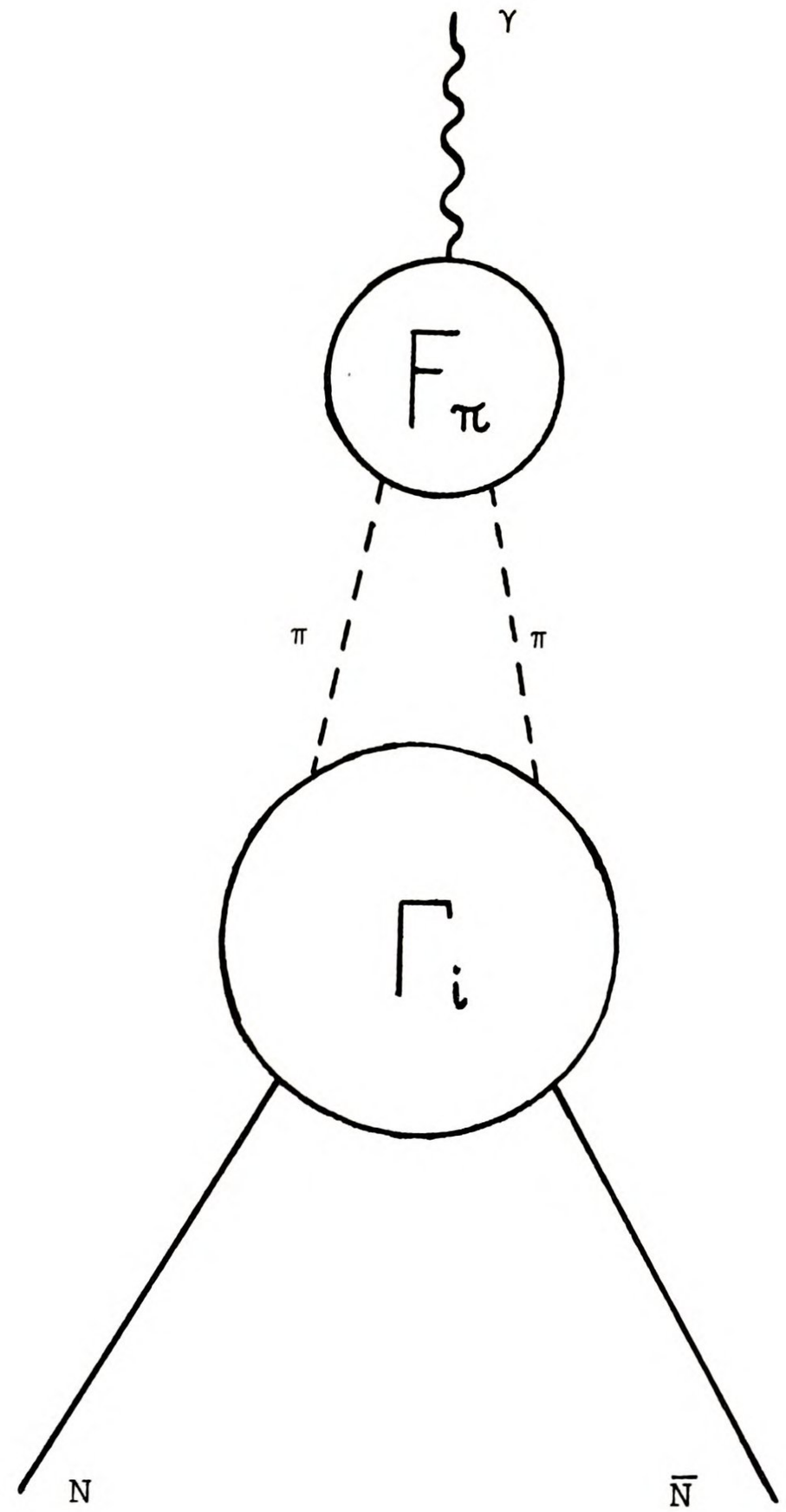

Figure 19. The two-pion contribution to the imaginary parts of the nucleon form factors.

The isov

given by

where τ

magneti

where

$$\langle p' | j_\mu | p \rangle = e\sqrt{\frac{m^2}{p_0' p_0}}\, i\bar{u}(p')\left[F_1(q^2)\gamma_\mu + F_2(q^2)\sigma_{\mu\nu}(p-p')_\nu\right]u(p) \qquad \text{(III.29)}$$

The isovector (I=1) and isoscalar (I=0) combinations are given by

$$F_1 = F_1^S + \tau_3 F_1^V ,$$
$$F_2 = F_2^S + \tau_3 F_2^V , \qquad \text{(III.30)}$$

where τ_3 is +1 (-1) for proton (neutron).

More commonly encountered are the electric and magnetic form factors G_E and G_M defined by

$$G_E = F_1 - 2m\tau F_2 , \qquad \text{(III.31a)}$$
$$G_M = F_1 + 2m F_2 , \qquad \text{(III.31b)}$$
$$F_1 = \frac{G_E + \tau G_M}{1+\tau} , \qquad \text{(III.31c)}$$
$$F_2 = \frac{G_M - G_E}{1+\tau} , \qquad \text{(III.31d)}$$

where $\tau \equiv \frac{-t}{4m^2}$.

The form factors are normalized to the values

$$G_E^V(0) = \tfrac{1}{2} \quad , \quad G_M^V(0) = \tfrac{1}{2} + g , \qquad \text{(III.32a)}$$
$$F_1^V(0) = \tfrac{1}{2} \quad , \quad 2m F_2^V(0) = g , \qquad \text{(III.32b)}$$

where g

magneti

dispers

$$F_i^{\nu}(t$$

The Γ_i

couplir

vector

C.

amount

factor

$\gamma_i \equiv [$

Since r

The res

values

cited

agreeme

where $g = 1/2\ (\lambda_p - \lambda_n) = 1.8530$ and λ_p, λ_n are the anamolous magnetic ratios.

The $N\bar{N}\to\pi\pi$ amplitudes Γ_i are related to F_i by the dispersion relation[25]

$$F_i^v(t) = F_i^v(0) - \frac{t}{\pi}\int_4^\infty \left[\frac{(t'-4)^3}{64t'}\right]^{1/2} \frac{F_\pi^*(t')\,\Gamma_i(t')\,dt'}{t'(t'-t)}. \qquad \text{(III.33)}$$

The Γ_i are just the $N\bar{N}\to\pi\pi$ amplitudes for vector and tensor coupling. They are, therefore, related to the rho meson vector and tensor coupling constants, as shown in Appendix C.

Without detailed fitting, because of the large amount of computation involved, we found that the form factor data were reproduced with the following values of $\gamma_i \equiv [D_1(30)\Gamma_i(30) - \Gamma_{iB}(30)]$:

$$\gamma_1 = 0.136\ , \qquad \text{(III.34)}$$
$$\gamma_2 = 0.0116\ .$$

Since $m_\rho^2 \simeq 30$ and $\mathrm{Re}\Gamma(m_\rho^2)=0$ we found, with $D_1(30)=0.168$, that

$$\mathrm{Im}\ \Gamma_1(30) = -0.121\ , \qquad \text{(III.35)}$$
$$\mathrm{Im}\ \Gamma_2(30) = -0.0544\ .$$

The resulting form factors are compared with experimental values in Figures 20, 21. The relevant experiments are cited in Reference 71. The calculated curves are in good agreement with the data for $t>-40$.

0.5

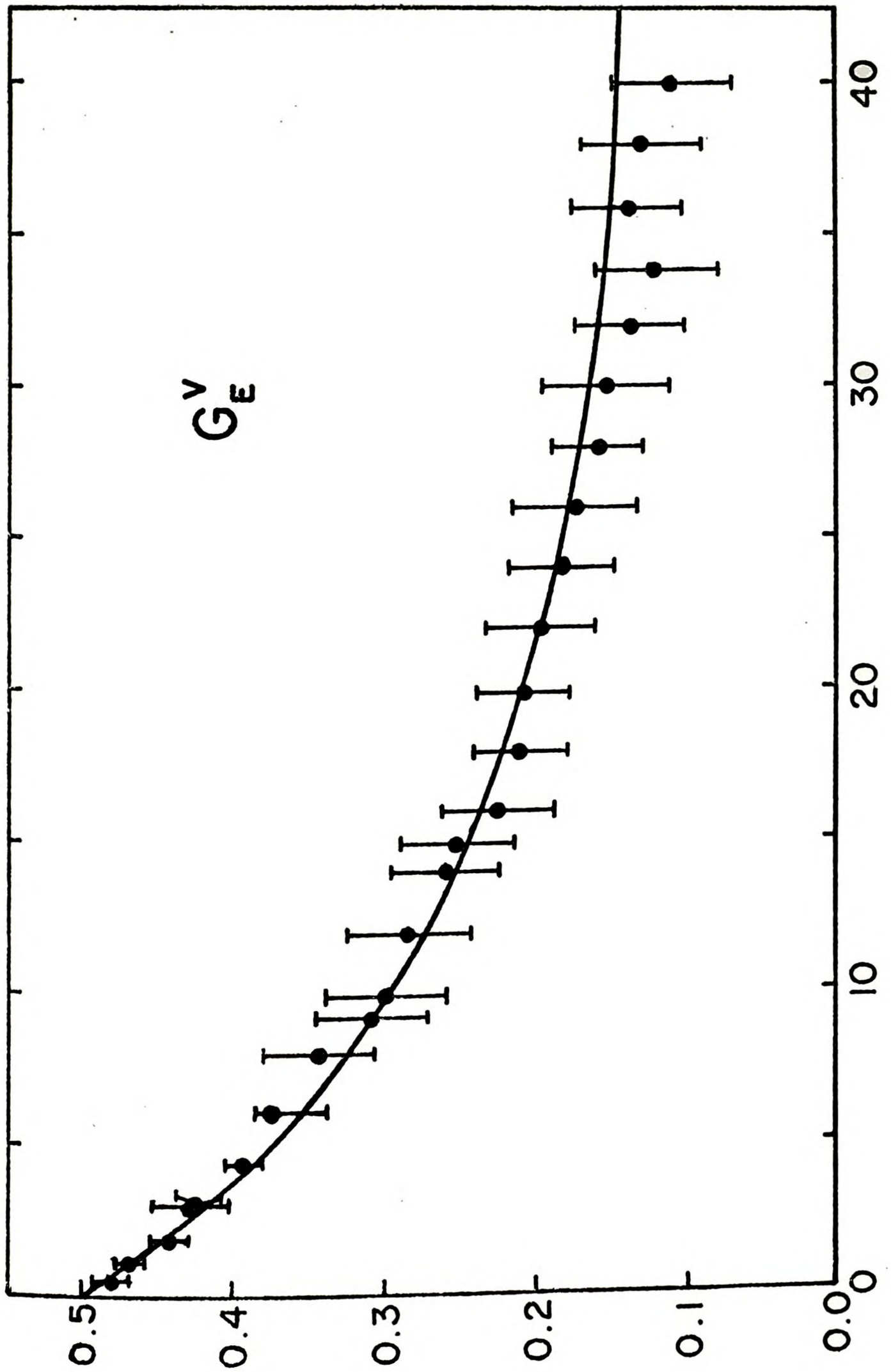

Figure 20. Fit to the nucleon electric form factor.

2.5

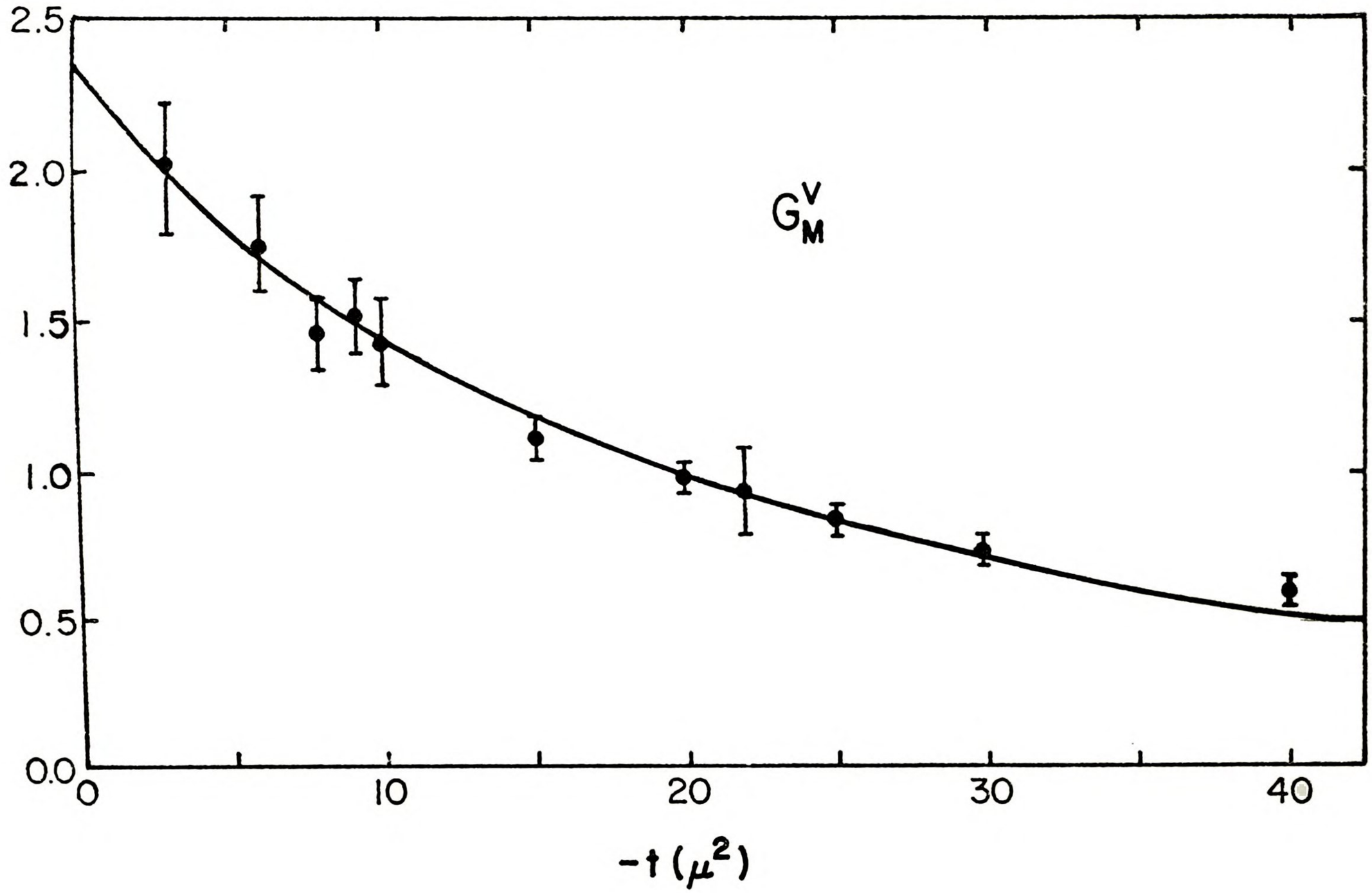

Figure 21. Fit to the nucleon magnetic form factor.

with th

Schwar

the ρ,

tude a

$$b_r$$

$$k$$

where

parame

found

is jus

The results for $\mathrm{Im}f_{+}^{1}$ are shown in Figure 22 along with the Nielsen-Oades[15] results.

The nucleon form factors were calculated by Schwarz[74] by a procedure which rather elegantly included the ρ, N, and Δ. Schwarz wrote the ππ scattering amplitude as

$$(q^3/t^{1/2})^{-1}\, b_{\pi\pi}(t) = e^{i\delta_1'} \sin\delta_1', \qquad \text{(III.36)}$$

$$b_{\pi\pi}^{-1}(t) = -i\, q^3/t^{1/2} + k(t) - k(m_\rho^2) + (m_\rho^2 - t)\left[k'(m_\rho^2) + 1/\gamma_\rho\right] + \lambda(m_\rho^2 - t)^2, \qquad \text{(III.37)}$$

$$k(t) = \left[2q^2/(\pi t^{1/2})\right] \mathrm{Log}\left(q + \tfrac{1}{2}t^{1/2}\right), \qquad \text{(III.38)}$$

where $q=(t/4-1)^{1/2}$, and γ_ρ determines the rho width. The parameter λ is an arbitrary entire function; Schwarz found an acceptable pion form factor with $\lambda=0$.

Since $b_{\pi\pi}(t)$ has no left cut, the pion form factor is just

$$F_{\pi\pi}(t) = b_{\pi\pi}(t) \Big/ b_{\pi\pi}(0). \qquad \text{(III.39)}$$

The $N\bar{N}\to\pi\pi$ amplitudes

$$b_1(t) = -2\Gamma_1(t), \qquad \text{(III.40a)}$$

where

b_i

where

has no

$b_i(t)$

where

b_i is

rho co

ment

and Δ

nucle

shown

from

120 M

The r

small

$$b_2(t) = -\left(\frac{2m}{g}\right)\Gamma_2(t), \qquad \text{(III.40b)}$$

where g=1.853, satisfy the dispersion relation

$$b_i(t) = b_i^L(t) + \frac{1}{\pi}\int_4^\infty \frac{q(t')^3\, b_i(t')\, b^*_{\pi\pi}(t')}{(t')^{1/2}(t'-t)}\, dt', \qquad \text{(III.41)}$$

where $b_i^L(t)$ is the left cut contribution. Since $b_{\pi\pi}(t)$ has no left cut Schwarz could solve this equation for $b_i(t)$ to obtain

$$b_i(t) = b_i^L(t) + b_{\pi\pi}(t)\left[\mu(t) + \frac{t}{\pi}\int_4^\infty \frac{q(t')^3\, b_i^L(t')}{(t')^{3/2}(t'-t)}\, dt'\right], \qquad \text{(III.42)}$$

where $\mu(t)$ is an entire function. Of course, the phase of b_i is equal to the phase of $b_{\pi\pi}$. Assuming universality of rho couplings, Schwarz required $\mu(0)=1$, and the requirement that $b_i(t)\to 0$ as $t\to\infty$ ensured that $\mu(t)$ is a constant.

The left cut contribution b_i^L was approximated by N and Δ exchange. Schwarz then proceeded to calculate the nucleon form-factors.

Unfortunately, the $N\bar{N}\to\pi\pi$ amplitudes b_i were not shown by Schwarz. We have, therefore, calculated the Γ_i from (III.40, 42) using $\lambda=0$, $\gamma_\rho=1.53$ ($\Gamma_\rho=120$ MeV), $\Gamma_\Delta=$ 120 MeV (Δ parameters from (B.6)), and a cutoff at t'=150. The results for $|\Gamma_1|$ and $|\Gamma_2|$, shown in Figures 22, 23 are smaller than we have obtained from (III.28). This fact is

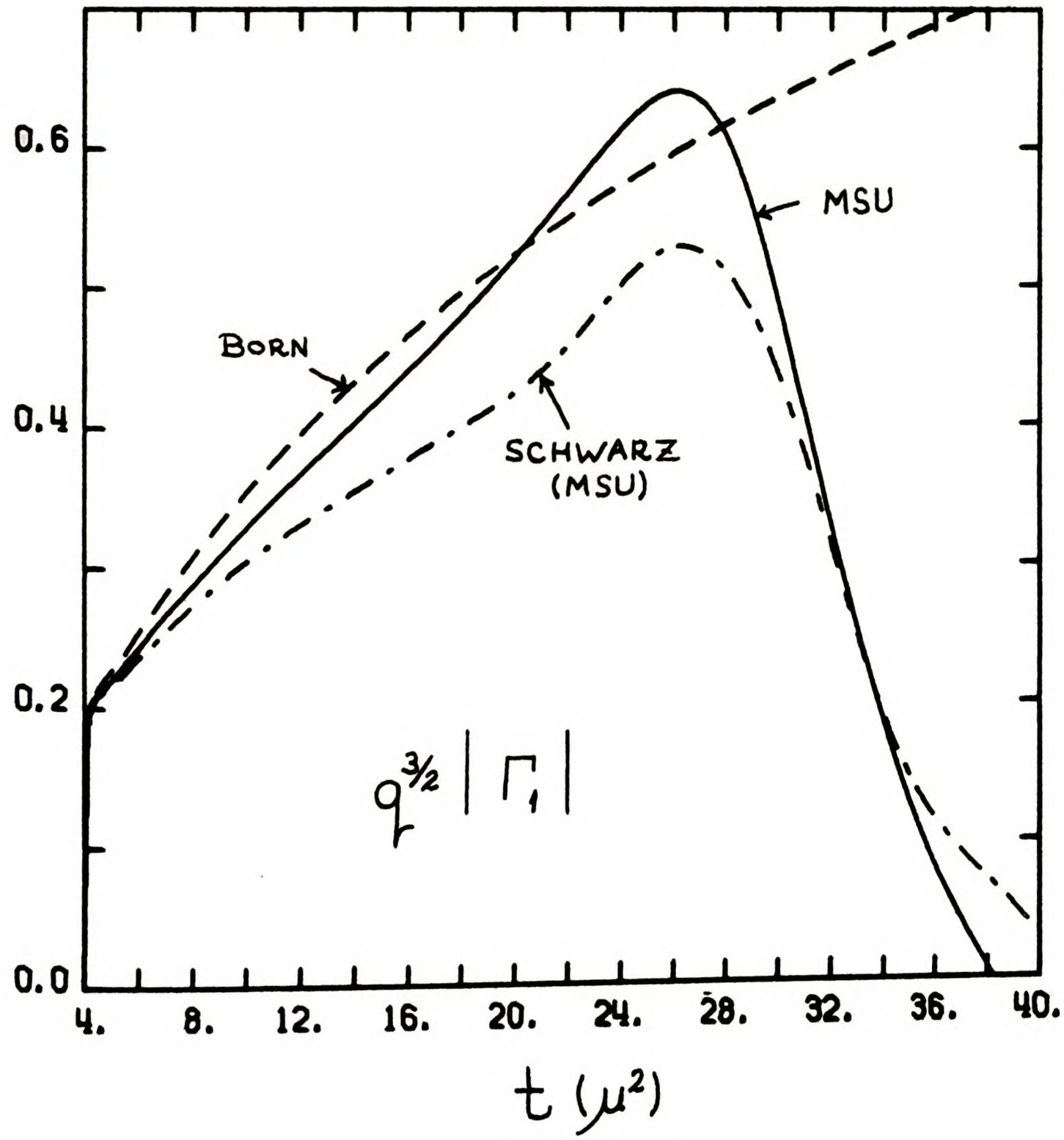

Figure 22. The $N\bar{N}\to\pi\pi$ amplitude $q^{3/2}|\Gamma_1|$.

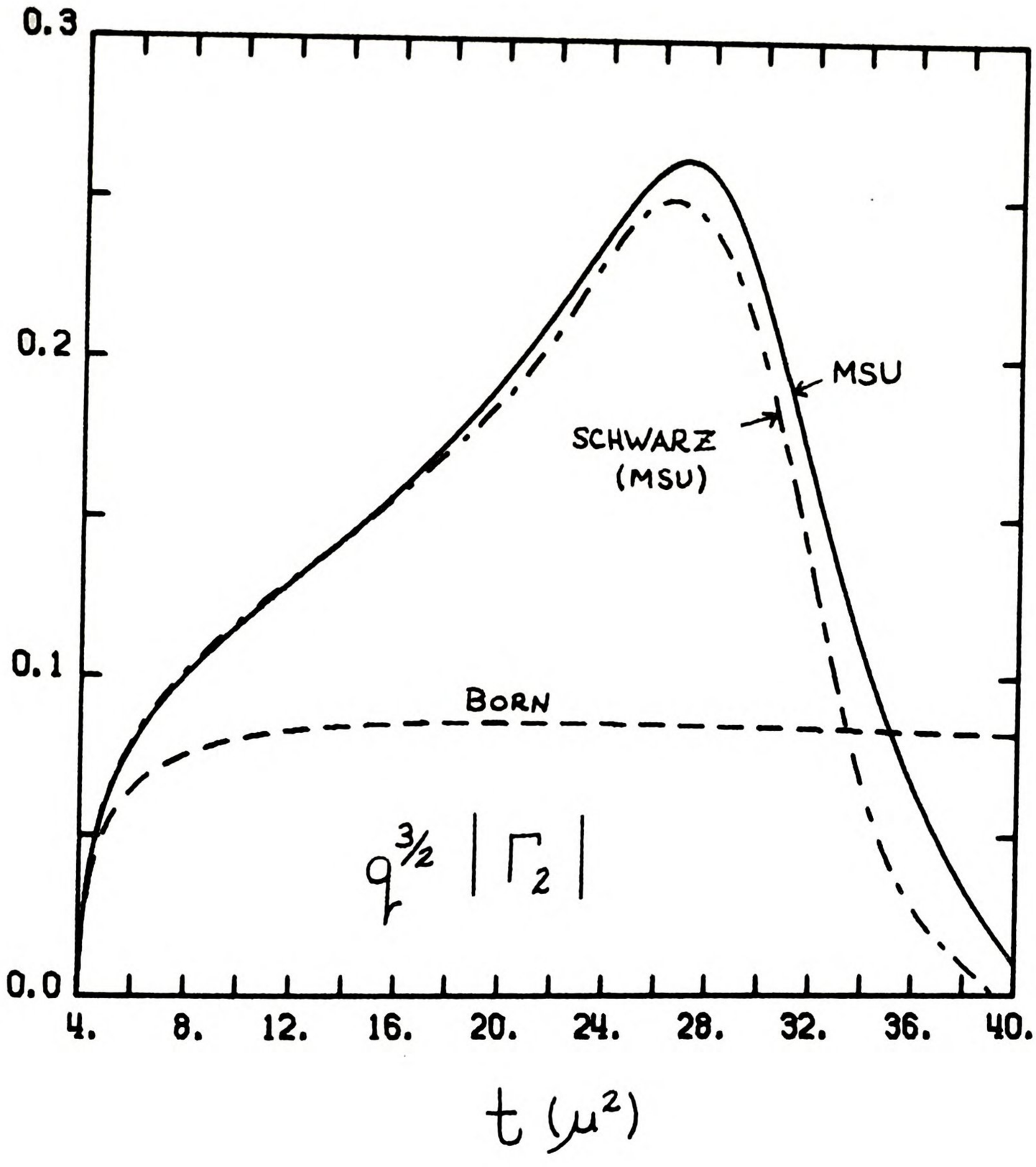

Figure 23. The $N\bar{N}\to\pi\pi$ amplitude $q^{3/2}|\Gamma_2|$.

consisten

nucleon f

relation

mediate s

However,

(left cu

procedur

logarith

f_{+}^{2} is

$D_2(t)$

As was

relatio

case to

Imf_{-}^{2}(t

tudes

f_{+B}^{2}

Multip

gives

consistent with Schwarz's observation that the resulting nucleon form factors calculated from a subtracted dispersion relation are too large. Possibly the higher mass intermediate states ($K\bar{K}$, $\pi\omega$) are the culprits, as Schwarz felt. However, using the N,Δ-poles to represent the πN scattering (left cut of Γ_i) and pushing it beyond t=100 is a dubious procedure. The Δ-pole contribution to Γ_1 is, in fact, logarithmically divergent, as Schwarz pointed out.

G. The $N\bar{N}\to\pi\pi$ d-Wave Helicity Amplitudes

The once subtracted Omnès dispersion relation for $f^2_{\pm}$ is

$$D_2(t) f^2_{\pm}(t) = D_2(t_0) f^2_{\pm}(t_0) + \frac{t-t_0}{\pi}\int_{-\infty}^{a} \frac{D_2(t')\, Im f^2_{\pm}(t')\, dt'}{(t'-t_0)(t'-t)} \quad . \tag{III.43}$$

As was the case for Γ_i, we have subtracted from this relation a similar one for the Born amplitudes, in this case to suppress the effect of rapid variation in $Imf^2_{-}(t')$ near t'=a. Having no right cut, the Born amplitudes satisfy

$$f^2_{\pm B}(t) = f^2_{\pm B}(t_0) + \frac{t-t_0}{\pi}\int_{-\infty}^{a} \frac{Im\, f^2_{\pm B}(t')\, dt'}{(t'-t_0)(t'-t)} \quad . \tag{III.44}$$

Multiplying (III.44) by $D_2(t)$ and subtracting from (III.43) gives

D_2

The f

for v

$[D_2(t$

Born

Niels

calcu

point

Table

t_o	
1	
3	

depen

The v

table

$$D_2(t)\,\tilde{f}^2_{\pm}(t) = D_2(t_o)\,\tilde{f}^2_{\pm}(t_o) + \left[D_2(t_o)-D_2(t)\right] f^2_{\pm B}(t_o)$$

$$+ \frac{t-t_o}{\pi}\int_{-\infty}^{a} \frac{D_2(t')\,\mathrm{Im}\,\tilde{f}^2_{\pm}(t') + \left[D_2(t')-D_2(t)\right]\mathrm{Im}\,f^2_{\pm B}(t')}{(t'-t_o)(t'-t)}\,dt'. \qquad \text{(III.45)}$$

The function $D_2(t)$ is a very slowly varying function of t for values of t of interest here. Therefore, the factor $[D_2(t')-D_2(t)]$ considerably reduces the contribution of the Born amplitude to the dispersion integral.

The non-Born amplitudes Re $\tilde{f}^2_{\pm}(t_o)$ interpolated from Nielsen's[27] tables are given together with the explicitly calculated Re $f^2_{\pm B}(t_o)$ in Table 8 for two subtraction points.

Table 8.--Values used as subtraction constants for the evaluation of the d-wave helicity amplitudes.

t_o	$\tilde{f}^2_+$	Re f^2_{+B}	$\tilde{f}^2_-$	Re f^2_{-B}
1	0.0156	-.01079	-.00719	-.3517
3	0.0170	-.09903	-.00600	-1.055

Calculations with (III.45) are increasingly dependent on the dispersion integral cutoff as t increases. The values of Im $\tilde{f}^2_{\pm}(t)$ can be extrapolated from Nielsen's tables to t=-30 with some confidence. In an attempt to

furthe

extrap

in Fi

term.

intro

is ra

δ_2^o by

effec

any c

nearl

further decrease the cutoff error we have used a hand extrapolation to t=-45.

The results for $q^{\frac{5}{2}}|f^2_{+-}|$, where $q^2=t/4-1$, are shown in Figure 24. The f^2_- amplitude is quite close to the Born term. The right cuts of the helicity amplitudes are introduced through $D_2(t)$. Since the input phase shift δ^o_2 is rather uncertain we have investigated the dependence on δ^o_2 by setting $D_2(t)=1$, thus eliminating the right cut. The effect of the right cut is greatest on f^2_+ but not large in any case. The $f^2_{+-}(t)$ results with either $t_o=1$ or 3 are very nearly the same.

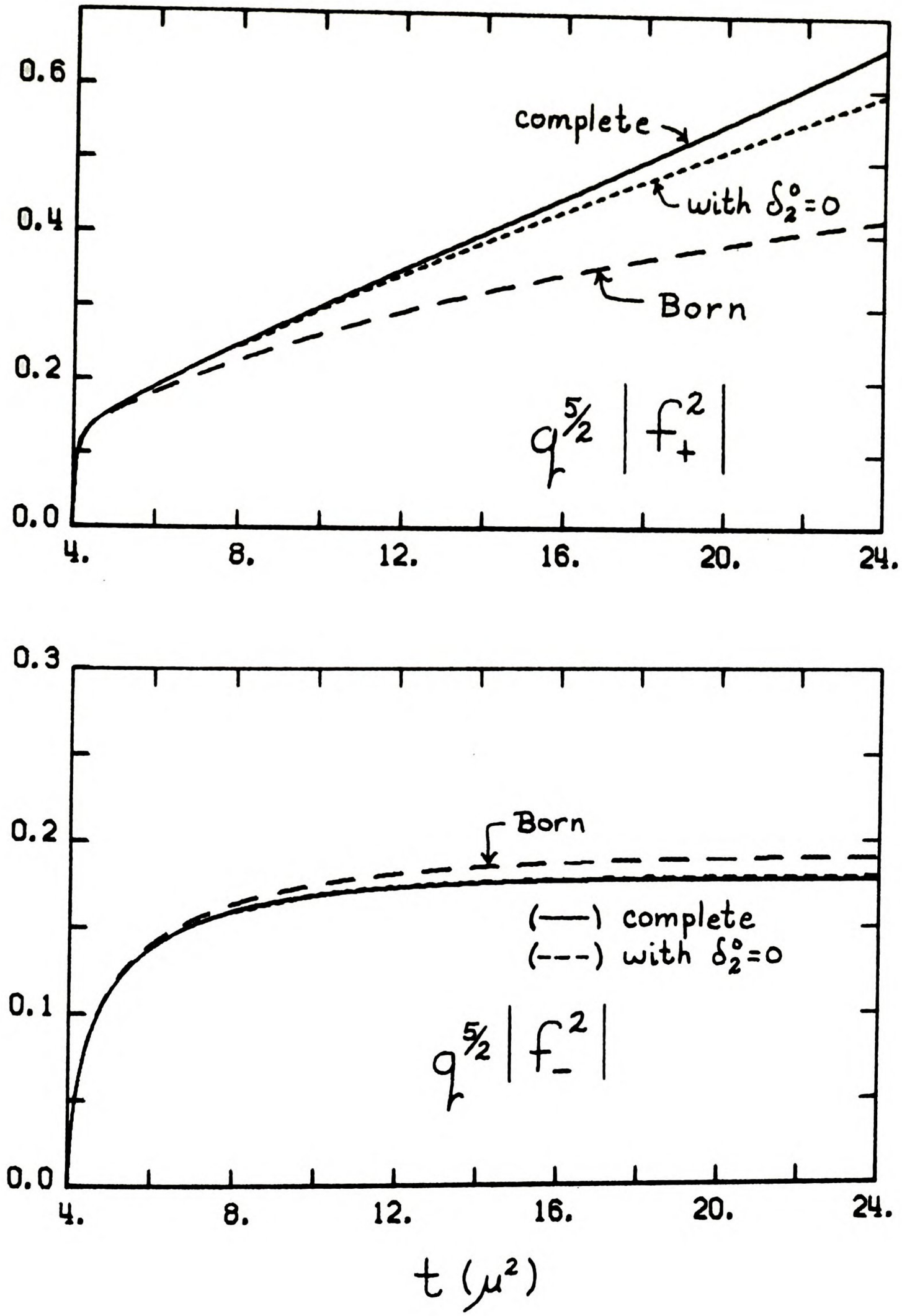

Figure 24. The $N\bar{N}\to\pi\pi$ amplitudes $q^{5/2} \mid f_{\pm}^2 \mid$.

one-p

pole

stant

show

S1 we

label

we ha

inclu

somew

the s

ener

MacG

Figu

nome

Figu

nate

IV. THE NUCLEON-NUCLEON AMPLITUDE AND POTENTIAL

A. Phase Shifts

To the two-pion-exchange amplitude we have added a one-pion-exchange pole with $g^2/4\pi=14.4$ and an omega-exchange pole with $g_\omega^2/4\pi=4.7$, $f_\omega/g_\omega=-0.12$. The omega coupling constants are discussed in Appendix G. In Figures 25-38 we show results for two $\pi\pi$ s-wave inputs. The curves labelled S1 were calculated with the Morgan-Shaw[28] δ_o^o as input; those labelled S2 used the GS+LBL[39,36] δ_o^o as input. In each case we have used n=3. The spectral functions have been included to t=45. The results from the GS+LBL δ_o^o are somewhat less attractive than S1, as one would expect from the smaller $|f_+^o|$ this phase shift produces.

The theoretical phase shifts can be compared to the energy independent phase shift analysis results of Arndt, MacGregor and Wright[75] (MAW-X), shown as data points in the Figures. We have also shown the Hamada-Johnston[76] phenomenological potential values as small squares in the Figures. The pion + fourth-order contribution is designated N and the pion-exchange by π.

$^1O_2$ PHASE SHIFT

9.

.5

2

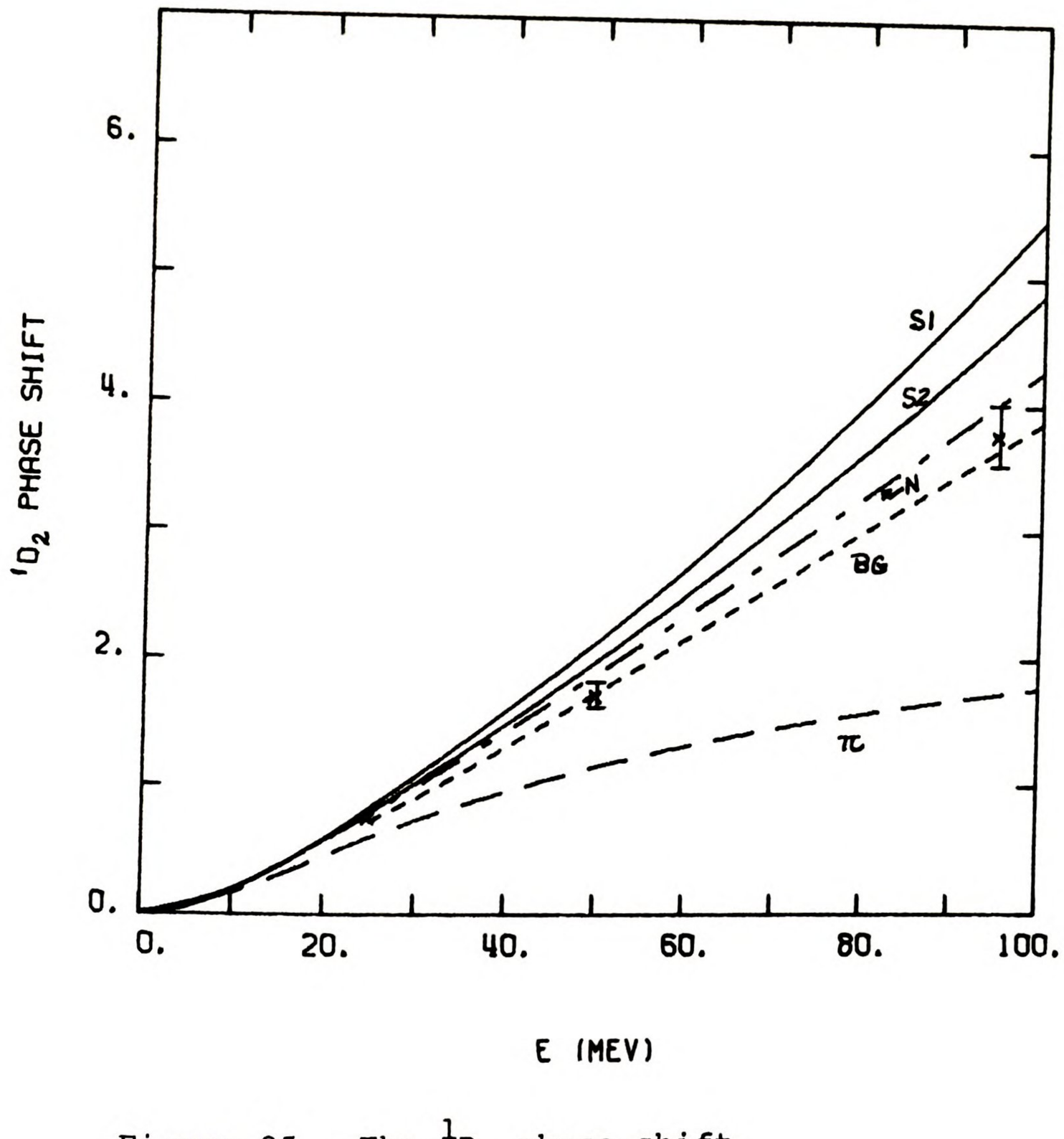

Figure 25. The $^1D_2$ phase shift.

'G_4 PHASE SHIFT

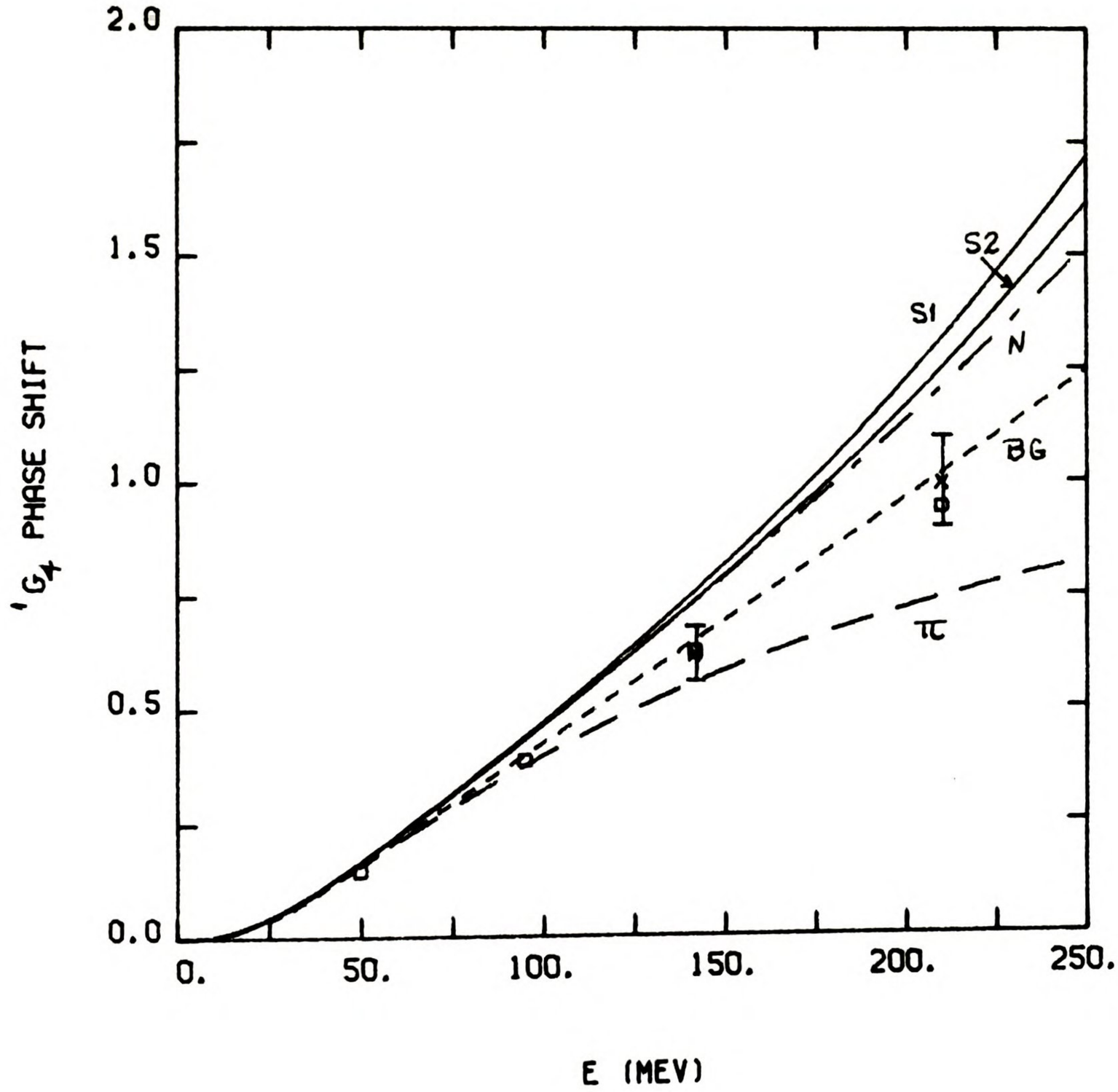

Figure 26. The $^1G_4$ phase shift.

$^3P_1$ PHASE SHIFT

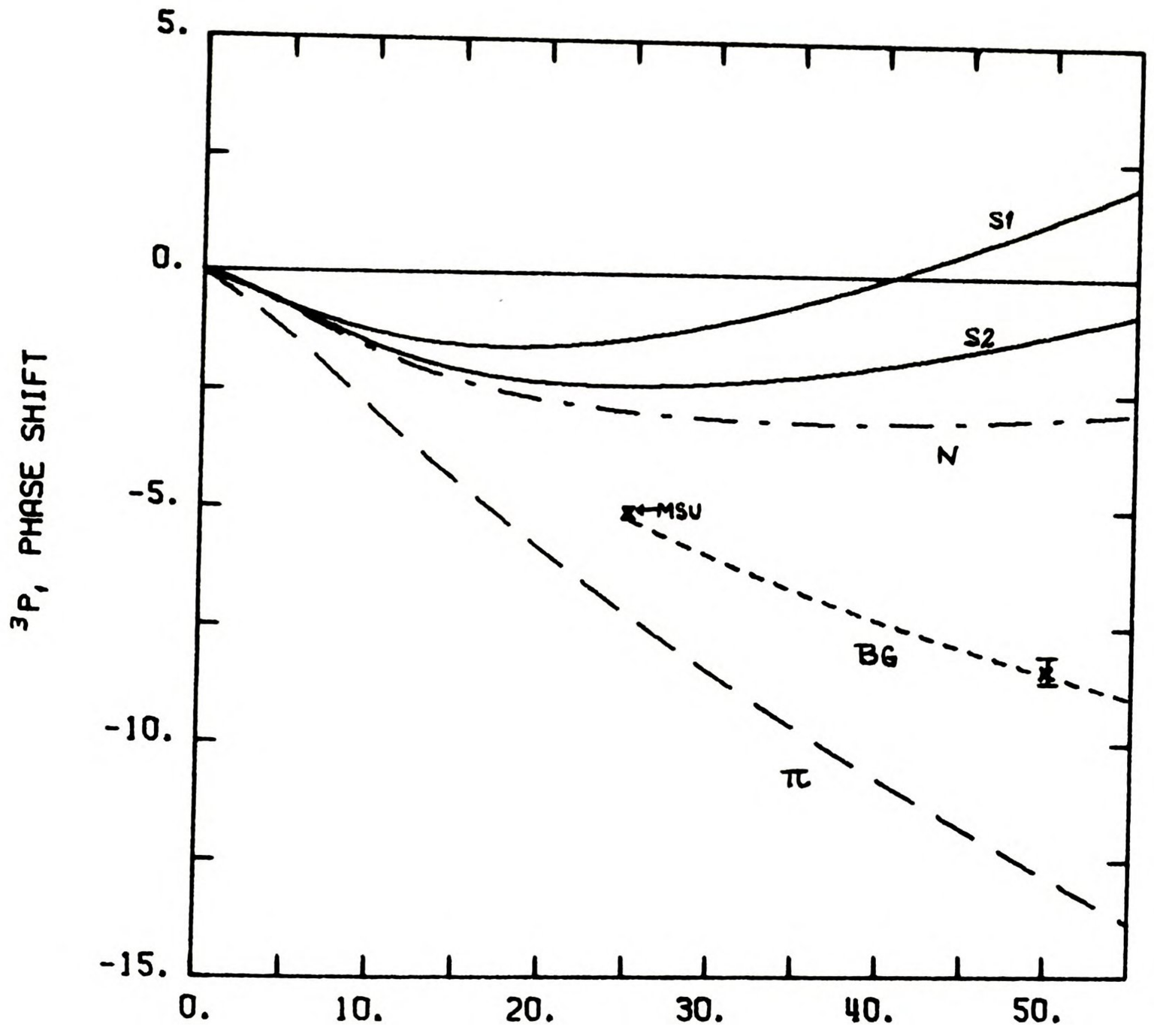

Figure 27. The $^3P_1$ phase shift.

$^3\bar{P}_2$ PHASE SHIFT

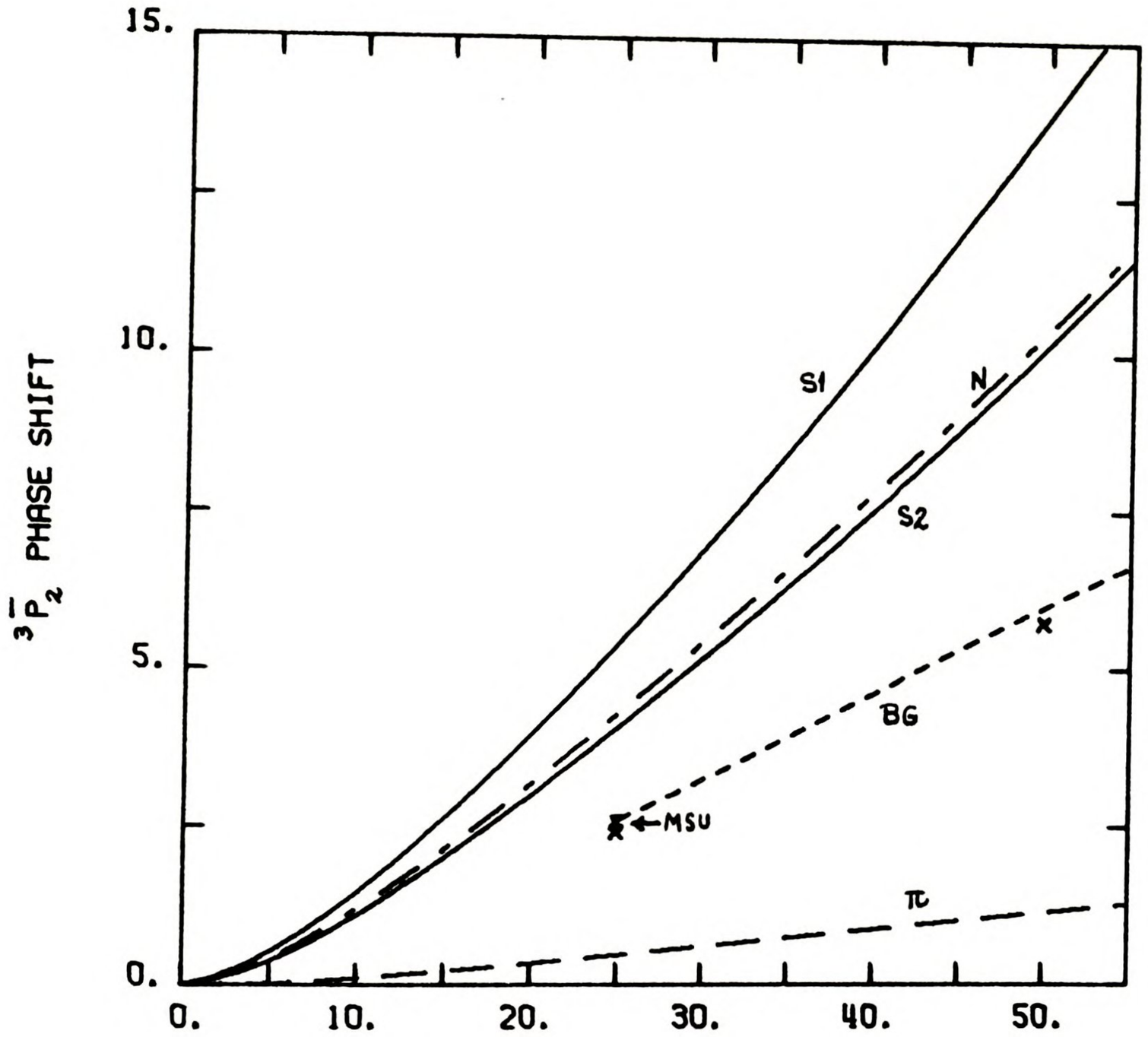

Figure 28. The $^3\bar{P}_2$ phase shift.

$3\overline{F}_c$ PHASE SHIFT

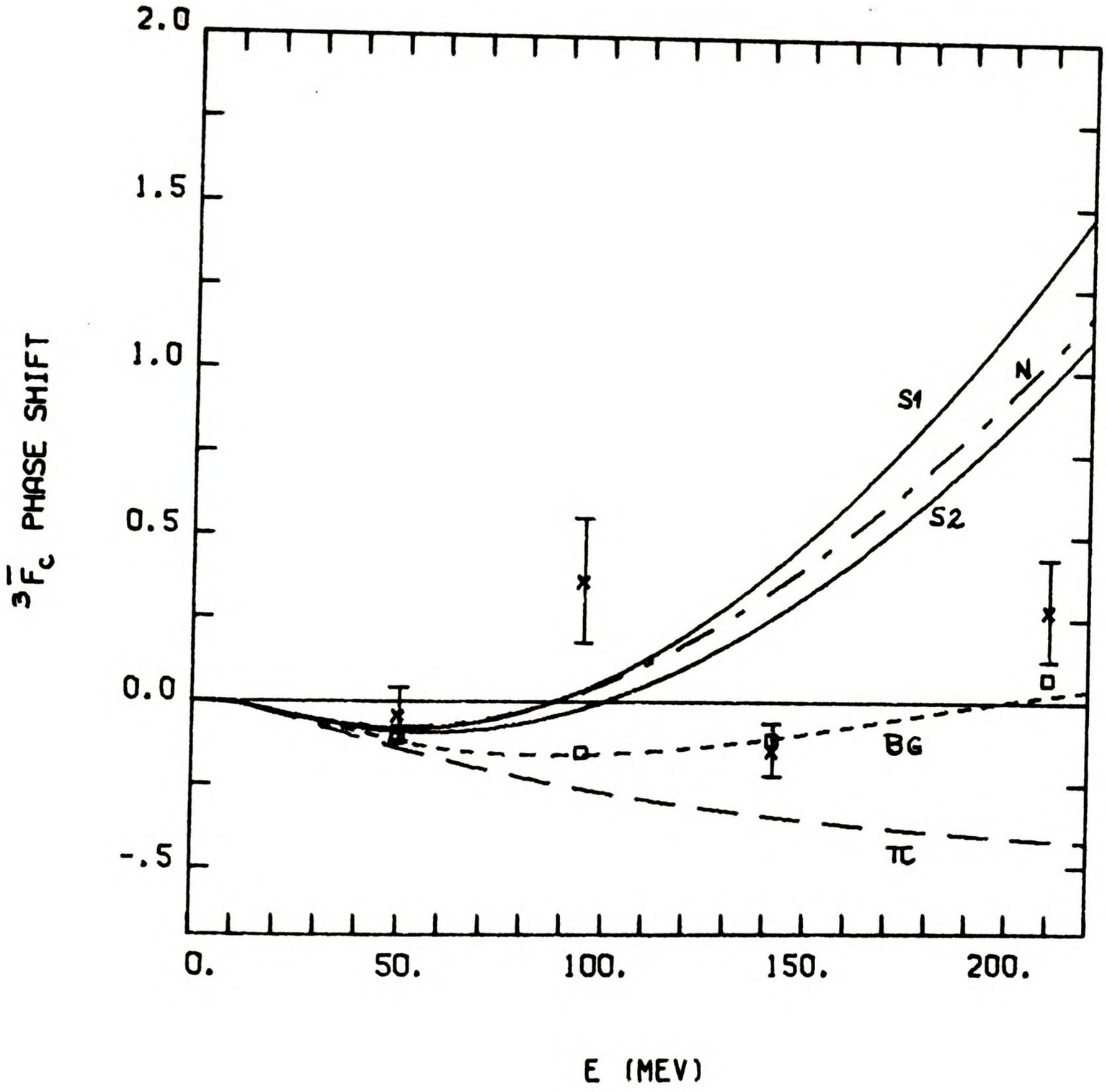

Figure 29. The $^3\bar{F}_C$ phase shift.

$^3\bar{F}_1$ PHASE SHIFT

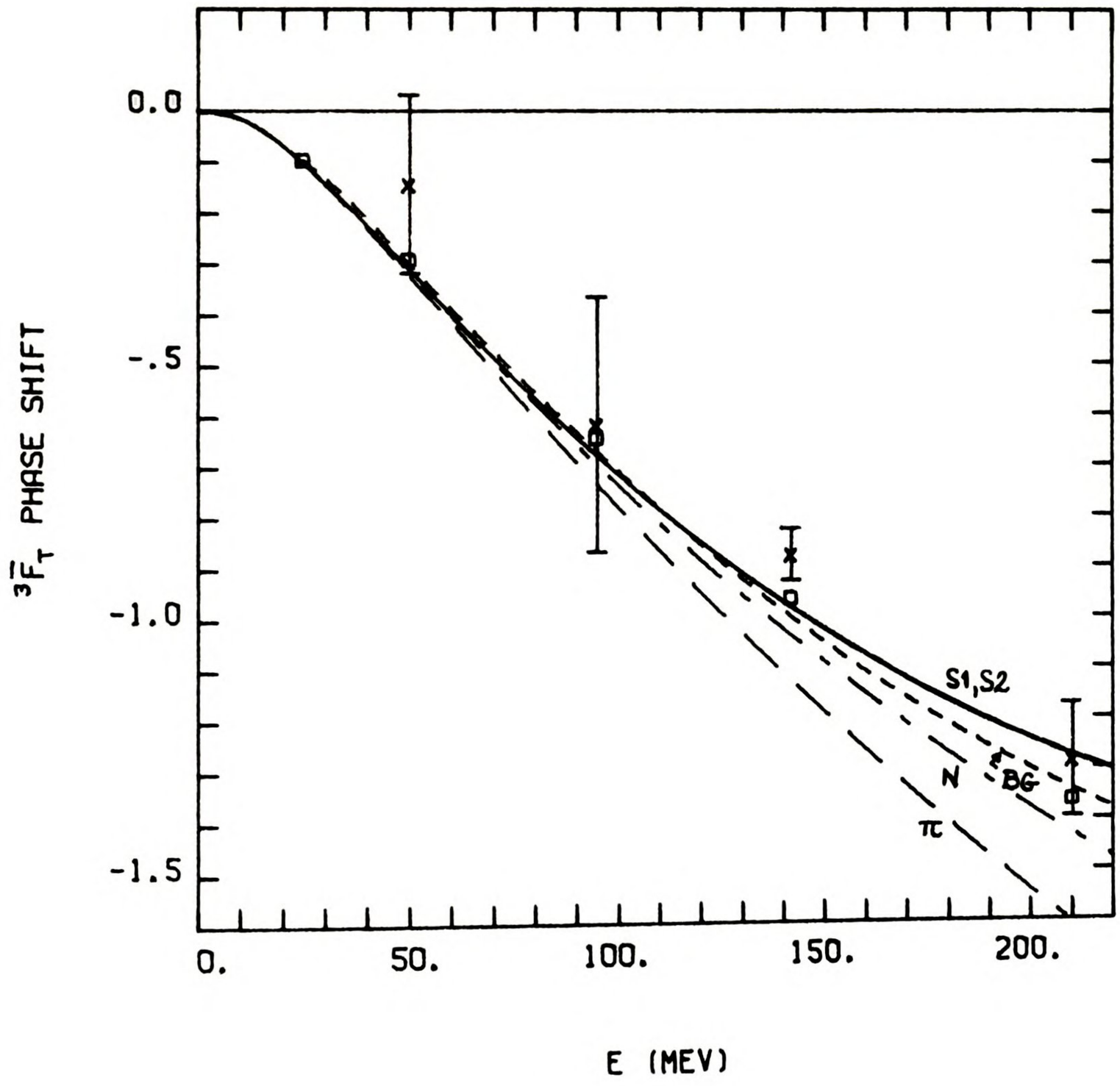

Figure 30. The $^3\bar{F}_T$ phase shift.

$3\bar{F}_{LS}$ PHASE SHIFT

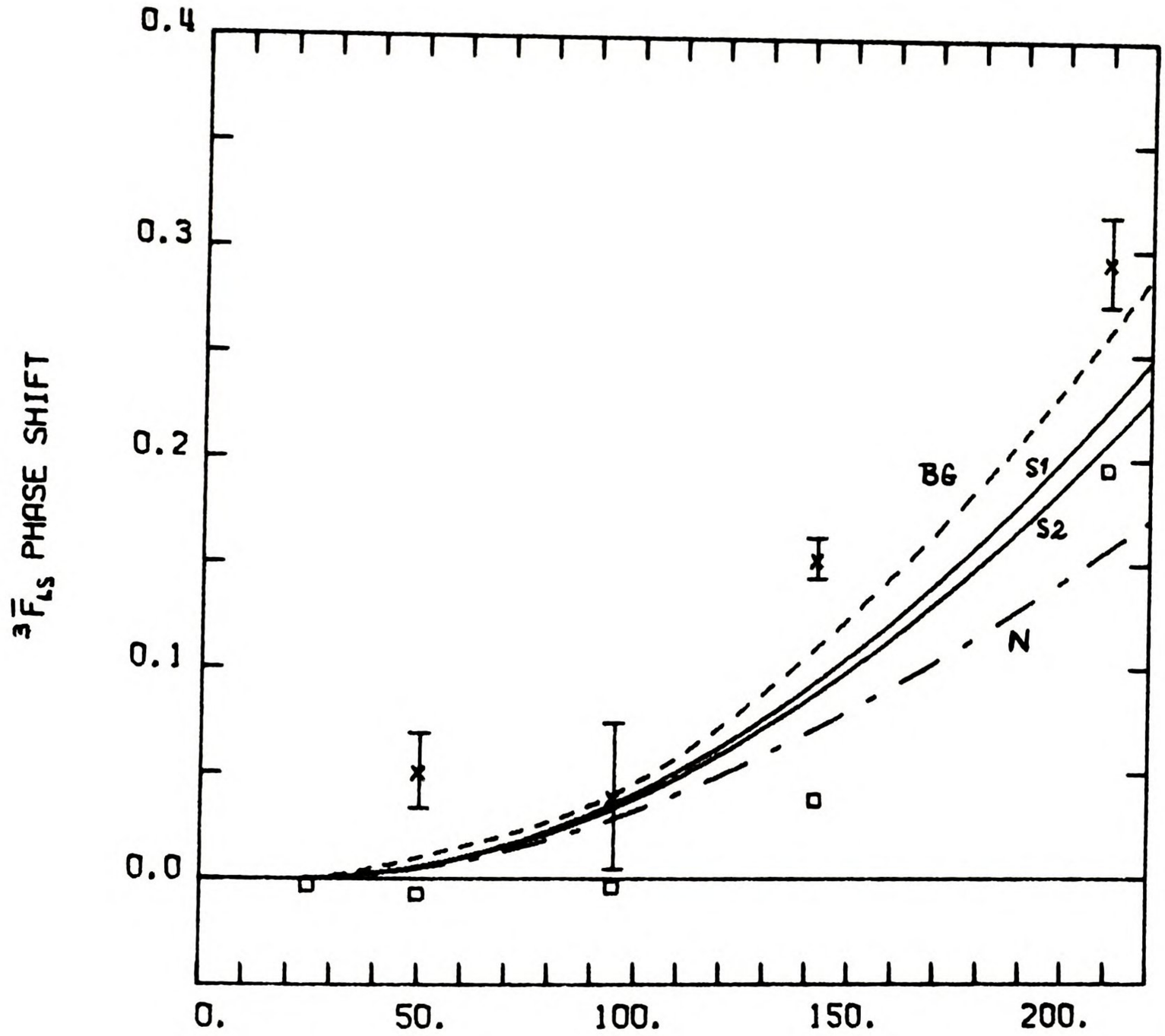

Figure 31. The $^3\bar{F}_{LS}$ phase shift.

$^3\bar{F}_2$ PHASE SHIFT

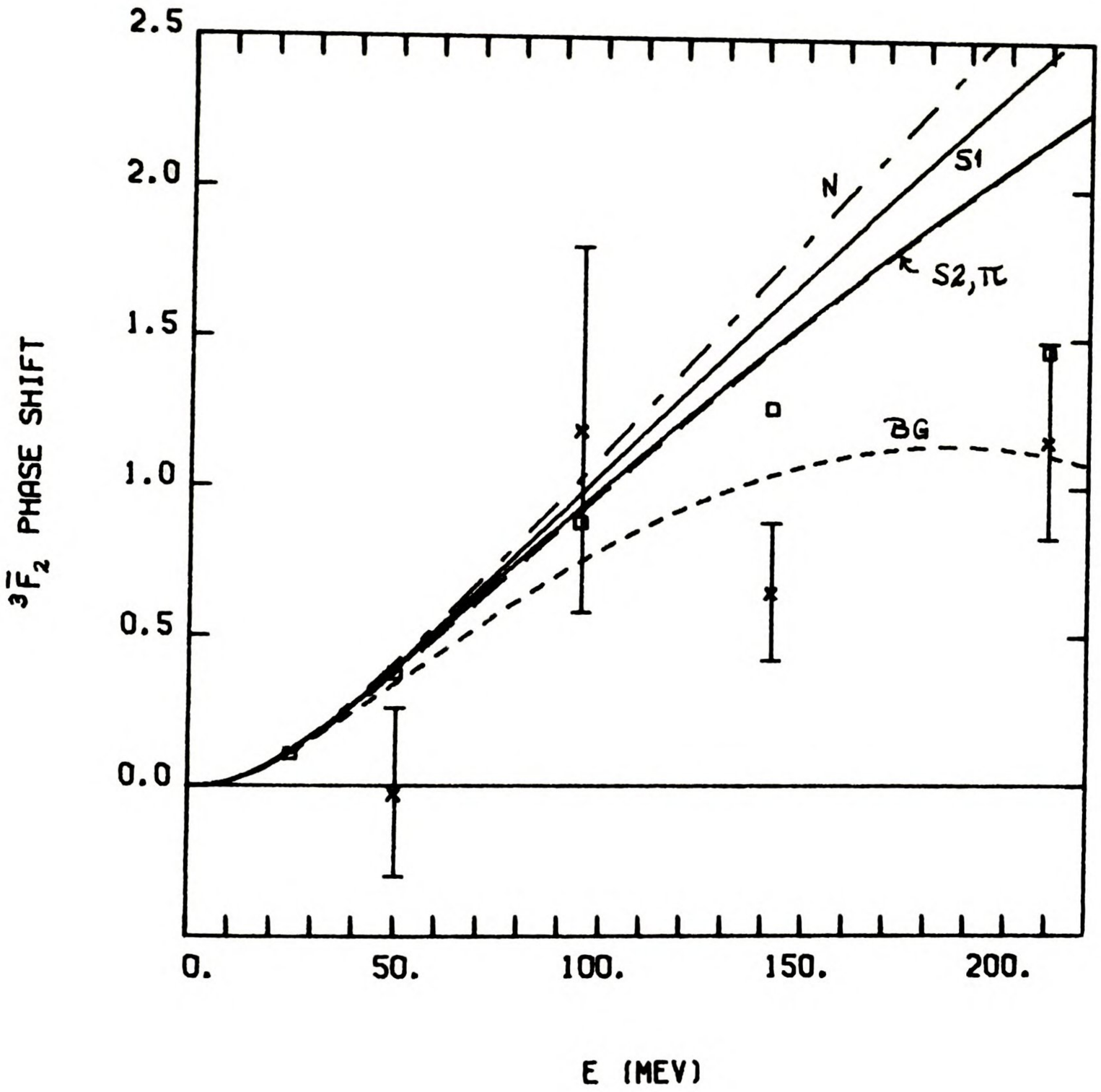

Figure 32. The $^3\bar{F}_2$ phase shift.

$^3F_3$ PHASE SHIFT

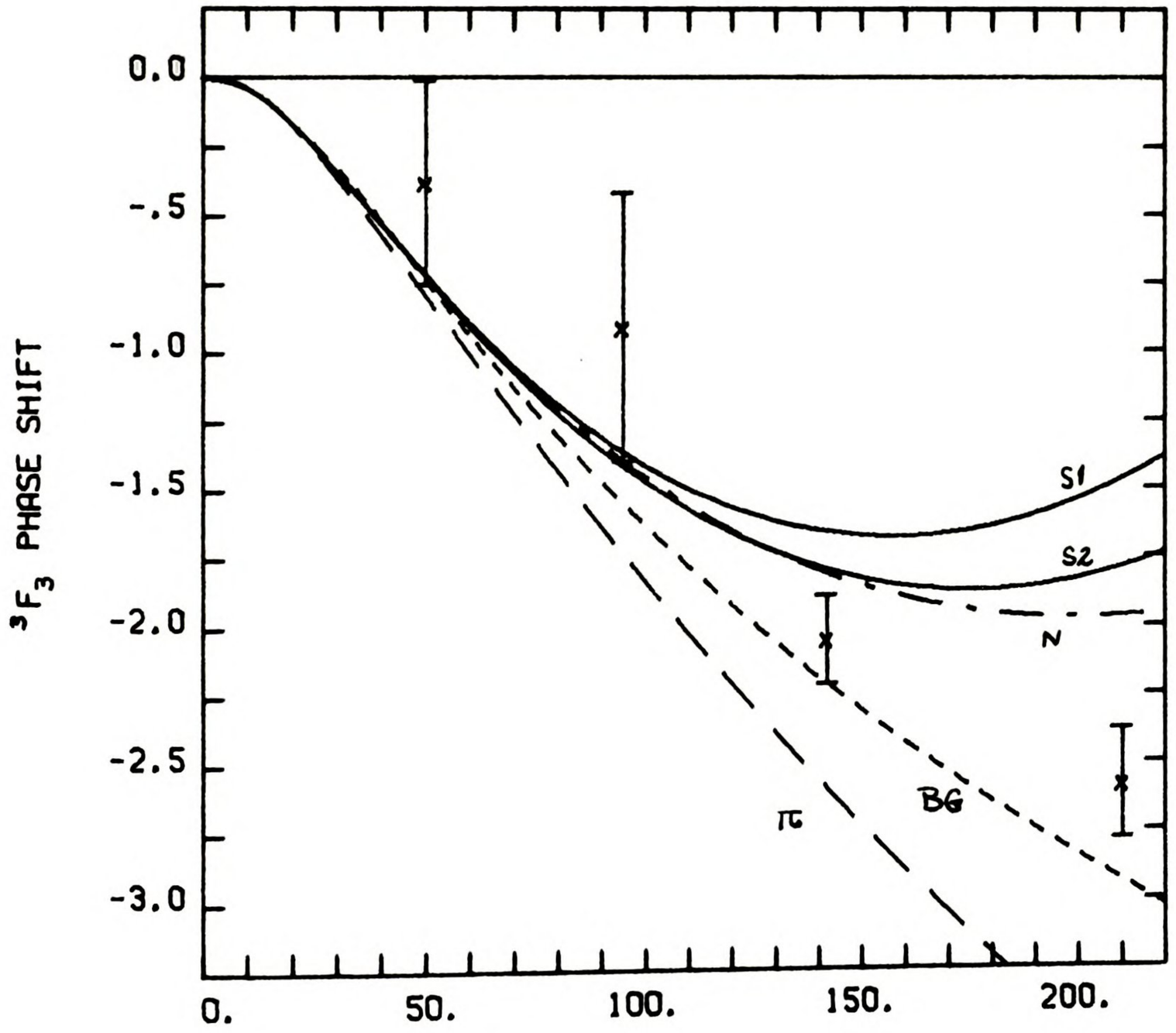

Figure 33. The $^3F_3$ phase shift.

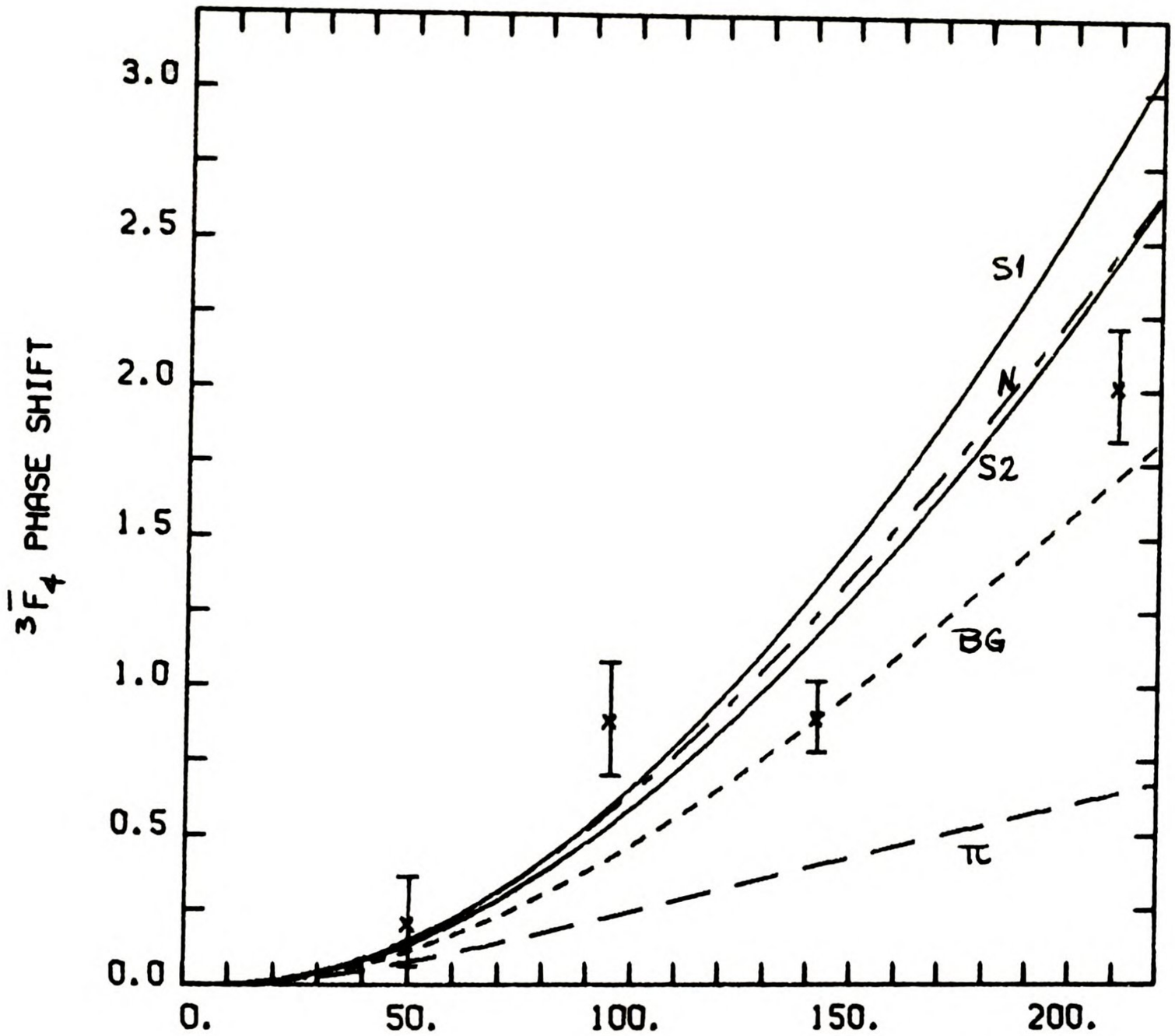

Figure 34. The $^3\bar{F}_4$ phase shift.

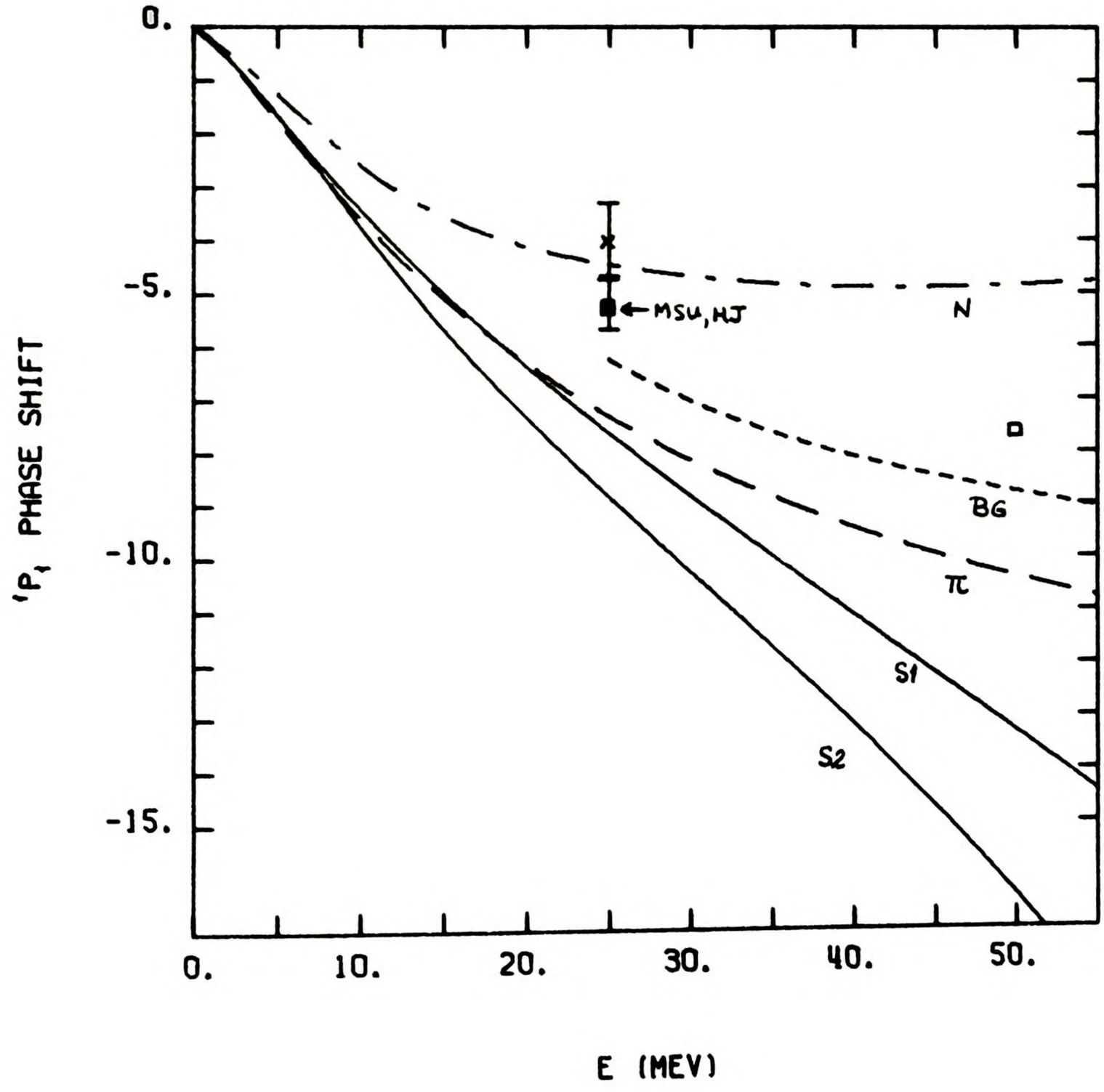

Figure 35. The $^1P_1$ phase shift.

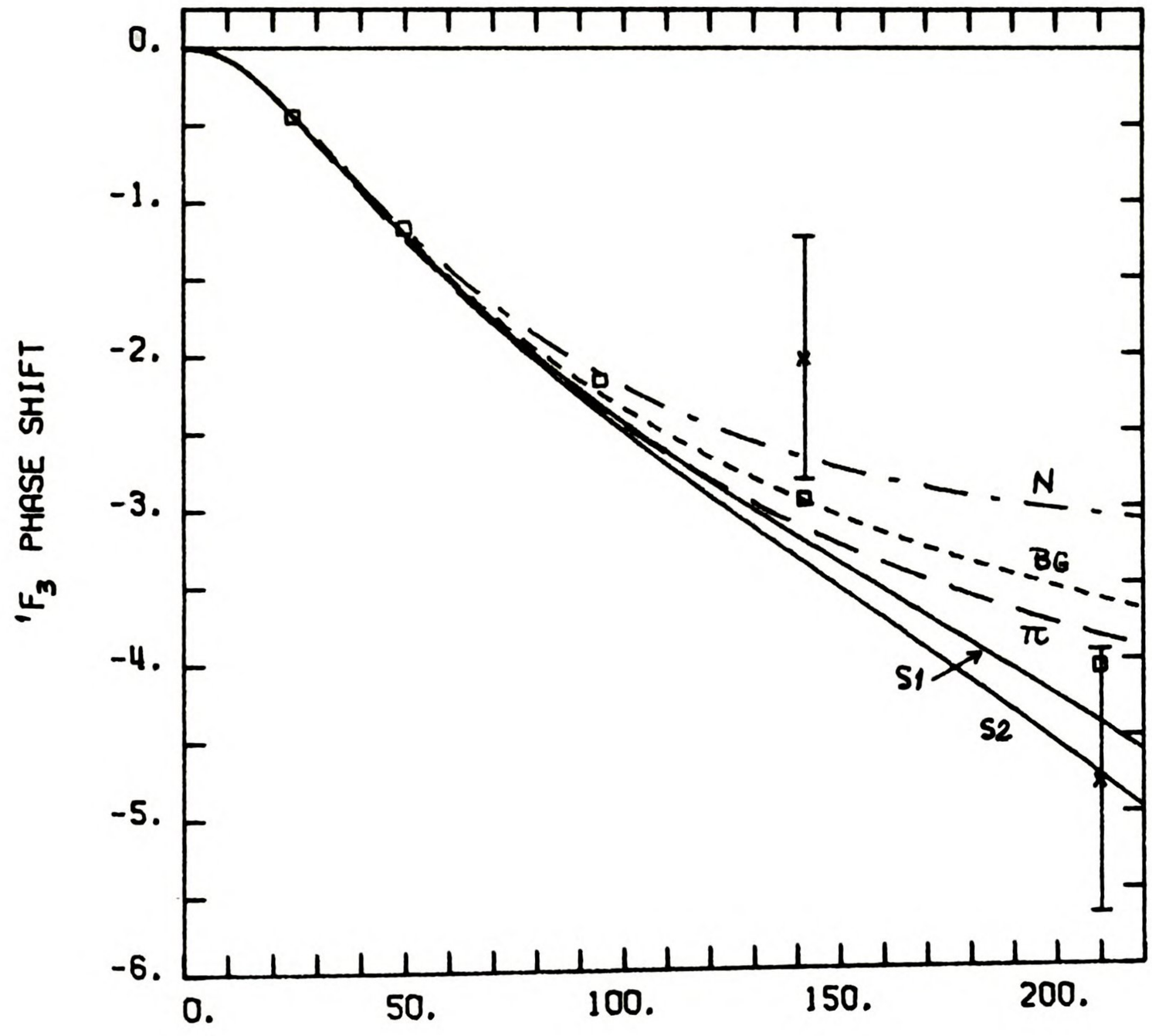

Figure 36. The $^1F_3$ phase shift.

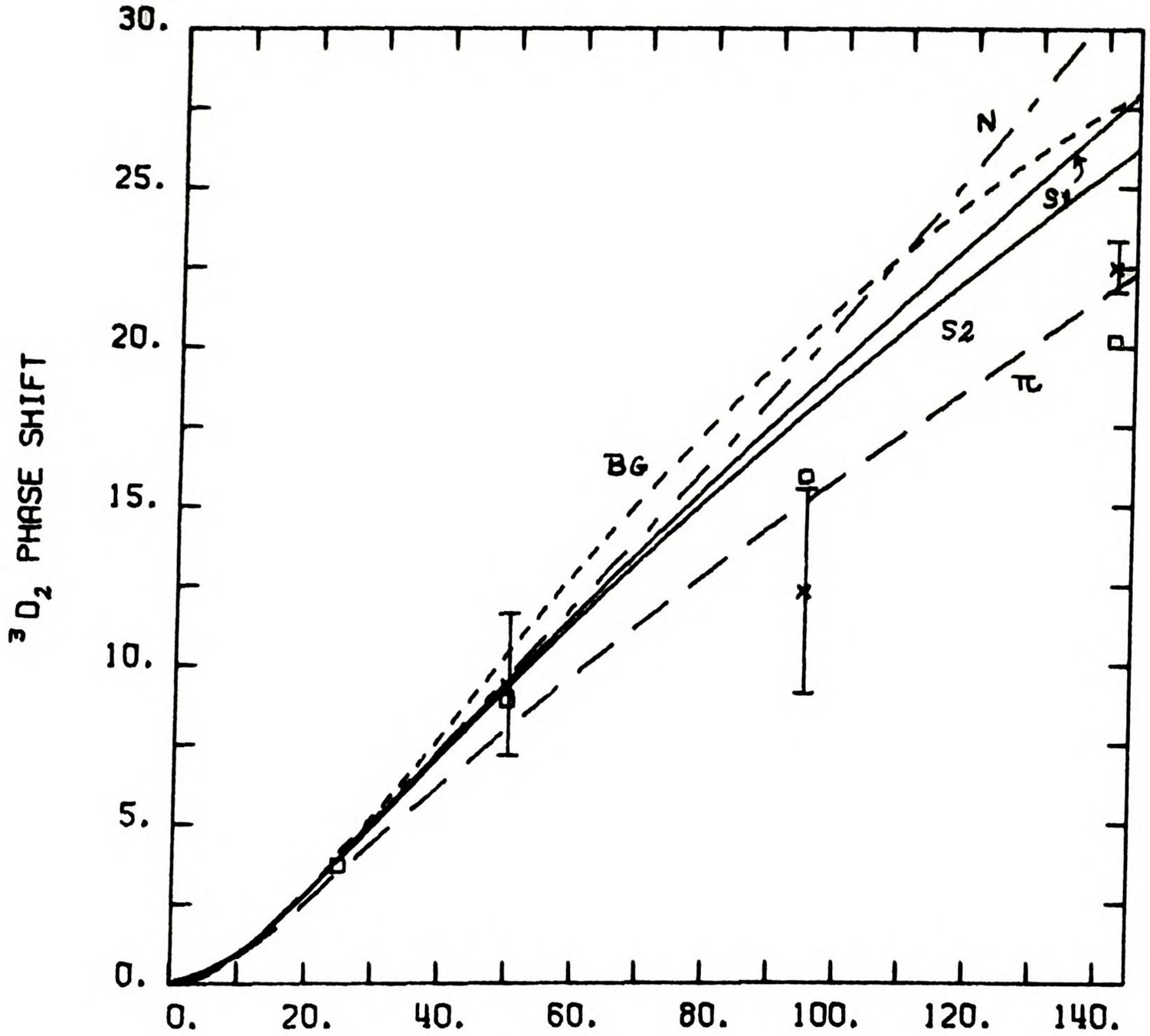

Figure 37. The $^3D_2$ phase shift.

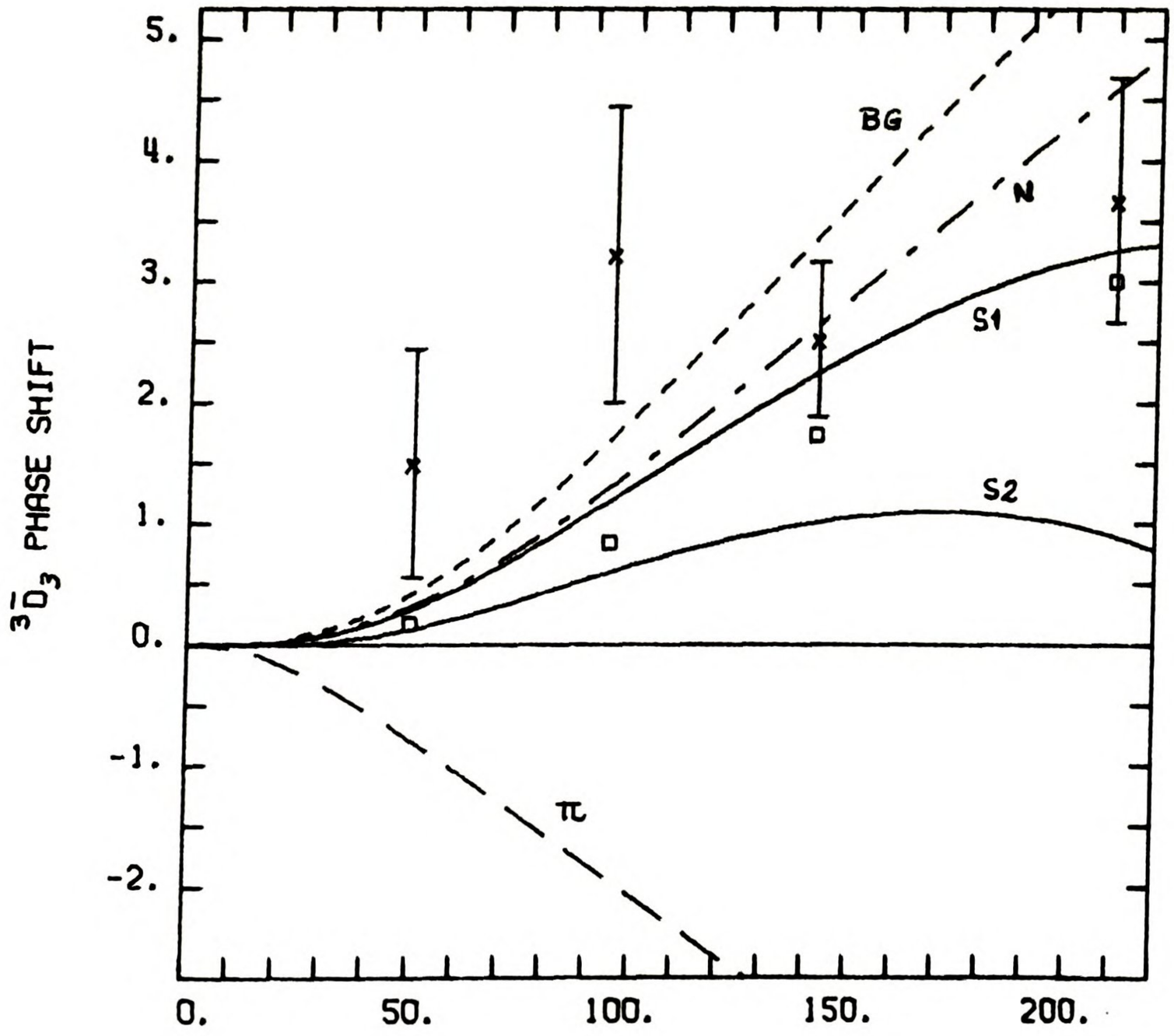

Figure 38. The $^3\bar{D}_3$ phase shift.

We have also shown the results of a recent boson-exchange-model fit, labelled BG. These results, the fit C of Bryan and Gersten,[77] were obtained by fitting with the MAW-X phase shift analysis error matrix, including the s-wave phase shifts.

The singlet even state is displayed by the $^1D_2$ and $^1G_4$ phase shifts. The theoretical result S1 (MS δ_o^o) is somewhat too attractive above 25 MeV in the $^1D_2$ case. As mentioned, reducing the $|f_+^o|$ input as in S2 (GS+LBL δ_o^o) decreases the attraction. We have removed the Coulomb effect in the phase shift analysis $^1D_2$ values via the Hamada-Johnston[76] potential (see Ref. 78).

The excess attraction is also present in the triplet odd state, as evidenced by the ^3F_J phase shifts. The failure of the theory to produce the L=1 phase shifts should possibly not be taken seriously since the dispersion relation (II.11) may require one subtraction. As noted in Chapter I, if one subtraction is required then the neglected high-t' dispersion integral would be a first order polynomial in t. We have shown the 25 MeV ^3P_J phase shifts, Coulomb effect removed, which were found in a recent analysis.[78] The ^3F_J phase shifts are also shown in linear combinations which approximately separate the central, tensor, and spin-orbit components of the amplitude. The combinations are defined for arbitrary L as

$$^3L_c = \frac{1}{3(2L+1)}\left[(2L-1)\delta_{L-1} + (2L+1)\delta_L + (2L+3)\delta_{L+1}\right],$$

$$^3L_T = \frac{-(2L-1)(2L+3)}{12L(2L+1)(L+1)}\left[(L+1)\delta_{L-1} - (2L+1)\delta_L + L\,\delta_{L+1}\right],$$

$$^3L_{LS} = \frac{-1}{2L(2L+1)(L+1)}\left[(2L-1)(L+1)\,\delta_{L-1} + (2L+1)\,\delta_L - L(2L+3)\,\delta_{L+1}\right]$$

The theoretical L=3 central component is much too attractive, but the tensor component, which is not directly dependent on the s-wave $\pi\pi$ interaction, is very well produced. The spin-orbit component is insufficiently attractive, but superior to that produced by the Hamada-Johnston potential.

The singlet odd phase shifts are apparently too repulsive, although the $^1F_3$ case is somewhat unclear. For the singlet odd state we found that using the GS+LBL rather than Morgan-Shaw δ_o^o input does not improve the agreement with nucleon-nucleon phase shift analysis.

The triplet even state is shown by the $^3D_2$ and $^3\bar{D}_3$ phase shifts. The theoretical $^3D_2$ phase shift is too attractive, as is the BG boson-exchange fit. The $^3\bar{D}_3$ phase shift is very sensitive to the high-t spectral function input. For example, changing the dispersion integral cut-off (Equation (II.11)) from $45\mu^2$ to $35\mu^2$ results in a 23% change in $^3\bar{D}_3$ at 210 MeV but a less than 3% change in other L>1 phase shifts.

B. Potentials

The potentials, calculated with the same input as for the phase shifts, are shown in Figures 39-48. The Hamada-Johnston[76] potential is also shown, and one may consider the phase shifts produced by the HJ potential in

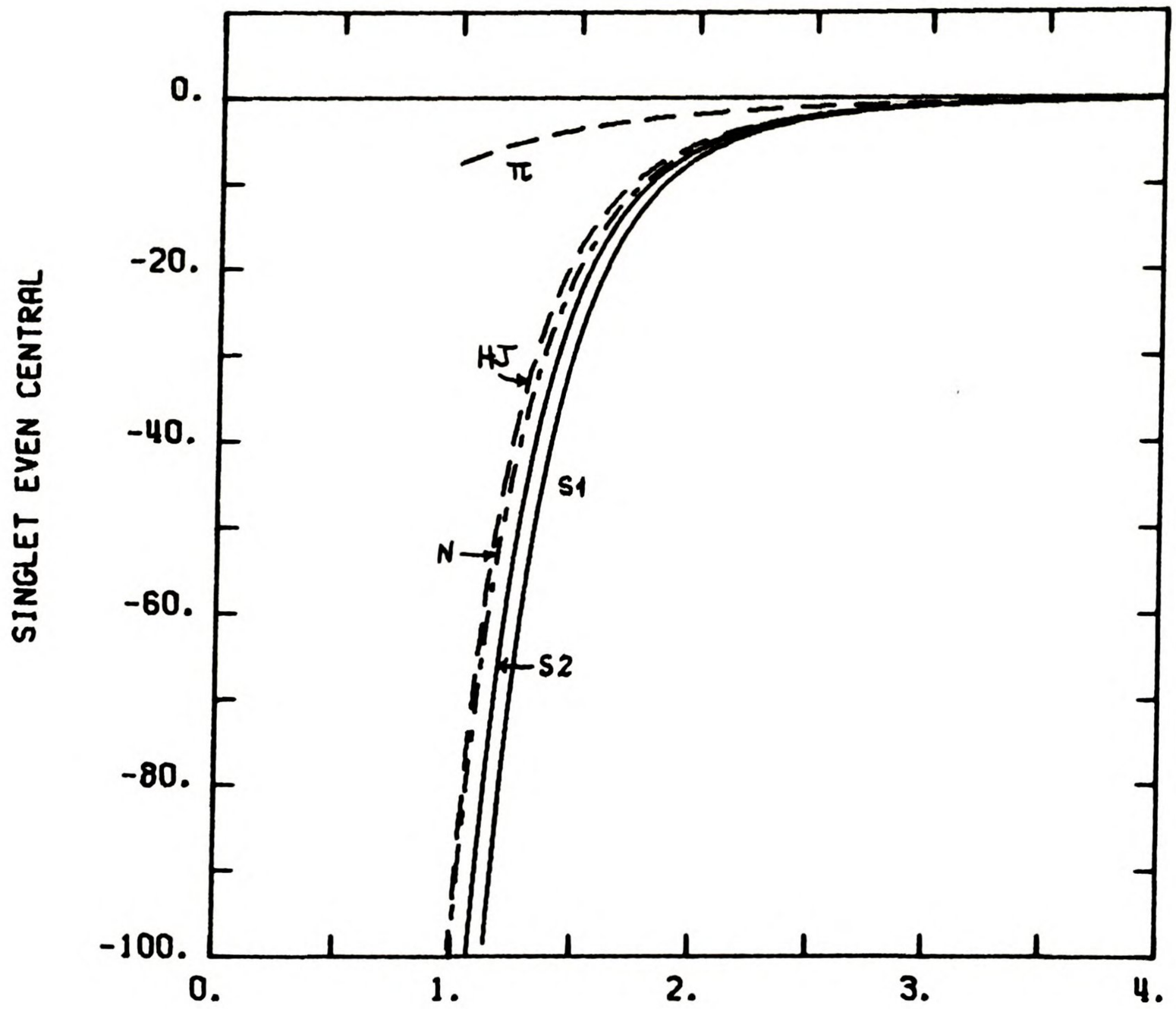

Figure 39. The singlet even central potential.

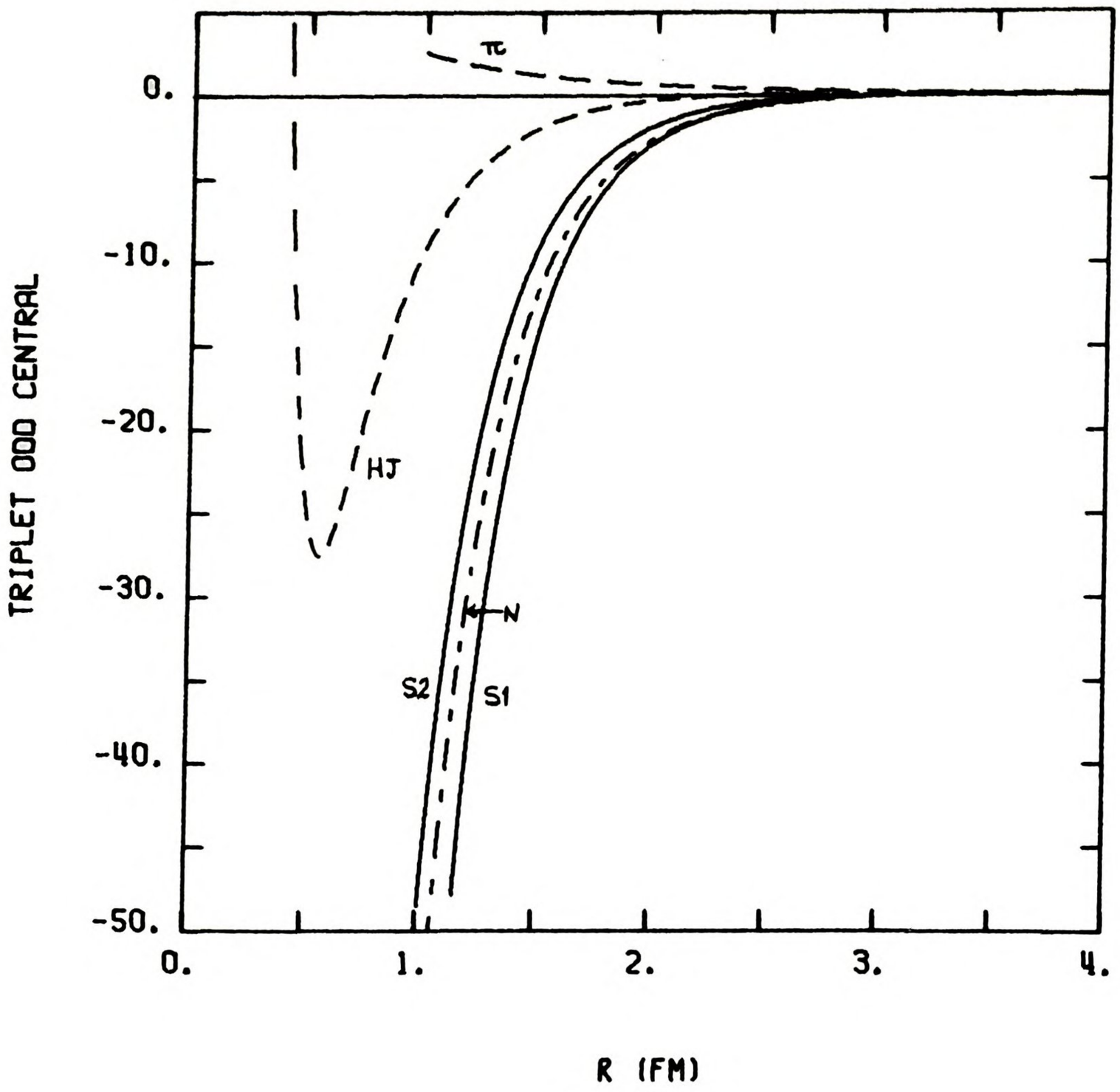

Figure 40. The triplet odd central potential.

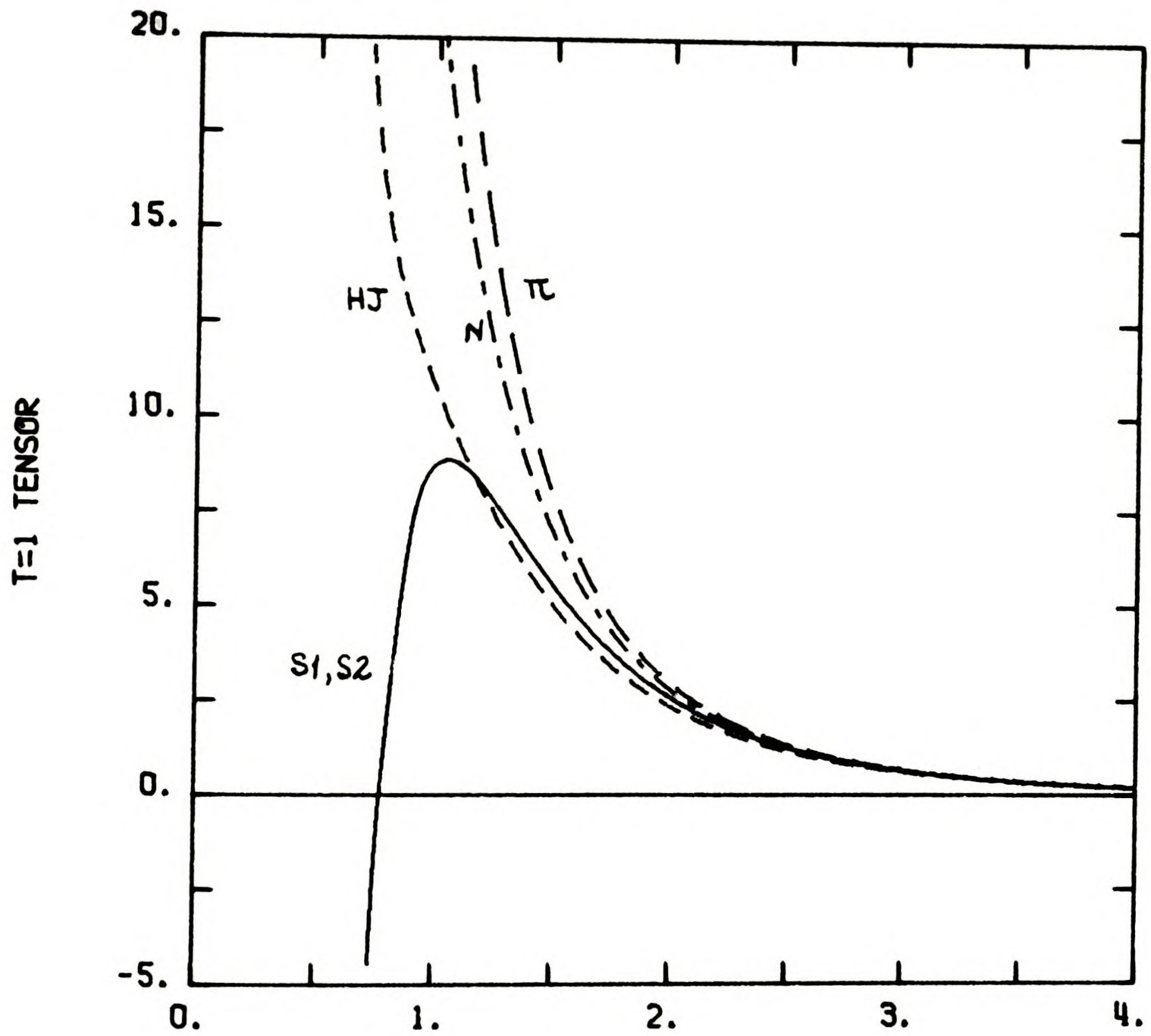

Figure 41. The T=1 tensor potential.

$$\Gamma_{\text{GaAs}} \cdot t=1$$

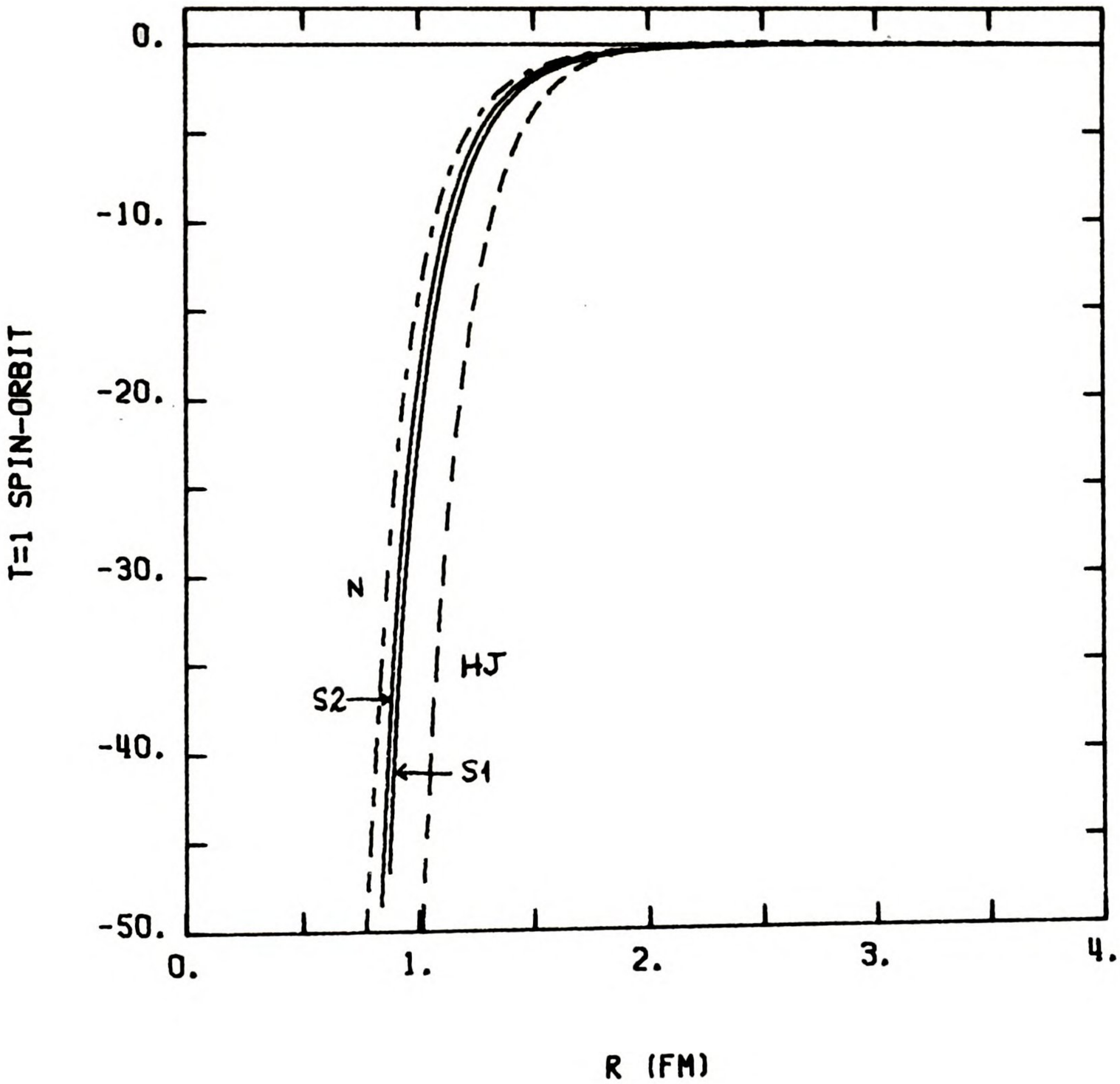

Figure 42. The T=1 spin-orbit potential.

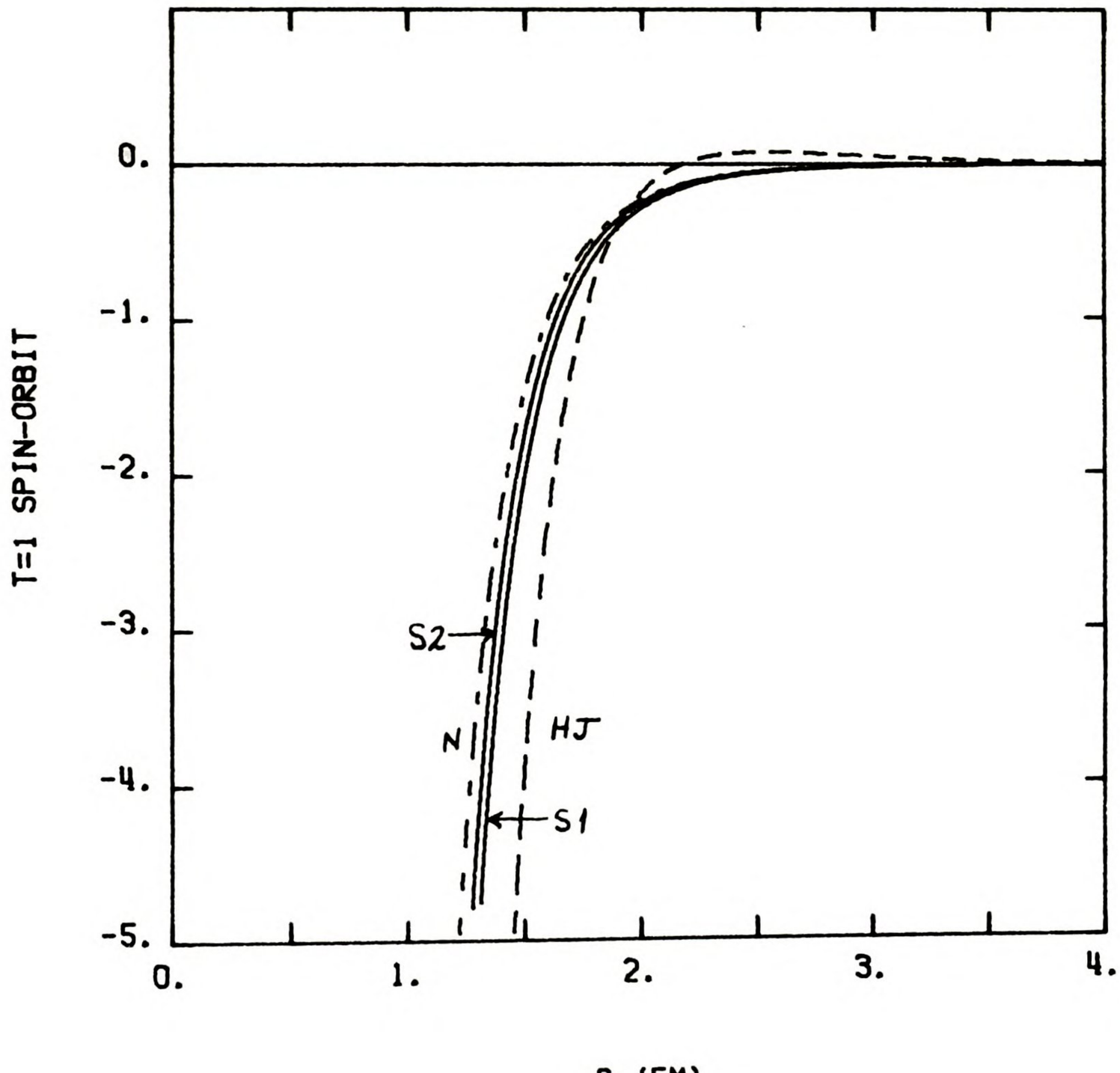

Figure 43. The long range T=1 spin-orbit potential.

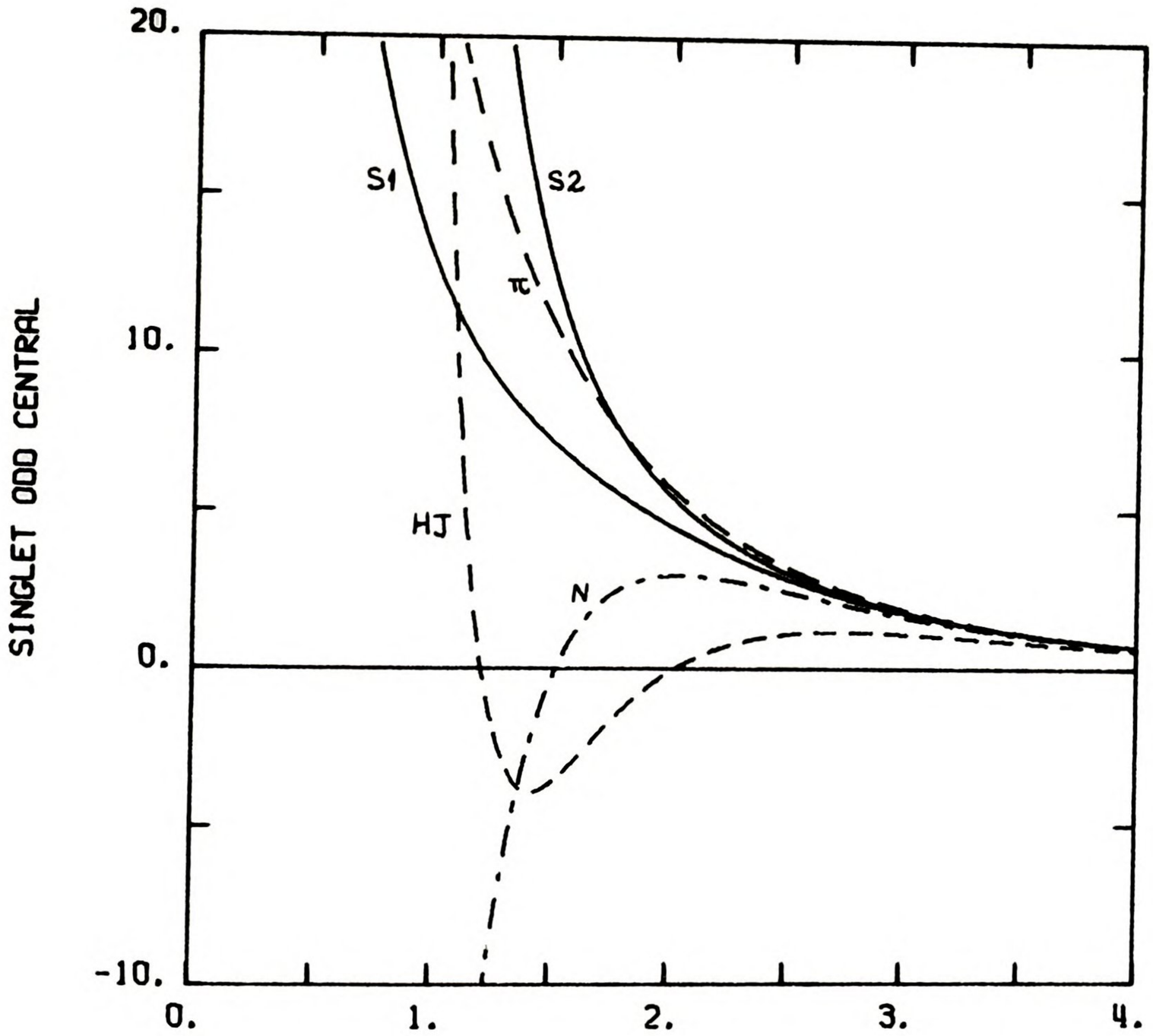

Figure 44. The singlet odd central potential.

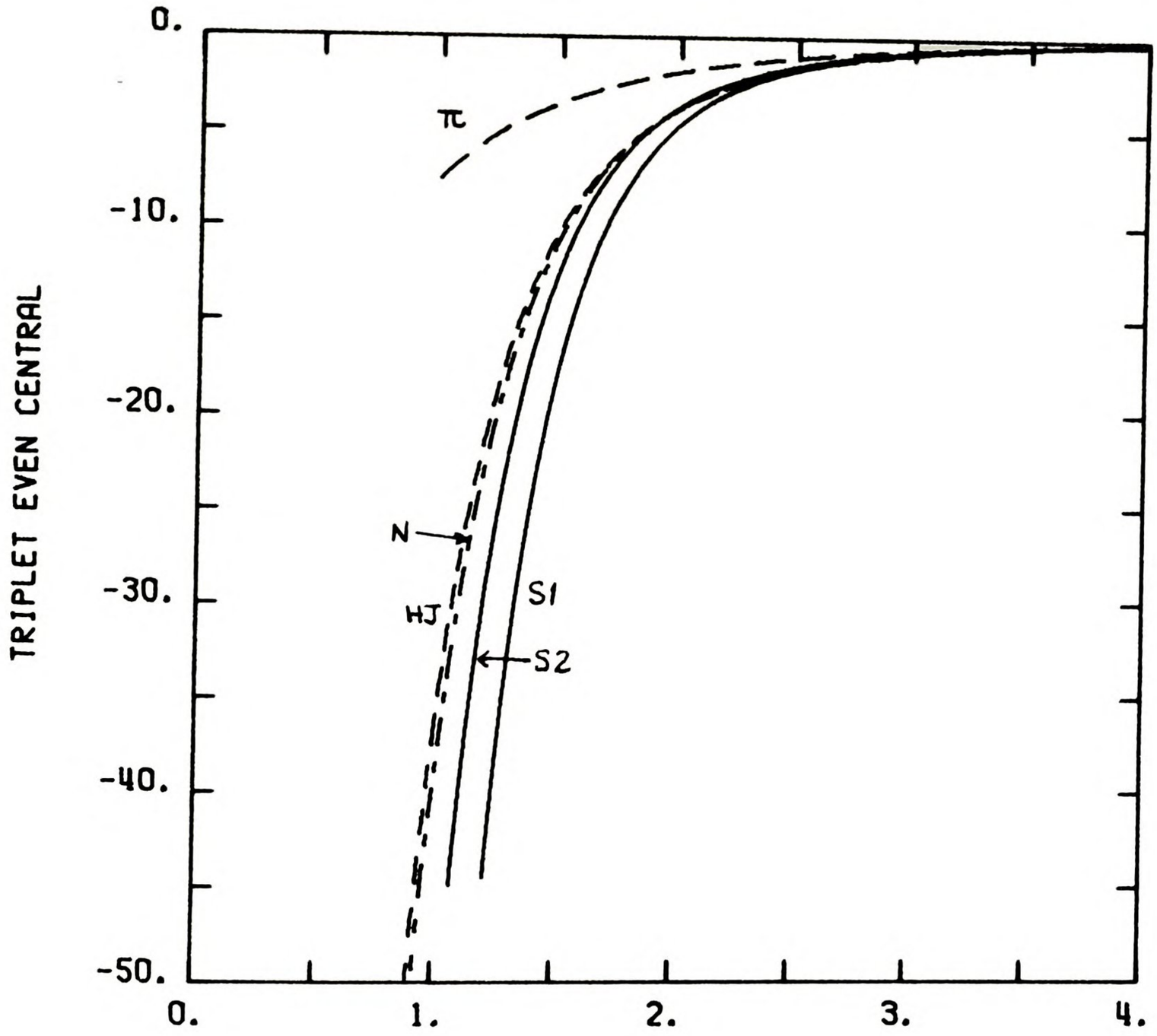

Figure 45. The triplet even central potential.

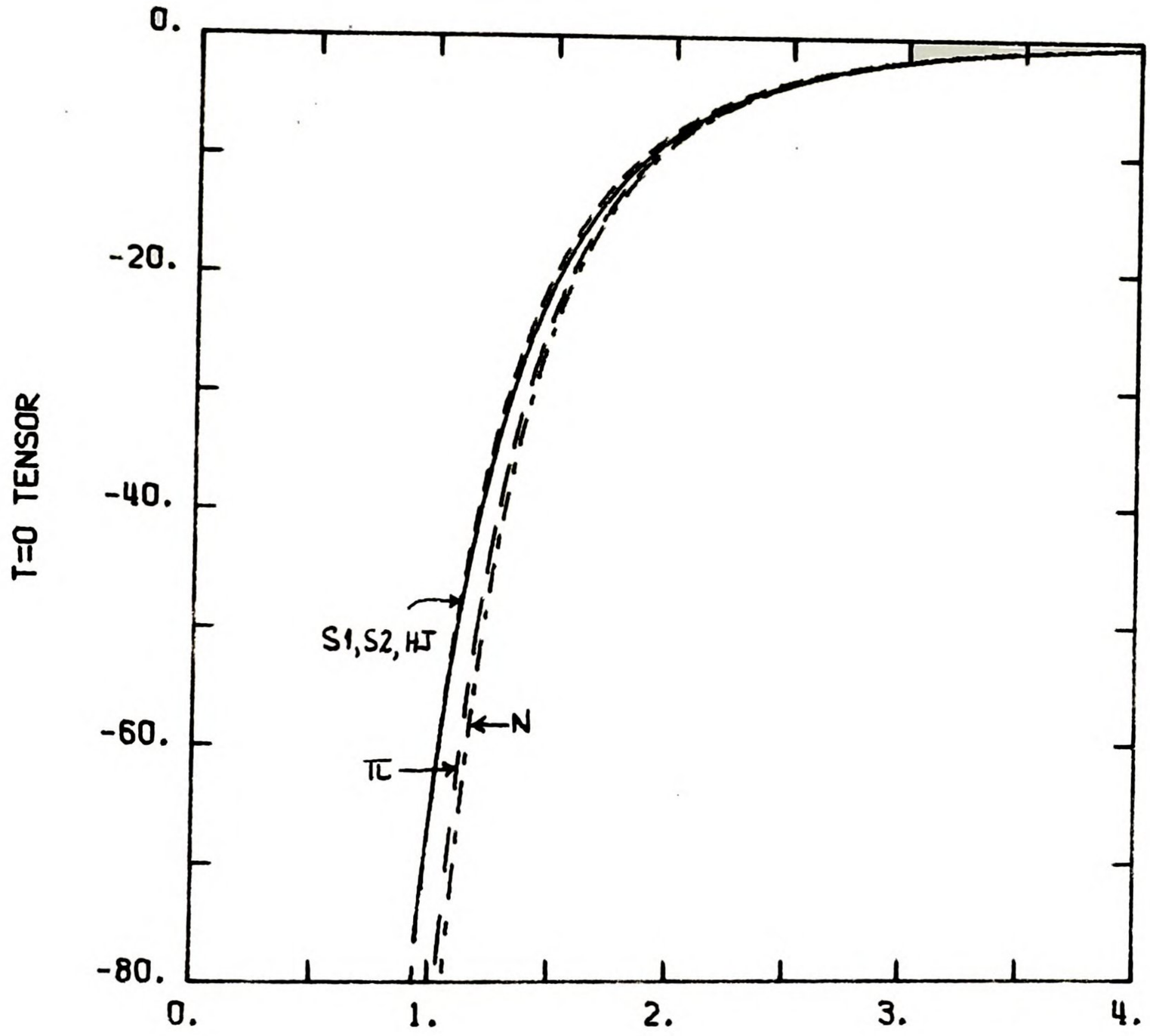

Figure 46. The T=0 tensor potential.

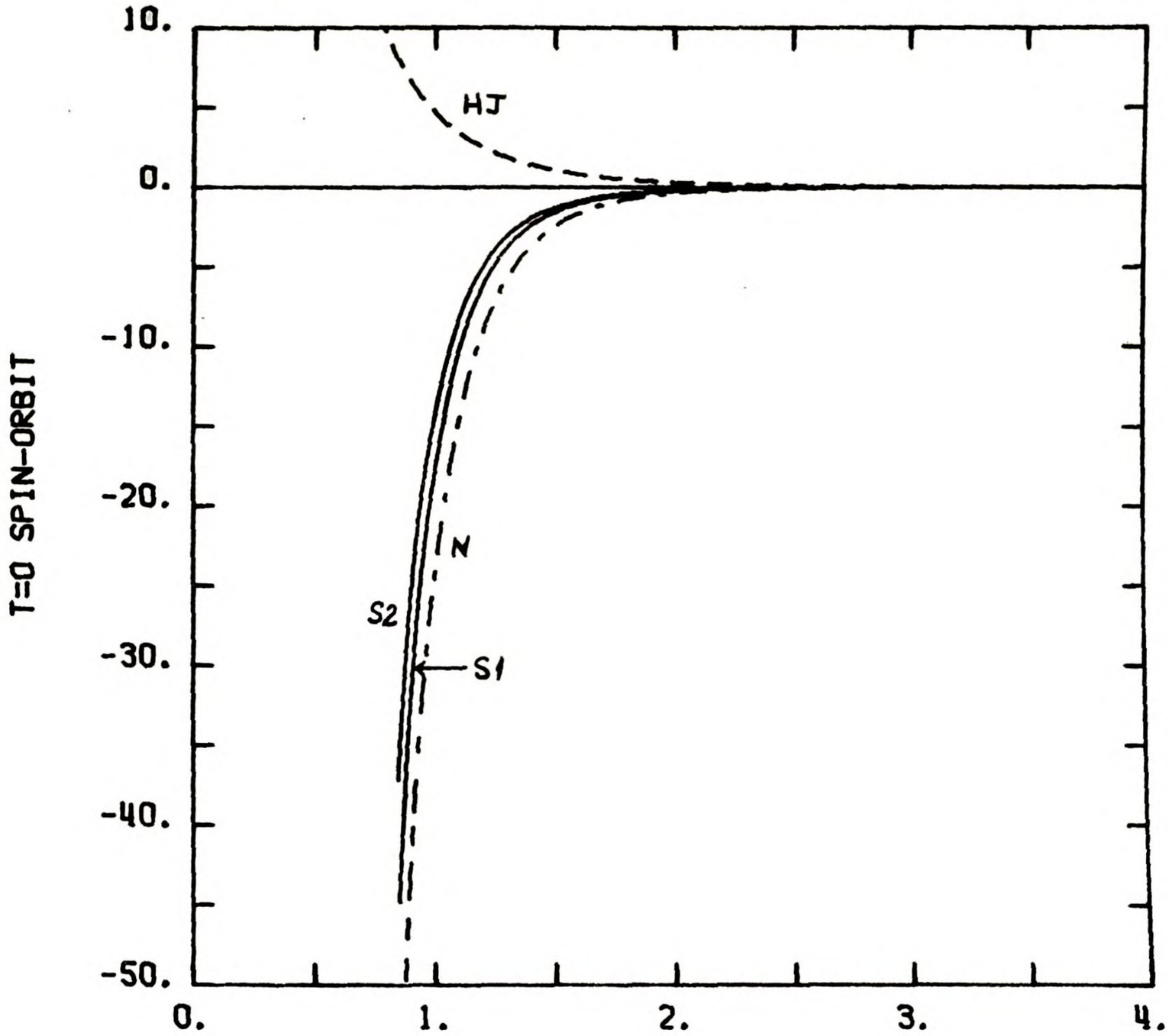

Figure 47. The T=0 spin-orbit potential.

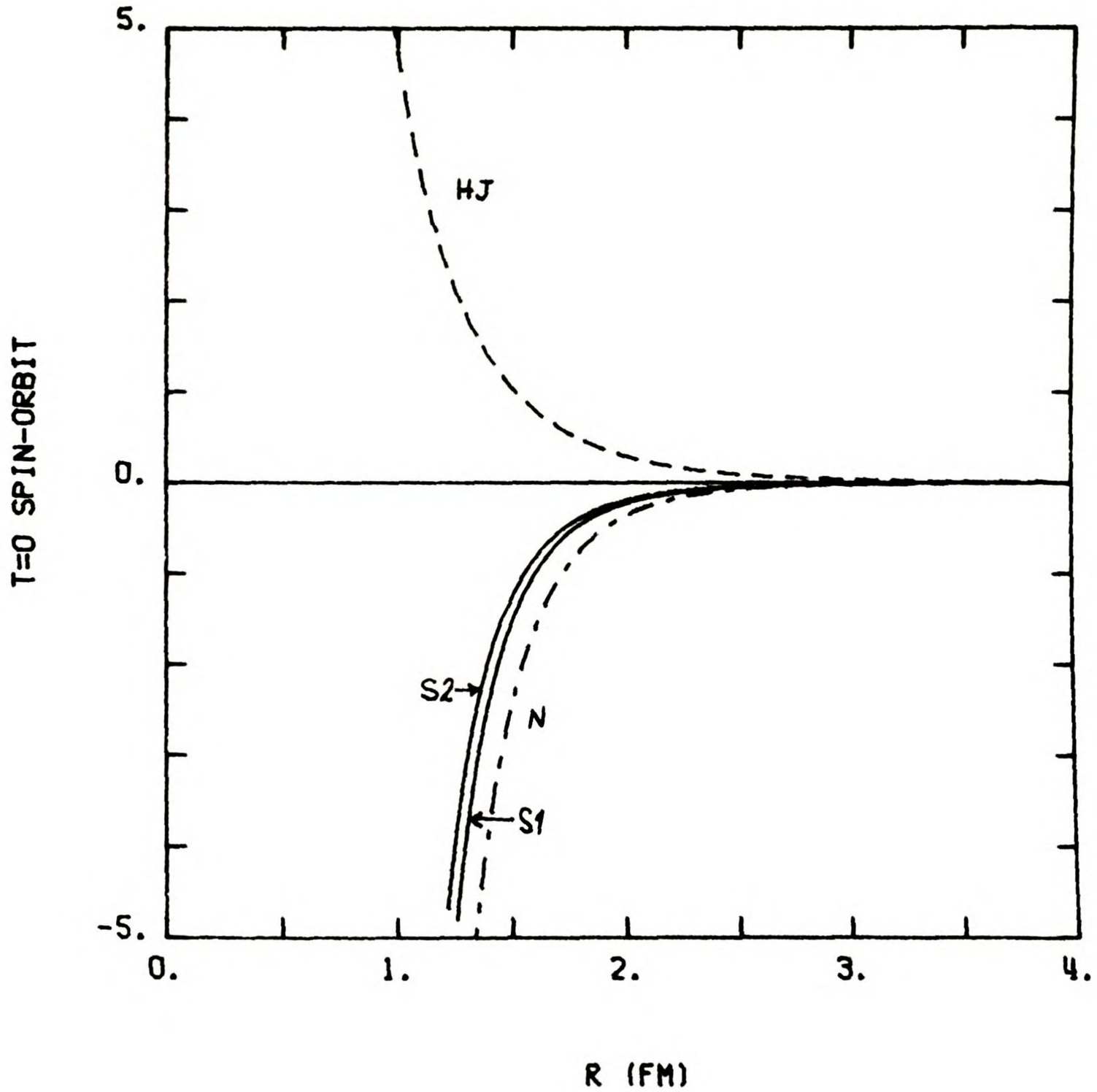

Figure 48. The long range T=0 spin-orbit potential.

judging its correctness. We do not imply that the two-pion-exchange + π + ω potential should necessarily reproduce the HJ one.

In Figure 39 we see that the theoretical singlet even potential is somewhat more attractive than the HJ potential, consistent with our conclusions from the $^1D_2$ and $^1G_4$ phase shifts. The 4th-order + π potential, labelled N, is remarkably close to the HJ potential, a fact noted by Partovi and Lomon.[1] It is interesting that increasing the low-t $\pi\pi$ s-wave enhancement brings the theoretical potential closer to HJ and N.

The tendency to be overly attractive is also seen in the triplet odd central and the triplet even central potentials, although the agreement with the HJ triplet even is good at long range. The discrepancy with the HJ triplet odd central potential is remarkably large.

The tensor potentials are in good agreement with HJ in to one Fermi. The tensor force is not directly dependent on the s-wave $\pi\pi$ interaction.

The $^3F_{LS}$ phase shift indicated that at low energy the HJ spin orbit force is less attractive than the 4th order + π or the theoretical values, but that at higher energies (above 200 MeV) the HJ $^3F_{LS}$ increases rapidly. The HJ T=1 spin-orbit potential is actually more attractive than the 4th-order + π or theoretical potentials even at two Fermis. The HJ potential becomes repulsive at ~2.2

Ferm

are

agre

curv

non-

cal

Howe

from

the

ππ

red

spo

enh

Gen

mos

Sha

we

Ber

t=4

by

tic

orb

Fermis. The L=3 phase shifts at energies less than 200 MeV are very sensitive to the potential at r>2fm.

The HJ T=0 spin-orbit potential is in strong disagreement with the calculated potentials. None of the curves changes sign between one and four Fermis.

The singlet odd state is interesting in that the HJ non-π-exchange potential is very long range. The theoretical potentials do not show the very long range behavior. However, the calculations S1, S2 do differ considerably from the 4-order + π potential.

C. Discussion

The largest uncertainty in TPE is the magnitude of the s-wave $N\bar{N}\rightarrow\pi\pi$ amplitude f^{o}_{+}. If the uncertainties in the $\pi\pi$ phase shift δ^{o}_{o}, especially at t<20 ($M_{\pi\pi}$<620 MeV), were reduced, the magnitude $|f^{o}_{+}|$ could be evaluated with correspondingly greater certainty. We have seen that the enhancement of the near-threshold δ^{o}_{o}, as reported by the Geneva-Saclay[39] group, gives much better agreement with most of the NN phase shifts than the no-enhancement Morgan-Shaw[28] δ^{o}_{o}. Although perhaps it is an insignificant fact, we note that the GS+LBL phase shift is very similar to the Berkeley[36] case 3 solution at t<10 (interpolation between t=4 and the t>15 fit). However, the improvement produced by the GS+LBL phase shift is not in all states. In particular, the singlet odd central and long-range T=1 spin-orbit forces suffer somewhat from this enhanced low-t δ^{o}_{o}.

very

combi

confo

this

accu

the

shel

exac

ener

a TP

scat

lat

effe

acc

et

the

cal

app

but

be

one

in

ac

The dependence of $|f_+^o|$ on the t>50 f_+^o phase is not very serious for most NN higher partial waves. Perhaps combining the Omnès dispersion relation approach with conformal mapping, à la Nielsen and Oades,[15] could decrease this uncertainty once the correct $t<50\mu^2$ phase is known accurately. Lack of an accurate knowledge of $|f_+^o|$ is now the only thing preventing a reliable calculation of the on-shell TPE amplitude.

One- and two-pion-exchange cannot be expected to exactly produce the NN amplitude, particularly at higher energies or lower partial waves. It may be possible to use a TPE calculation in a phenomenological analysis of NN scattering. Provided one is confident of the TPE calculation, he could perhaps study the higher mass exchange effects, determine the ωNN, ηNN coupling constants more accurately than at present, etc. We note here that Barker et al.[79] have shown that $\pi\eta$ exchange may be important.

Before we can claim to have a real understanding of the intermediate range NN force it may be necessary to calculate the low-t three-pion-exchange in at least some approximate way. Because of the broad ε and ρ distributions, and the small pion mass, we must be very cautious before neglecting three-pion-exchange, especially at, say, one Fermi. A three-pion-exchange calculation should include the J=0,1 $\pi\pi$ interactions.

The exchange of the $\pi\pi$ p-wave system is probably accurately included. We have obtained very good agreement

with the experimental nucleon form factors using our $N\bar{N}\to\pi\pi$ p-wave amplitudes. The fit to both G_E^V and G_M^V using only two parameters, Im $\Gamma_i(m_\rho^2)$, gives some support to our belief that the two pion state gives by far the dominant contribution to the small $|t|$ nucleon form factors and is consistent with p-wave elasticity to well beyond the ρ. We have found that the nucleon form factors are more sensitive to the $\Gamma_i(t\lesssim 30)$ than are the higher partial wave NN amplitudes below 200 MeV. Thus, the form factors provide a stringent test of the validity of the p-wave input.

Our evaluation of $\Gamma_i(t)$ depended on the pion form factor $F_\pi(t)$. The experimental situation for timelike t ($t>0$) is not yet very satisfying. The form factor which we have used is in good agreement with the Novosibirsk[70] experimental results. When better experimental F_π results are available they may be used in the study of the nucleon form factors. We do not expect better F_π results to significantly affect the TPE calculation.

We have accurately determined the d-wave $N\bar{N}\to\pi\pi$ amplitudes at $4<t<25$, the most important region for TPE. We do not, therefore, have to rely upon theoretical models for the d-wave exchange. The nucleon pole contribution is expected to adequately represent all higher-J $\pi\pi$ exchange. However, theoretical models can be tested against our amplitudes. We have, for example, shown how one can approximate the d-wave exchange by nucleon and Δ_{33} poles. The d-wave $\pi\pi$ interaction was shown to have a rather small

effect on the $N\bar{N}\to\pi\pi$ amplitudes. We can conclude that Vinh Mau et al.[14] were justified in neglecting the $J\geq 2$ t-channel branch cut.

Finally, we can conclude that the Mandelstam representation has once again shown its great value to particle physics calculations.

LIST OF REFERENCES

129a

LIST OF REFERENCES

1. M. H. Partovi and E. L. Lomon, Phys. Rev. D2, 1999 (1970); Phys. Rev. Letters 22, 438 (1969).

2. S. N. Gupta, R. D. Haracz and J. Kaskas, Phys. Rev. 138, B1500 (1965); S. N. Gupta, Phys. Rev. 117, 1146 (1960); B. M. Barker and R. D. Haracz, Phys. Rev. 186, 1624 (1969); references therein.

3. J. Binstock, Phys. Rev. D3, 1139 (1971); J. Binstock and R. Bryan, Phys. Rev. D4, 1341 (1971).

4. D. Amati, E. Leader and B. Vitale, Nuovo Cimento 17, 68 (1960); Nuovo Cimento 18, 409 (1960); Phys. Rev. 130, 750 (1963).

5. J. Bowcock, W. N. Cottingham and D. Lurié, Nuovo Cimento 16, 918 (1960).

6. J. W. Durso, Phys. Rev. 149, 1234 (1966).

7. P. D. Kapadia, Nucl. Phys. B3, 291 (1967).

8. P. Signell, Advances in Nuclear Physics 2, 223 (1969).

9. P. Signell, Amsterdam International Conference (1971).

10. G. E. Brown and J. W. Durso, Phys. Letters 35B, 120 (1971).

11. S. L. Adler, Phys. Rev. 137, B1022 (1965); Phys. Rev. 139, B1638 (1965). Also see Ref. 83.

12. H. Nielsen, J. L. Petersen and E. Pietarinen, Nucl. Phys. B22, 525 (1970).

13. M. Chemtob, J. W. Durso, and D. O. Riska, Nucl. Phys. B38, 141 (1972).

14. R. Vinh Mau, J. M. Richard, B. Loiseau, M. Lacombe and W. N. Cottingham, Phys. Letters 44B, 1 (1973); Phys. Rev. D8, 800 (1973).

15. H. Nielsen and G. C. Oades, Nucl. Phys. B49, 586 (1972).

16. G. Epstein and B. McKellar, Lettere al Nuovo Cimento 5, 807 (1972); G. Epstein, Ph.D. Thesis (1973).

17. S. Mandelstam, Phys. Rev 112, 1344 (1958); Phys. Rev. 115, 1741 and 1752 (1959).

18. The Mandelstam representation has been discussed in Dispersion Relations and Elementary Particles, ed. by C. DeWitt and R. Omnès, Wiley, New York (1960).

19. For example see J. J. Sakurai, Advanced Quantum Mechanics, Addison-Wesley (1967), Reading, Mass. Our field-theory amplitude is defined with the sign opposite to that of Sakurai.

20. G. F. Chew, M. L. Goldberger, F. E. Low and Y. Nambu, Phys. Rev. 106, 1377 (1957).

21. For a discussion of the various scattering amplitudes, their relations to the S-matrix, their Lorentz transformation properties, the unitarity relation, and the Lippmann-Schwinger equation for the amplitude see M. L. Goldberger and K. M. Watson, Collision Theory, Wiley, New York (1964). The T_{ba} of this reference is related to our M_{fi} by

$$\mathcal{M}_{fi} = -(2\pi)^3 \left(\frac{E_{p_1} E_{n_1} E_{p_2} E_{n_2}}{m^4} \right)^{1/2} T_{ba}$$

In our Equation (II.42) we interpret k^2 as E^2-m^2 rather than replacing k^2 by $2m(E-m)$. This interpretation is suggested by the relations between T_{fi}, M_{fi} and the cross section.

22. L. Heller, private communication.

23. R. Blankenbecler and R. Sugar, Phys. Rev. 142, 1051 (1966).

24. A. A. Logunov and A. N. Tavkhelidze, Nuovo Cimento 29, 380 (1963).

25. W. R. Frazer and J. R. Fulco, Phys. Rev. 117, 1603 (1960); Phys. Rev. 119, 1420 (1960).

26. R. Omnès, Nuovo Cimento 8, 316 (1958).

27. H. Nielsen, Nucl. Phys. B33, 152 (1971).

28. D. Morgan and G. Shaw, Phys. Rev. D2, 520 (1970).

29. For copious references see the Review of Particle Properties: T. A. Lasinski et al., Rev. Mod. Phys. 45, S73 (1973).

30. L. W. Jones et al., Phys. Letters 21, 590 (1966).

31. W. D. Walker, J. Carroll, A. Garfinkel and B. Y. Oh, Phys. Letters 18, 630 (1967).

32. C. Goebel, Phys. Rev. Letters, 337 (1958).

33. G. F. Chew and F. E. Low, Phys. Rev. 113, 1640 (1959).

34. J. P. Baton, G. Laurens and J. Reignier, Phys. Letters 33B, 525 and 528 (1970).

35. P. Baillon et al., Phys. Letters 38B, 555 (1972).

36. S. D. Protopopescu et al., Phys. Rev. D7, 1279 (1973).

37. P. Estabrooks, A. D. Martin et al., International Conference on $\pi\pi$ Scattering and Associated Topics, Tallahasee, AIP (1972); G. Grayer et al., Experimental Meson Spectroscopy, 1972, Proceedings of the Third International Conference, Philadelphia, AIP (1972).

38. W. D. Apel et al., Phys. Letters 41B, 542 (1972).

39. P. Basile et al., Phys. Letters 36B, 619 (1971); A. Zylbersztejn et al., Phys. Letters 38B, 457 (1971).

40. E. W. Beir et al., Phys. Rev. Letters 30, 399 (1972).

41. M. R. Pennington and S. D. Protopopescu, Phys. Rev. D7, 1429 and 2591 (1973).

42. M. G. Olsson, Wisconsin preprint COO-282 (1970), unavailable.

43. W. M. Bugg et al., Phys. Rev. D7, 3264 (1973).

44. K. Symanzik, Phys. Rev. 105, 743 (1957); N. N. Bogoliubov, B. V. Medvedev and M. K. Polivanov, Problems of the Theory of Dispersion Relations, lecture notes, Institute for Advanced Study; M. L. Goldberger, Phys. Rev. 99, 979 (1955).

45. D. V. Bugg, A. A. Carter and J. R. Carter, Physics Letters 44B, 278 (1973).

46. J. Hamilton and W. S. Woolcock, Rev. Mod. Phys. 35, 737 (1963).

47. G. Höhler, H. Schaile and R. Strauss, Z. Phys. 229, 217 (1969).

48. Data Tape UCRL-20030 πN, Particle Data Group, University of California.

49. A. T. Davies, Nucl. Phys. B40, 157 (1972).

50. R. Ayed, P. Bareyre and G. Villet, Phys. Letters 31B, 598 (1970).

51. L. D. Roper, R. M. Wright and B. T. Feld, Phys. Rev. 138, B190 (1965).

52. S. Almehed and C. Lovelace, Nucl. Phys. B40, 157 (1972); references therein.

53. V. Barger and R. J. N. Phillips, Phys. Rev. 187, 2210 (1969). I am thankful to Paul Stevens for pointing out the errors in this paper.

54. G. Höhler, H. P. Jakob and R. Strauss, Nucl. Phys. B39, 232 (1972); Phys. Letters 35B, 445 (1971).

55. J. Engels, Nucl. Phys. B36, 73 (1972).

56. C. Lovelace, Pion-Nucleon Scattering (Irvine Conference), ed. by G. L. Shaw and D. Y Wong, Wiley-Interscience, New York (1969).

57. J. Hamilton, Phys. Letters 20, 687 (1966).

58. V. Samaranake and W. S. Woolcock, Nucl. Phys. B48, 205 (1972).

59. N. S. Hald, Nucl, Phys. B48, 549 (1972).

60. V. Samaranayake and W. S. Woolcock, Phys. Rev. Letters 15, 936 (1965). Also see Ref. 58.

61. M. H. MacGregor, R. A. Arndt and R. M. Wright, Phys. Rev. 182, 1714 (1972).

62. S. I. Bilen'kaya, L. N. Glonti, Yu. M. Kazarinov and V. S. Kiselev, JETP (Sov. Phys.) 32, 569 (1971).

63. R. E. Cutkosky and B. B. Deo, Phys. Rev. Letters, 20, 1272 (1968).

64. P. Lichard and P. Prešnajder, Nucl. Phys. B33, 605 (1971).

65. D. Morgan and G. Shaw, Nucl. Phys. B43, 365 (1972).

66. Y. A. Chao and R. K. P. Zia, Phys. Rev. D8, 4085 (1973).

67. S. Furuichi and K. Watanabe, Prog. Theoret. Phys. 37, 465 (1967).

68. See for example W. R. Frazer, in Dispersion Relations, ed. by. G. R. Screaton, Oliver and Boyd, Edinburgh, Great Britain (1961).

69. J. E. Augustin et al., Phys. Letters 28B, 508 (1969).

70. V. L. Auslander et al., Sov. J. Nucl. Phys. 9, 69 (1969).

71. P. Signell and J. W. Durso, Phys. Rev. Letters 18, 185 (1967).

72. J. S. Ball and D. Y. Wong, Phys. Rev. 130, 2112 (1963).

73. P. Federbush, M. L. Goldberger and S. B. Treiman, Phys. Rev. 112, 642 (1958).

74. J. Schwarz, Phys. Rev. 179, 1487 (1969).

75. M. H. MacGregor, R. A. Arndt and R. M. Wright, Phys. Rev. 182, 1714 (1969).

76. T. Hamada and I. D. Johnston, Nucl. Phys. 34, 382 (1962).

77. R. A. Bryan and A. Gersten, Phys. Rev. D6, 341 (1972).

78. G. E. Bohannon, T. Burt and P. Signell, to be published.

79. B. M. Barker, S. N. Gupta and R. D. Haracz, Phys. Rev. 142, 1144 (1966).

80. H. P. Stapp, T. J. Ypsilantis and N. Metropolis, Phys. Rev. 105, 302 (1957).

81. M. L. Goldberger, I. Nambu and R. Oehme, Ann. Phys. 2, 226 (1957).

82. See for example R. P. Feynman, Photon-Hadron Interactions, W. A. Benjamin, Reading, Mass. (1972).

83. See for example J. J. Sakurai, Currents and Mesons, U. of Chicago Press, Chicago (1969).

84. L. H. Chan et al., Phys. Rev. 141, 1298 (1966).

85. S. C. C. Ting, Proceedings of the 14th International Conference on High Energy Physics, Vienna (1968), CERN.

APPENDICES

137a

APPENDIX A

THE HELICITY EXPANSION

1376

APPENDIX A

THE HELICITY EXPANSION

The momenta for the $N\bar{N}\to\pi\pi$ process are labelled as in Figure 3. The corresponding Mandelstam variables are

$$s = -(p - q)^2 ,$$

$$t = -(p + p')^2 , \qquad (A.1)$$

$$u = -(p - q')^2 ,$$

and the nucleon momentum, pion momentum, and scattering angle, all in the c.m. frame are

$$p^2 = t/4 - m^2 ,$$

$$q^2 = t/4 - 1 , \qquad (A.2)$$

$$\cos\theta = (s - u)/(4pq) .$$

In the pseudophysical region ($4 \leq t < 4m^2$) the nucleon c.m. momentum is positive imaginary while below the pseudophysical threshold ($t<4$) both nucleon and pion c.m. momenta

are positive imaginary. It is customary to define the variables p_- and q_- as $p = ip_-$ and $q = iq_-$.

Taking the quantization axis along the antinucleon momentum $\underline{p}'$, Frazer and Fulco[25] gave the helicity expansion for $A^{(\pm)}$ and $B^{(+)}$:

$$A^{(t)} = -\sum_{J=0}^{\infty} (J+\tfrac{1}{2}) \frac{8\pi}{p^2} (pq)^J \left\{ P_J(\cos\theta) f_+^J(t) \right.$$

$$\left. - \frac{m \cos\theta\, P_J'(\cos\theta)}{\sqrt{J(J+1)}} f_-^J(t) \right\}, \qquad \text{(A.3a)}$$

$$B^{(t)} = \sum_{J=1}^{\infty} \frac{8\pi(J+\frac{1}{2})}{\sqrt{J(J+1)}} (pq)^{J-1} P_J'(\cos\theta) f_-^J(t) . \qquad \text{(A.3b)}$$

Generalized Bose-Einstein statistics requires that the t-channel isospin is 0 (1) when J is even (odd). We recall that the superscript on A and B is + (-) for t-channel isospin 0 (1). The subscript on $f_{\pm}^J$ indicates that the nucleon and antinucleon helicities are the same (+) or opposite (-). The partial wave projections of A and B are

$$f_+^J(t) = \frac{1}{8\pi} \left[\frac{-p^2}{(pq)^J} A_J + \frac{m}{(2J+1)(pq)^{J-1}} \left\{ (J+1) B_{J+1} \right.\right.$$

$$\left.\left. + J B_{J-1} \right\} \right], \qquad \text{(A.4a)}$$

$$f_-^J(t) = \frac{1}{8\pi} \frac{\sqrt{J(J+1)}}{(2J+1)(pq)^{J-1}} \left\{ B_{J-1} - B_{J+1} \right\}, \qquad \text{(A.4b)}$$

where

$$A_J = \int_{-1}^{1} P_J(\cos\theta)\, A^{(\pm)}\, d\cos\theta \,,$$

$$B_J = \int_{-1}^{1} P_J(\cos\theta)\, B^{(\pm)}\, d\cos\theta \,.$$

APPENDIX B

POLE CONTRIBUTIONS TO THE

$N\bar{N}\to\pi\pi$ AMPLITUDES

1402

APPENDIX B

POLE CONTRIBUTIONS TO THE $N\bar{N}\to\pi\pi$ AMPLITUDES

The contributions of s- and u-channel poles to $f^J_{\pm}$ are found by putting the poles into the appropriate term of the s- and u-channel partial expansions of A and B, and applying (A.4).

The following forms for J=0,1,2 are most convenient for $t\geq 4$:

$$f^0_+(t) = \frac{1}{4\pi}\left[\frac{p_-}{q_b} G_A^{(+)} \arctan\frac{1}{h_r} + m\, G_B^{(+)}\left(h_r \arctan\frac{1}{h_r} - 1\right)\right], \qquad \text{(B.1)}$$

$$f^1_+(t) = \frac{1}{4\pi}\left[\frac{1}{q_b^2} G_A^{(-)}\left(1-\arctan\frac{1}{h_r}\right) + \frac{m}{p_- q_b} G_B^{(-)}\left(h_r - h_r^2 \arctan\frac{1}{h_r}\right)\right], \qquad \text{(B.2a)}$$

$$f^1_-(t) = \frac{1}{4\pi\sqrt{2}\, p_- q_b} G_B^{(-)}\left[(1+h_r^2)\arctan\frac{1}{h_r} - h_r\right], \qquad \text{(B.2b)}$$

$$f^2_+(t) = \frac{1}{8\pi p_- q_b^3} G_A^{(+)}\left[(3h_r^2+1)\arctan\frac{1}{h_r} - 3h_r\right], \qquad \text{(B.3a)}$$

$$f^2_-(t) = \frac{\sqrt{6}}{8\pi (p_- q_b)^2} G_B^{(+)}\left[\frac{2}{3} + h_r^2 - (h_r^3+h_r)\arctan\frac{1}{h_r}\right], \qquad \text{(B.3b)}$$

where $$h_r = \frac{t - 2(m^2 + 1 - m_r^2)}{4p \cdot q} ,$$

and m_r^2 is the pole position in s and u.

The nucleon pole (Born term) residues are

$$G_A^{\pm} = 0 ,$$

$$G_B^{\pm} = g^2 = 4\pi(14.6) . \qquad \text{(B.4)}$$

For a "zero-width" $\Delta(1234)$ they are

$$G_A^{(+)} = \frac{16\pi m_\Delta \Gamma_\Delta}{3} \left[\frac{3(m_\Delta + m)}{(m_\Delta + m)^2 - 1} \left(1 + \frac{t}{2q_\Delta^2}\right) + \frac{m_\Delta - m}{(m_\Delta - m)^2 - 1} \right] , \qquad \text{(B.5a)}$$

$$G_B^{(+)} = \frac{16\pi m_\Delta \Gamma_\Delta}{3} \left[\frac{3}{(m_\Delta + m)^2 - 1} \left(1 + \frac{t}{2q_\Delta^2}\right) - \frac{1}{(m_\Delta - m)^2 - 1} \right] , \qquad \text{(B.5b)}$$

$$G_{A,B}^{(-)} = -\frac{1}{2} G_{A,B}^{(+)} , \qquad \text{(B.5c)}$$

where

$$q_\Delta^2 = \left[m_\Delta^2 - (m+1)^2 \right] \left[m_\Delta^2 - (m-1)^2 \right] / (4 m_\Delta^2) .$$

With m_Δ = 1234 MeV, m_π = 139.576 MeV, m = 938.259 MeV, and Γ_Δ = 120 MeV we find

$$G_A^+ = 4\pi(43.7 + 1.96\ t)\ ,$$
$$G_B^+ = 4\pi(-15.0 + 0.126\ t)\ . \qquad \text{(B.6)}$$

Often one will see the residues for the Δ determined not by the physical width but by other criteria, such as the πN scattering lengths or the integral of the partial wave amplitude over the region of the Δ. The latter method was used by Epstein[16] to obtain

$$G_A^{(+)} = 4\pi(36.0 + 1.6\ t)\ ,$$
$$G_B^{(+)} = 4\pi(-12.2 + 0.1\ t)\ . \qquad \text{(B.7)}$$

Note that with the masses used in (A.10) one should maintain the following relations regardless of how the residues are determined:

$$G_A^{(+)} = 4\pi(1 + 0.0449\ t)x\ ,$$
$$G_B^{(+)} = 4\pi(-0.343 + 0.00288\ t)x\ . \qquad \text{(B.8)}$$

with x to be determined.

Also useful are the p-wave amplitudes[25]

$$\Gamma_1(t) = \frac{m}{p^2}\left(f_+^1(t) - \frac{t}{4\sqrt{2}\,m} f_-^1(t)\right), \qquad \text{(B.9a)}$$

$$\Gamma_2(t) = \frac{1}{2p^2}\left(-f_+^1(t) + \frac{m}{\sqrt{2}} f_-^1(t)\right), \qquad \text{(B.9b)}$$

where, again, $p^2 = t/4 - m^2$.

For reference, the following relations are also given:

$$f_+^1 = -m\Gamma_1 - \frac{t}{2}\Gamma_2,$$

$$f_-^1 = -\sqrt{2}\,(\Gamma_1 + 2m\Gamma_2),$$

$$\Gamma_1 = -2m\Gamma_2 - \frac{1}{\sqrt{2}} f_-^1.$$

The values at t = 4 are

$$f_+^0(4) = \frac{p_-^2 G_A^{(+)}}{\pi(4-t_r)}, \tag{B.10}$$

$$f_+^1(4) = \frac{4p_-^2 G_A^{(-)}}{3\pi(4-t_r)^2} + \frac{m G_B^{(-)}}{3\pi(4-t_r)}, \tag{B.11a}$$

$$f_-^1(4) = \frac{\sqrt{2}\, G_B^{(-)}}{3\pi(4-t_r)}, \tag{B.11b}$$

$$f_+^2(4) = \frac{7p_-^2 G_A^{(+)}}{3\pi(4-t_r)^3} + \frac{7m G_B^{(+)}}{12\pi(4-t_r)}, \tag{B.12a}$$

$$f_-^2(4) = \frac{\sqrt{6}\, G_B^{(+)}}{4\pi(4-t_r)^2}, \tag{B.12b}$$

where $t_r = 2(m^2 + 1 - m_r^2)$ and $p_-^2 = p_-^2(4) = m^2 - 1$.

For $t < 4 - \frac{1}{m^2}$ the Born terms in $f_\pm^J$ become complex. Here the J=0,1,2 real parts are written in terms of logarithms.

$$\mathrm{Re}\, f_+^0(t) = \frac{-mg^2}{4\pi}\left[1 + Q \log\frac{1-Q}{1+Q}\right], \tag{B.13}$$

$$\mathrm{Re}\, f_+^1(t) = \frac{mg^2}{4\pi(p-q_-)}\left[Q + Q^2 \log\frac{1-Q}{1+Q}\right], \tag{B.14a}$$

$$\mathrm{Re}\, f_-^1(t) = \frac{g^2}{4\pi\sqrt{2}\,p-q_-}\left[-Q + \frac{1-Q^2}{2}\log\frac{1-Q}{1+Q}\right], \tag{B.14b}$$

$$\mathrm{Re}\, f_+^2(t) = \frac{mg^2}{8\pi(p-q_-)^2}\left[\frac{1}{2}(Q-3Q^3)\log\frac{1-Q}{1+Q} - 3Q^2\right], \tag{B.15a}$$

$$\mathrm{Re}\, f_-^2(t) = \frac{\sqrt{6}\,g^2}{8\pi(p-q_-)^2}\left[-\frac{2}{3} + Q^2 + \frac{1}{2}(Q^3-Q)\log\frac{1-Q}{1+Q}\right]. \tag{B.15b}$$

$$\mathrm{Im}\, f_+^0(t) = \frac{mg^2}{8} Q, \tag{B.16}$$

$$\mathrm{Im}\, f_+^1(t) = \frac{-mg^2}{8\,p-q_-} Q^2, \tag{B.17a}$$

$$\mathrm{Im}\, f_-^1(t) = \frac{\sqrt{2}\,g^2}{16\,p-q_-}(Q^2-1), \tag{B.17b}$$

$$\mathrm{Im}\, f_+^2(t) = \frac{mg^2}{16(p-q_-)^2}(3Q^3-Q), \tag{B.18a}$$

$$\mathrm{Im}\, f_-^2(t) = \frac{\sqrt{6}\,g^2}{16(p-q_-)^2}(Q-Q^3), \tag{B.18b}$$

$$\mathrm{Im}\, \Gamma_1(t) = \frac{m^2g^2}{8p^3q_-}\left[Q^2 + \frac{(Q^2-1)t}{8m^2}\right], \tag{B.19a}$$

$$\mathrm{Im}\, \Gamma_2(t) = \frac{mg^2}{32\,p^3q_-}(1-3Q^2), \tag{B.19b}$$

where $Q = \frac{2 - t}{4p_-q_-}$.

These equations may be obtained from (A.5,6,7) by the substitutions

$$h \rightarrow iQ,$$

$$\arctan 1/h \rightarrow \pi/2 + i/2 \log \frac{1-Q}{1+Q} . \qquad \text{(B.20)}$$

In the case J=0 one may not expect the nucleon + Δ pole approximation to be adequate as given in (A.5). The $A^{(+)}$ s-channel dispersion relation is rather slowly convergent and one can expect f_+^o to be sensitive to the large s behavior of the absorptive parts in an unsubtracted relation. One can, however, project f_+^o from a once subtracted relation for $A^{(+)}$ (unsubtracted for $B^{(+)}$) to obtain

$$f_+^o(t) = \frac{1}{4\pi}\left\{ p_-^2 A^{(+)}(s=m^2,t) - 2p_-^2 G_A^{(+)}\left[1 - h_r \arctan 1/h_r \right.\right.$$

$$\left. - \frac{t-2}{2(m_r^2-m^2)(m_r^2-m^2-2+t)}\left(1 - (h_r+h)\arctan 1/h_r\right)\right]$$

$$\left. - m\, G_B^{(+)}\left(1 - h_r \arctan 1/h_r\right)\right\}, \qquad \text{(B.21)}$$

where the subtraction is at $s = m^2$ and $h = \frac{t - 2}{4p_-q}$.

Brown and Durso[10] have obtained a particularly simple expression for f_+^o by keeping only the Born contributions to $B^{(+)}$ and approximating $A^{(+)}$ by its current algebra value g^2/m at the Adler[11] point. They obtained

$$f_+^o(t) = \frac{mg^2}{4\pi}\left(h \arctan 1/h - \frac{t}{4m^2}\right) . \qquad \text{(B.22)}$$

APPENDIX C

PARTIAL WAVE PROJECTIONS

1460

APPENDIX C

PARTIAL WAVE PROJECTIONS

To compare the theoretical NN amplitude with experiment we project out the partial wave amplitudes.

The bar phase shifts and mixing parameters are defined in terms of the α-matrix,[80] where $i\alpha = S$.

singlet: $$i\alpha_\ell = e^{2i\delta_\ell} \tag{C.1a}$$

triplet uncoupled: $$i\alpha_{\ell,\ell} = e^{2i\delta_{\ell,\ell}} \tag{C.1b}$$

triplet coupled: $$i\alpha_{j\pm1,j} = \cos 2\epsilon_j \; e^{2i\delta_{j\pm1,j}} \tag{C.1c}$$

$$i\alpha^j = i\sin 2\epsilon_j \exp\left[i\left(\delta_{j+1,j} + \delta_{j-1,j}\right]\right.$$

The α-matrix elements are written in terms of the singlet-triplet partial wave amplitudes $T_{ij}(\ell)$ as[81,4]

$$\alpha_\ell = \frac{k}{2\ell+1} \; T_{00}(\ell)$$

$$\alpha_{\ell,\ell} = \frac{k}{2\ell+1}\left[T_{11}(\ell) - (\ell+2)(\ell-1)\,T_{1-1}(\ell) + \sqrt{2}\;T_{01}(\ell)\right]$$

$$\alpha_{\ell,\ell+1} = \frac{k}{(2\ell+1)(2\ell+3)} \Big[(\ell+2)\, T_{11}(\ell) + \sqrt{2}\,\ell(\ell+1)\, T_{10}(\ell)$$

$$+ \ell(\ell+2)(\ell-1)\, T_{1-1}(\ell) - \sqrt{2}\,\ell(\ell+2)\, T_{01}(\ell)$$

$$+ (\ell+1)\, T_{00}(\ell) \Big]$$

$$\alpha_{\ell,\ell-1} = \frac{k}{(2\ell+1)(2\ell-1)} \Big[(\ell-1)\, T_{11}(\ell) - \sqrt{2}\,\ell\,(\ell+1)\, T_{10}(\ell)$$

$$+ (\ell+2)(\ell+1)(\ell-1)\, T_{1-1}(\ell)$$

$$+ \sqrt{2}\,(\ell+1)(\ell-1)\, T_{01}(\ell) + \ell\, T_{00}(\ell)$$

$$\alpha^{\ell+1} = \frac{-k\,[(\ell+1)(\ell+2)]^{1/2}}{(2\ell+1)(2\ell+3)} \Big[T_{11}(\ell) - \sqrt{2}\,\ell\, T_{10}(\ell)$$

$$+ \ell(\ell-1)\, T_{1-1}(\ell) - \sqrt{2}\,\ell\, T_{01}(\ell) - T_{00}(\ell) \qquad \text{(C.2)}$$

where k is the NN center of mass frame momentum.

The partial wave amplitudes $T_{ij}(\ell)$ are given by

$$T_{ij}(\ell) = \frac{2\ell+1}{2} \frac{(\ell-m)!}{(\ell+m)!} \int_{-1}^{1} T_{ij}(\cos\theta)\, P_\ell^m(\cos\theta)\, d\cos\theta \qquad \text{(C.3)}$$

where $m = |i-j|$ and

$$T_{ij}(\cos\theta) = \sum_r \sum_t V_{ij}^r(w,\cos\theta) \Big\{ U_{rt}(w,\cos\theta)\, p_t(wt\bar{t})$$

$$+ (-1)^{r+\Gamma}\, U_{rt}(w,-\cos\theta)\, p_t(w\bar{t}t) \Big\} (1-\cos^2\theta)^{\frac{m}{2}} \qquad \text{(C.4)}$$

where T is the NN isospin and $p_t = p_t^T$.

The matrices V_{ij}^r and U_{rt} are as follows:[4]

$$\frac{4\pi\lambda}{m} V_{ij}^r(w,y) =$$

i j	r=1	r=2	r=3	r=4	r=5
SS	0	0	2	$-2y^2(y^2-1)$	$2\lambda^2$
11	0	$\lambda[\lambda+1+(\lambda-1)y^2]$	$2y(1-y^2)$	$1+\lambda-(\lambda-1)y^2$	0
1-1	0	$\lambda(\lambda-1)$	0	$1-\lambda$	0
10	$\sqrt{2}(\lambda^2-1)$	$\sqrt{2}\,y(\lambda-1)$	0	$-\sqrt{2}\,y\lambda(\lambda-1)$	0
01	0	$\sqrt{2}\,y\lambda(\lambda-1)$	$-\sqrt{2}(\lambda^2-1)$	$-\sqrt{2}\,y(\lambda-1)$	0
00	$2y(1-\lambda^2)$	$2[\lambda-(\lambda-1)y^2]$	0	$2\lambda[1+(\lambda-1)y^2]$	0

where $\lambda = \frac{\sqrt{W}}{2m}$ and m = nucleon mass.

$4\,U_{rt}(w,y) =$

r	t=1	t=2	t=3	t=4	t=5
1	1	$2m - 4yk^2/m$	$-3m^2 - 4k^2(1+y)$	-4	1
2	1	$-2m$	$m^2 + 4k^2$	2	-1
3	1	$2m$	$-3m^2 - 4k^2$	-2	-1
4	1	$-2m - 4k^2/m$	m^2	0	1
5	1	$-6m - 4yk^2/m$	$5m^2 + 4k^2 + 4yk^2$	4	1

where $k^2 = W/4 - m^2$.

The amplitudes $p_t(wt\bar{t})$ were calculated via the dispersion relation (II.11). Introducing (II.11) and (C.4) into (C.3) and interchanging integrations yields

$$T_{ij}(\ell) = (\mathrm{OPE}) + \frac{2\ell+1}{2\pi}\,\frac{(\ell-m)!}{(\ell+m)!}\int_4^\infty dt' \int_{-1}^{1} dx$$

$$\times\, P_\ell^m(x)\,\frac{(1-x^2)^{m/2}}{2k^2(y-x)} \sum_r \sum_t V_{ij}^{rt}(w,x)$$

$$\times \left\{ U_{rt}(w,x)\,\rho'_t(wt'\bar{t}(x)) + (-1)^{r+T}\,(x \to -x) \right\}. \qquad (C.5)$$

We have defined $y(t') = 1 + t'/2k^2$ and $x = \cos\theta = 1 + t/2k^2$.

The x-dependence of ρ' generates some difficulty in evaluating the integral on x. Recall from (II.23) that

$$\rho_t'^{(\pm)}(wt'\bar{t}(x)) = \rho_t^{(t)}(wt') \mp (-1)^t\,\rho_t^{(t)}(\bar{t}(x)\,t'). \qquad (C.6)$$

The Mandelstam representation assures us that[4]

$$\rho_k(\bar{t}\,t') = \frac{1}{\pi}\int_{4m^2}^{\infty} dz\ \frac{\mathcal{H}_k(z\,t')}{z-\bar{t}}\,. \qquad (C.7)$$

Now for physical NN scattering $\bar{t}$ is negative and, at low energies, small:

$$-4k^2<\bar{t}<0\ .$$

Thus it is reasonable to neglect $\bar{t}$ with respect to $4m^2$, the lower limit in (C.7). We have, therefore, set $\bar{t}=0$ ($t=4m^2-w \to -4k^2$) in (C.5). This prescription for handling the x-dependence in (C.5) is not that used by ALV.[4] ALV replaced x by y(t'), equivalent to replacing t by t'. The prescription $\bar{t}=0$ was also used by Epstein and McKellar[16] and by Chemtob et al.[13]

The x-integration in (C.5) can now be performed. We note that the product $V^r_{ij}(w,x)U_{rt}(w,x)$ is a second order polynomial in x. The integration can, therefore, be written in terms of the associated Legendre functions of the second kind. Define

$$W^t_{ij}(w,x) = \sum_r V^r_{ij}(w,x)\,U_{rt}(w,x)$$

and

$$W^t_{ij}(w,x) = W^t_{ij}(w,0) + \alpha^t_{ij}\,x + \beta^t_{ij}\,x^2\ .$$

For the case $\ell \neq 0$ the P_ℓ^m satisfy

$$\frac{1}{2}\int_{-1}^{1} \frac{W_{ij}^t(w,x)(1-x^2)^{\frac{m}{2}} P_\ell^m(x)}{y-x}\, dx$$

$$= W_{ij}^t(w,y)(y^2-1)^{\frac{m}{2}} Q_\ell^m(y)$$

$$- \frac{2}{3}\alpha_{ij}^t \delta_{m1}\delta_{\ell 1}$$

$$- \frac{1}{3}\beta_{ij}^t(\delta_{m0} + 2y\,\delta_{m1})\delta_{\ell 1} . \qquad \text{(C.10)}$$

The linear and quadratic terms in W_{ij}^t are

$$\frac{16\pi\lambda}{m}\alpha_{ij}^t =$$

ij	t=1	t=2	t=3	t=4	t=5
SS	$2(1-\lambda^2)$	$4m(1-\lambda^2)$	$2m^2(1-4\lambda^2)(1-\lambda^2)$	0	$2(1-\lambda^2)$
11	$2(1-\lambda^2)$	$4m(1-\lambda^2)$	$2m^2(1-4\lambda^2)(1-\lambda^2)$	$-4(1-\lambda^2)$	$-2(1-\lambda^2)$
1-1	0	0	0	0	0
10	$-\sqrt{2}(1-\lambda^2)$	$-2\sqrt{2}(1-2\lambda^2)\times(1-\lambda)$	$\sqrt{2}\,m^2(1+3\lambda-4\lambda^3)(\lambda-1)$	$2\sqrt{2}(\lambda-1)$	$\sqrt{2}(1-\lambda^2)$
01	$\sqrt{2}(\lambda-1)^2$	$2\sqrt{2}\,m(1+2\lambda)\times(1-\lambda)^2$	$-m^2\sqrt{2}(1+3\lambda-4\lambda^3)(\lambda-1)$	$2\sqrt{2}\lambda(\lambda-1)$	$\sqrt{2}(1-\lambda^2)$
00	$2(1-\lambda^2)$	$4m(1-\lambda^2)$	$2m^2(1-4\lambda^2)\times(1-\lambda^2)$	0	$2(1-\lambda^2)$

$$\frac{16\pi\lambda}{m}\,\beta_{ij}^{t} =$$

ij	t=1	t=2	t=3	t=4	t=5
SS	0	0	0	0	0
11	$(\lambda-1)^2$	$2m(1+2\lambda)\times(1-\lambda)^2$	$m^2(4\lambda^3-3\lambda-1)(\lambda-1)$	$2\lambda(\lambda-1)$	$1-\lambda^2$
1-1	0	0	0	0	0
10	0	0	0	0	0
01	0	0	0	0	0
00	$2(\lambda-1)^2$	$4m(1+2\lambda)\times(1-\lambda)^2$	$2m^2(1+2\lambda-3\lambda^2-4\lambda^3+4\lambda^4)$	$4(1-\lambda)$	$2(\lambda^2-1)$

where m = nucleon mass.

The partial wave amplitudes are finally obtained by numerically performing the t'-integration in (C.5).

APPENDIX D

POTENTIAL EQUATIONS

153a

APPENDIX D

POTENTIAL EQUATIONS

The iterated one-pion-exchange contribution to the potential was calculated by Chemtab, Durso, and Riska[13] and earlier by Partovi and Lomon.[1] CDR wrote the iterated one-pion-exchange contribution $\mathcal{J}_{\pi 2}$ of (II.55) in terms of spectral functions

$$\mathcal{J}_{\pi 2}(k',k) =$$

$$\bar{u}_p(\underset{\sim}{k}')\,\bar{u}_n(-\underset{\sim}{k}')\sum_{j=1}^{5}\frac{1}{\pi}\int_4^\infty dt'\;\frac{3\eta_j^+(k^2,t')+2\tau_p\cdot\tau_n\,\eta_j^-(k^2,t')}{t'-t}\,Q_j\;u_p(\underset{\sim}{k})\,u_n(-\underset{\sim}{k}), \tag{D.1}$$

where

$$\begin{aligned} Q_1 &= 1, \\ Q_2 &= \gamma_4^p\gamma_4^n, \\ Q_3 &= \gamma_4^p+\gamma_4^n, \\ Q_4 &= \gamma^p\cdot\gamma^n, \\ Q_5 &= \gamma_5^p\gamma_5^n. \end{aligned} \tag{D.2}$$

The $\eta_j^{\pm}$ were given by CDR and are not repeated here. However, we correct a printing error in CDR's (4.29):

$$T_2(p^2,t') = \frac{1}{w} S_1(p^2,t')$$

$$+ \frac{2}{(p^2-k_-^2)\sqrt{k_+^2+m^2}} \left\{ \frac{k_-^2+m^2}{p^2+m^2} \tilde{\Pi}(\gamma;\alpha) - \tilde{F}(\alpha) \right\}, \qquad (D.3)$$

where p^2 is the same as our k^2. Also there should be a closing bracket immediately preceeding the T_o in CDR's (4.31b).

Another form for T_2 is

$$Re\ T_2 = \frac{2}{(k_+^2-p^2)\sqrt{k_+^2+m^2}} \tilde{\Pi}(n;\alpha), \qquad (D.4)$$

where $n = (k_+^2 - k_-^2)/(k_+^2 - p^2) < 1$.

The transformation from $\eta_-^{\pm}$ to the $\bar{\eta}_-^{\pm}$ occurring in the potential (II.62) is

$$\bar{\eta}_\alpha^{\pm} = \sum_j \tilde{X}_{\alpha j}^{Q\Omega} \eta_j^{\pm} . \qquad (D.5)$$

The matrix $\tilde{X}^{Q\Omega}$ evaluated at $w = 4m^2$, $t=0$ is

$\tilde{X}^{Q\Omega}_{\alpha j}$ =

α	j=1	j=2	j=3	j=4	j=5
C	1	1	2	0	0
SO	$\frac{-1}{2m^2}$	$\frac{1}{2m^2}$	0	$\frac{1}{m^2}$	0
T	0	0	0	$\frac{-1}{12m^2}$	$\frac{1}{12m^2}$
SS	0	0	0	$\frac{-1}{6m^2}$	$\frac{-1}{12m^2}$
SO2	$\frac{-1}{16m^4}$	$\frac{-1}{16m^4}$	$\frac{1}{8m^4}$	0	0

The transformation from $\rho^{\pm}$ to $\bar{\rho}^{\pm}$ is

$$\bar{\rho}^{\pm}_{\alpha} = \sum_{j} \tilde{X}^{P\Omega}_{\alpha j} \rho^{\pm}_{j} . \qquad \text{(D.6)}$$

The matrix $\tilde{X}^{P\Omega}_{\alpha j}$ evaluated at $w=4m^2$, $t=0$ is

$$\widetilde{\chi}^{P\Omega}_{\alpha j} =$$

α	$j=1$	$j=2$	$j=3$	$j=4$	$j=5$
C	1	$-2m$	m^2	1	0
SO	$\frac{-1}{2m^2}$	$\frac{-1}{m}$	$\frac{3}{2}$	$\frac{3}{2m^2}$	0
T	0	0	0	$\frac{-1}{12m^2}$	$\frac{1}{12m^2}$
SS	0	0	0	$\frac{-1}{6m^2}$	$\frac{-1}{12m^2}$
SO2	$\frac{-1}{16m^4}$	$\frac{-3}{8m^3}$	$\frac{-9}{16m^2}$	$\frac{-1}{16m^4}$	0

APPENDIX E

DIRAC ALGEBRA

157a

APPENDIX E

DIRAC ALGEBRA

The Dirac algebra that we use is the Dirac-Pauli representation:

$$\{\gamma_\mu, \gamma_\nu\} = 2\delta_{\mu\nu}, \tag{E.1}$$

$$\gamma_k = \begin{pmatrix} 0 & -i\sigma_k \\ i\sigma_k & 0 \end{pmatrix}, \tag{E.2}$$

$$\gamma_4 = \begin{pmatrix} 1 & 0 \\ 0 & -1 \end{pmatrix}, \tag{E.3}$$

$$\gamma_5 = \gamma_1\gamma_2\gamma_3\gamma_4 = \frac{1}{4!}\epsilon_{\mu\nu\lambda\sigma}\gamma_\mu\gamma_\nu\gamma_\lambda\gamma_\sigma$$

$$= \begin{pmatrix} 0 & -1 \\ -1 & 0 \end{pmatrix}, \tag{E.4}$$

$$\sigma_{\mu\nu} = \frac{1}{2i}(\gamma_\mu\gamma_\nu - \gamma_\nu\gamma_\mu), \tag{E.5}$$

$$\gamma_\mu\gamma_\nu = \delta_{\mu\nu} + i\sigma_{\mu\nu}. \tag{E.6}$$

The free particle Dirac equations are

$$(i\gamma\cdot p + m)\, u(p) = 0 \,, \tag{E.7}$$

$$(i\gamma\cdot p - m)\, v(p) = 0 \,, \tag{E.8}$$

$$\bar{u}(p)(i\gamma\cdot p + m) = 0 \,, \tag{E.9}$$

$$\bar{v}(p)(i\gamma\cdot p - m) = 0 \,, \tag{E.10}$$

where

$$\bar{u}(p) = u^{\dagger}(p)\gamma_4 \,, \tag{E.11}$$

$$\bar{v}(p) = v^{\dagger}(p)\gamma_4 \,, \tag{E.12}$$

$$u^{\pm}(p) = \sqrt{\frac{E+m}{2m}} \begin{pmatrix} 1 \\ \frac{\sigma\cdot p}{E+m} \end{pmatrix} \chi^{\pm} \,, \tag{E.13}$$

$$v^{\pm}(p) = \mp\sqrt{\frac{E+m}{2m}} \begin{pmatrix} \frac{\sigma\cdot p}{E+m} \\ 1 \end{pmatrix} \chi^{\mp} \,. \tag{E.14}$$

The Feynman rules in this representation are summarized by Sakaurai.[19]

APPENDIX F

RHO-MESON COUPLING CONSTANTS

159a

APPENDIX F

RHO-MESON COUPLING CONSTANTS

The ρ-meson coupling constants are defined by the Lagrangian density for interacting nucleon and ρ-meson fields:

$$\mathcal{L} = i g_{\rho NN} \bar{\Psi} \vec{\tau}\cdot\vec{\phi}_\mu \gamma_\mu \Psi - \frac{f_{\rho NN}}{2m} \bar{\Psi} \sigma_{\mu\nu} \vec{\tau}\cdot(\partial_\nu \vec{\phi}_\mu)\Psi \quad , \tag{F.1}$$

where $\vec{\tau}$ is the nucleon isospin operator; g_{pNN} and $f_{\rho NN}$ are the vector and tensor coupling constants respectively. An equivalent expression is

$$\mathcal{L} = i(g_{\rho NN} + f_{\rho NN}) \bar{\Psi} \vec{\tau}\cdot\vec{\phi}_\mu \gamma_\mu \Psi - \frac{f_{\rho NN}}{2m} \bar{\Psi} \vec{\tau}\cdot[(p'+p)_\mu \vec{\phi}_\mu]\Psi, \tag{F.2}$$

where p(p') is the initial (final) nucleon momemtum operator.

As noted in Chapter III.F, the ρ coupling constants are related to the amplitudes Γ_i. We shall define the coupling constants in terms of the residues of Γ_i at the ρ-meson pole.

We write the $\mathrm{Im}\Gamma_i(t)$ near the pole position as

$$\Gamma_1 = \left(\frac{T_R}{T_R-4}\right)^{1/4}\left(\frac{4T_I}{3\pi(T_R-4)}\right)^{1/2}\frac{g_{\rho NN}}{t-T_{p1}} + B_1 , \quad \text{(F.3a)}$$

$$2m\Gamma_2 = \left(\frac{T_R}{T_R-4}\right)^{1/4}\left(\frac{4T_I}{3\pi(T_R-4)}\right)^{1/2}\frac{f_{\rho NN}}{t-T_{p2}} + B_2 , \quad \text{(F.3b)}$$

where B_i are regular at $t=T_{pi}$. For T_{pi} we use a form suggested by J. Pisut and M. Roos, Nucl. Phys. B6, 325 (1968):

$$T_{pi} = T_R + iT_I\left(\frac{q_b}{q_P}\right)^3\left(\frac{1+R_i^2 q_P^2}{1+R_i^2 q_b^2}\right), \quad \text{(F.4)}$$

$$q_b^2 = t/4 - 1 ,$$
$$q_P^2 = T_R/4 - 1 .$$

The B_i are expected to be approximately real (the nucleon pole terms are exactly real and the contributions from narrow s- and u-channel resonances are approximately real) so we shall work with the imaginary parts of (F.3). From the mass and width of the ρ we expect $T_I/T_R<0.2$ so that we may replace T_{pi} by T_R in the numerators.

The imaginary parts of (F.3) with B_i neglected and T_{pi} replaced by T_R in the numerators have been fitted near the pole to the Γ_i calculated in Chapter III. The resulting parameters are

$$T_R = 29.2 \pm 1. , \quad \text{(F.5a)}$$

$$T_I = 5.50 \pm 0.2 , \quad \text{(F.5b)}$$

$$R_1^2 = 0.0008 , \quad \text{(F.6a)}$$

$$R_2^2 = 0.0652 , \quad \text{(F.6b)}$$

$$g_{\rho NN} = 2.35 \pm 0.10 \ , \qquad \text{(F.7a)}$$

$$f_{\rho NN} = 13.6 \pm 0.06 \ . \qquad \text{(F.8a)}$$

Thus

$$\frac{g^2_{\rho NN}}{4\pi} = 0.44 \pm 0.05 \ , \qquad \text{(F.7b)}$$

$$\frac{f_{\rho NN}}{g_{\rho NN}} = 5.8 \pm 0.2 \ . \qquad \text{(F.7c)}$$

The fitted $\mathrm{Im}\Gamma_i$ are shown in Figure 49.

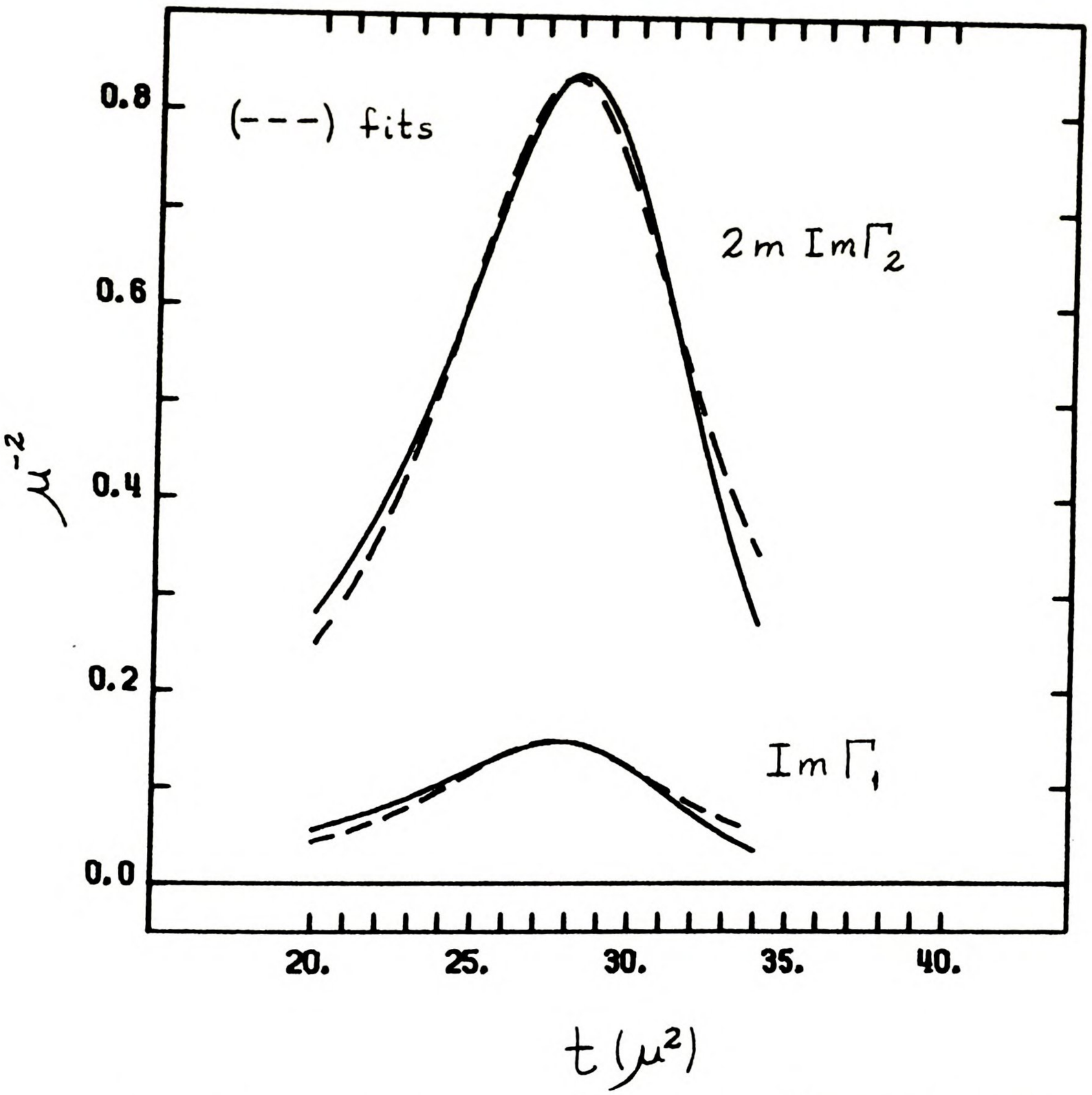

Figure 49. Imaginary parts of the $N\bar{N}\to\pi\pi$ amplitudes Γ_i and resonance fits.

APPENDIX G

OMEGA-MESON COUPLING CONSTANTS

163a

APPENDIX G

OMEGA-MESON COUPLING CONSTANTS

The ω-meson coupling constants are defined by a Lagrangian density similar to (F.1) but without the isospin factors. One can attempt to determine the coupling constants in several ways.

The simple quark model[82] relates the ω and ρ coupling constants. The quark structures of the ρ° and ω are

$$\rho^{\circ} = \frac{1}{\sqrt{2}} (p\bar{p} - n\bar{n}) , \tag{G.1a}$$

$$\omega = \frac{1}{\sqrt{2}} (p\bar{p} + n\bar{n}) , \tag{G.1b}$$

where p and n are the (isospin, charge) = (1/2, 2/3) and (-1/2, -1/3) nonstrange quarks. The meson-proton coupling is depicted in the quark diagrams, Figure 50. The proton → $\frac{1}{\sqrt{2}}(\rho+\omega)$ vertex is twice (because the proton contains two p-quarks) diagram 50a and the proton → $\frac{1}{\sqrt{2}}(\rho-\omega)$ vertex is diagram 50b. Each diagram has equal weight so $g_{\omega pp} = 3g_{\rho pp}$. Similarly one finds $g_{\omega nn} = -3g_{\rho nn}$. Thus

$$g^2_{\omega NN} = 9\ g^2_{\rho NN} . \tag{G.2}$$

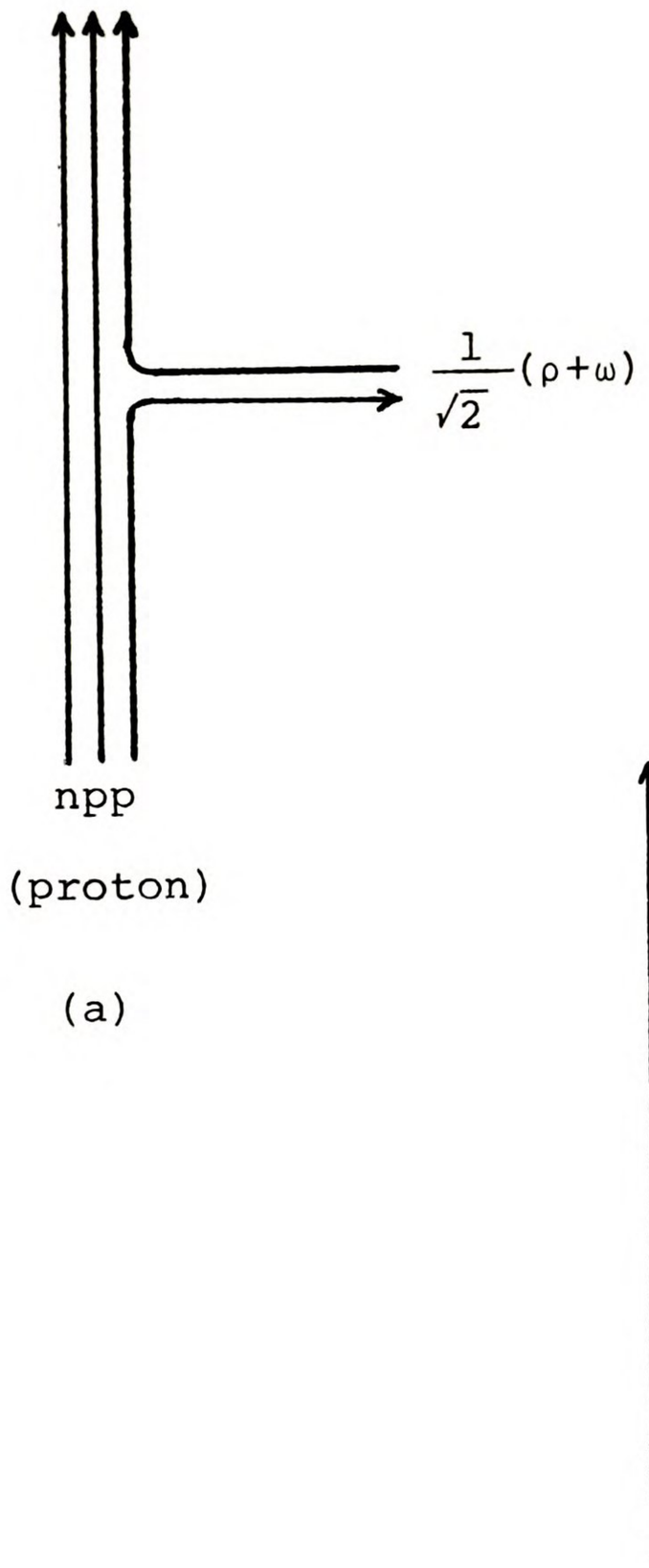

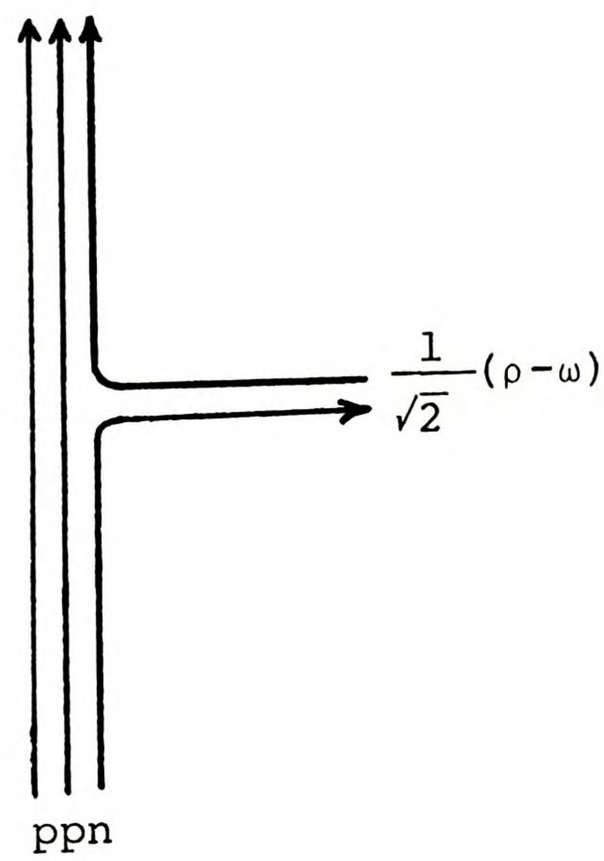

Figure 50. Meson-nucleon quark diagrams.

From (F.5) we find

$$\frac{g^2_{\omega NN}}{4\pi} = 4.0 . \qquad \text{(G.3)}$$

In the simple quark model the ϕ-meson is composed of only the (I,Q) = (0,-1/3) strange quarks:

$$\phi = \lambda\bar{\lambda} . \qquad \text{(G.1c)}$$

Thus ϕ does not couple to nucleon in this picture.

One can also use the quark model to predict[82] the electromagnetic couplings of the ρ,ω, and ϕ. These constants are defined by the current-field identity[83] in terms of the vector-meson electromagnetic current $j_\mu^{(\gamma VV)}$ and the meson field $\phi_\mu^{(V)}$:

$$j_\mu^{(\gamma VV)} = \frac{m_V}{2g_V}\,\phi_\mu^{(V)} . \qquad \text{(G.4)}$$

The corresponding interaction Lagrangian density is

$$\mathcal{L} = j_\mu^{(\gamma VV)} A_\mu . \qquad \text{(G.5)}$$

Coupling the photon to the individual quark charges we find

$$g_\omega^2 = 9\, g_q^2 = \frac{9}{2}\, g_\phi^2 \qquad \text{(G.6)}$$

The vector-meson-dominance (VMD) model[83] applied to the nucleon form factors postulates that the photon couples to the nucleon only through an intermediate vector-meson state. A rather strong statement of the model is that the

nucleon electromagnetic current is proportional to the nucleon's vector-meson current J_μ:

$$J_\mu^{\cdot(YNN)} = \frac{1}{2g_v} \Delta_{\mu\nu}^{(v)}(t)\, J_\nu \qquad \text{(G.7)}$$

where $\Delta_{\mu\nu}^{(V)}(t)$ is the vector-meson propagator normalized such that $\Delta_{\mu\nu}^{(V)}(0) = 1$.

Considering, for simplicity, only the I_3=0 components of (F.1) we can write

$$\langle p' | J_\mu | p \rangle = \sqrt{\frac{m^2}{p'_0 p_0}}\; i\,\bar{u}(p')\Big[g_{VNN}\,\gamma_\mu + \frac{f_{VNN}}{2m}\,\sigma_{\mu\nu}(p-p')_\nu \Big]\, u(p)\,. \qquad \text{(G.8)}$$

Thus (G.7) relates the form factors in (III.29) to the coupling constants in (G.8). The relation is

$$F_1^x(t) = \sum_v \frac{g_{VNN}}{2g_v}\,\Delta_{\mu\nu}^{(v)}(t) \qquad \text{(G.9a)}$$

$$2m\,F_2^x(t) = \sum_v \frac{f_{VNN}}{2g_v}\,\Delta_{\mu\nu}^{(v)}(t) \qquad \text{(G.9b)}$$

where the sum includes the ω and ϕ if x=S(isoscalar) and the ρ (and ρ') if x=V(isovector). Higher mass mesons may be included if they exist.

The normalizations

$$F_1^S(0) = \frac{1}{2} \qquad \text{(G.10a)}$$

$$2m F_2^S(0) = \frac{\lambda_p+\lambda_n}{2} = -0.06 \qquad \text{(G.10b)}$$

and (G.10) give

$$\frac{g_{\omega NN}}{g_\omega} + \frac{g_{\phi NN}}{g_\phi} = 1 \qquad \text{(G.11a)}$$

$$\frac{f_{\omega NN}}{g_\omega} + \frac{f_{\phi NN}}{g_\phi} = -0.12 \ . \qquad \text{(G.11b)}$$

From the simple quark model we have $g_{\phi NN}=f_{\phi NN}=0$. Then

$$g_{\omega NN} = g_\omega \ , \qquad \text{(G.12a)}$$

and

$$\frac{f_{\omega NN}}{g_{\omega NN}} = -.12 \ . \qquad \text{(G.12b)}$$

Then (G.2) follows from (G.5) and (G.13).

It is not necessary to rely on the quark model prediction $g_{\phi NN}=0$. The VMD model for the isoscalar form factors with narrow-width ω, ϕ is

$$F_1^S(t) = \frac{g_{\omega NN}}{2g_\omega}\frac{1}{1-t/m_\omega^2} + \frac{g_{\phi NN}}{2g_\phi}\frac{1}{1-t/m_\phi^2} \qquad \text{(G.13a)}$$

$$2m\,F_2^S(t) = \frac{f_{\omega NN}}{2g_\omega}\frac{1}{1-t/m_\omega^2} + \frac{f_{\phi NN}}{2g_\phi}\frac{1}{1-t/m_\phi^2} \ . \qquad \text{(G.13b)}$$

The coupling constant ratios $\frac{g_{\omega NN}}{g_\omega}$, etc. can be determined from the t=0 normalization of F_i^s and the derivatives at t=0. The form factors near t=0 were analyzed by L. H. Chan et al.[84] with the results

$$\left.\frac{dG_E^p}{dt}\right|_{t=0} = 2.95 \quad GeV^{-2},$$

$$\left.\frac{dG_E^n}{dt}\right|_{t=0} = -0.454,$$

$$\left.\frac{dG_M^p}{dt}\right|_{t=0} = 7.98,$$

$$\left.\frac{dG_M^n}{dt}\right|_{t=0} = -5.61 \quad . \tag{G.14}$$

From these values we find

$$\left.\frac{dF_1^s}{dt}\right|_{t=0} = 1.27 \quad GeV^{-2}, \tag{G.15a}$$

$$2m \left.\frac{dF_2^s}{dt}\right|_{t=0} = -0.0800 \cdot \tag{G.15b}$$

Solving (G.13) for the coupling constant ratios gives

$$\frac{g_{\omega NN}}{g_\omega} = 2.38, \tag{G.16a}$$

$$\frac{f_{\omega NN}}{g_\omega} = -0.067, \tag{G.16b}$$

$$\frac{g_{\phi NN}}{g_\phi} = -1.38, \tag{G.16c}$$

$$\frac{f_{\phi NN}}{g_\phi} = -0.053. \qquad \text{(G.16d)}$$

If, in addition to the ω, higher mass mesons also contribute to the isoscalar form factors (D.10) then such high mass contributions are somewhat suppressed in a subtracted dispersion relation, which we write as

$$F_i^S(t) = F_i^S(0) + \frac{t}{\pi}\int_q^\infty \frac{Im\ F_i^S(t')}{t'(t'-t)}\,dt' \quad . \qquad \text{(G.17)}$$

In the narrow resonance approximation the ω contributions to Im F_i^S are

$$Im\ F_1^S(t') = \pi m_\omega^2 \left(\frac{g_{\omega NN}}{2g_\omega}\right) \delta(t'-m_\omega^2), \qquad \text{(G.18a)}$$

$$2m\ Im\ F_2^S(t') = \pi m_\omega^2 \left(\frac{f_{\omega NN}}{2g_\omega}\right) \delta(t'-m_\omega^2), \qquad \text{(G.18b)}$$

so that

$$F_1^S(t) \simeq \frac{1}{2} + \frac{g_{\omega NN}}{2g_\omega}\frac{t}{m_\omega^2-t}, \qquad \text{(G.19a)}$$

$$2m\ F_2^S(t) \simeq -0.06 + \frac{f_{\omega NN}}{2g_\omega}\frac{t}{m_\omega^2-t}\ . \qquad \text{(G.19b)}$$

Again using the derivaties (G.16) yields

$$\frac{g_{\omega NN}}{g_\omega} = 1.56\ , \qquad \text{(G.20a)}$$

$$\frac{f_{\omega NN}}{g_{\omega}} = -.0983 \ . \qquad \text{(G.20b)}$$

The γ_{VV} coupling constants g_V can be determined[85] directly from the $V \to e^+e^-$ rate measured in e^+e^- colliding beam experiments. Combining (G.4) with QED one finds the partial decay width

$$\Gamma(V \to e^+e^-) = \frac{4\pi\alpha^2 m_V}{12 g_V^2}\left(1 + \frac{2m_e^2}{m_V^2}\right)\left(1 - \frac{4m_e^2}{m_V^2}\right)^{1/2}$$

$$\simeq \frac{4\pi\alpha^2 m_V}{12 g_V^2} \ . \qquad \text{(G.21)}$$

From the data tables $\frac{\Gamma(\omega \to e^+e^-)}{\Gamma(\omega)} = 7.6 \times 10^{-5}$ and $\Gamma(\omega) =$ 9.8 MeV. We therefore find

$$\frac{g_\omega^2}{4\pi} = 4.7 \qquad \text{(G.22)}$$

which also gives $g^2_{\omega NN}/4\pi$ if we accept (G.12).

Table 9 summerizes the predictions for the omega coupling constants.

Table 9.--Predictions for the omega coupling.

Source Equations	$\frac{g^2_{\omega NN}}{4\pi}$	$f_{\omega NN}/g_{\omega NN}$
(G.3)	4.0	-
(G.12), (G.22)	4.7	-.12
(G.11), (G.22)	26.6	-.028
(G.20), (G.22)	11.4	-.063

MICHIGAN STATE UNIVERSITY LIBRARIES
3 1293 03196 0176